QUANTIFYING NUCLIDE CONTRIBUTIONS TO REACTOR BEHAVIOUR OVER TIME

STUART CHRISTIE

Quantifying nuclide contributions to reactor behaviour over time

Quantifying nuclide contributions to reactor behaviour over time

Proefschrift

ter verkrijging van de graad van doctor
aan de Technische Universtiteit Delft,
op gezag van de Rector Magnificus Prof. ir. K.C.A.M. Luyben,
voorzitter van het College voor Promoties,
in het openbaar te verdedigen
op maandag 06 januari 2014 om 15:00 uur
door

Stuart Alexander CHRISTIE

Master of Science in the Physics and Technology of Nuclear Reactors,
University of Birmingham

geboren te Northampton, Verenigd Koninkrijk

Dit proefschrift is goedgekeurd door de promotor:

Prof. dr. ir. T.H.J.J. van der Hagen

Copromotor:

Dr. ir. D. Lathouwers

Samenstelling promotiecommissie:

Rector Magnificus,	voorzitter
Prof. dr. ir. T.H.J.J. van der Hagen,	Technische Universiteit Delft, promotor
Dr. ir. D. Lathouwers,	Technische Universiteit Delft, copromotor
Prof. T.J. Abram,	University of Manchester, Verenigd Koninkrijk
Prof. G.H. Lohnert,	University of Stuttgart, Duitsland
Prof. dr. ir. I.R. van der Poel,	Technische Universiteit Delft
Prof. dr. H.T. Wolterbeek,	Technische Universiteit Delft
Dr. ir. E.V. Verhoef,	Centrale Organisatie Voor Radioactief Afval

© 2013, Stuart Alexander Christie

All rights reserved. No part of this book may be reproduced, stored in a retrieval system, or transmitted, in any form or by any means, without prior permission from the copyright owner.

ISBN 978-90-8891-795-0

Keywords: Nuclear, fuel cycle, adjoint

Cover design by Lilee Nishizono

The research described in this thesis was performed in the section Nuclear Energy and Radiation Applications (NERA), of the department of Radiation Science and Technology (RST), of the Delft University of Technology, Delft, The Netherlands.

The work in this thesis was supported by the Centrale Organisatie Voor Radioactief Afval (COVRA).

Printed by: Proefschriftmaken.nl || Uitgeverij BOXPress

Published by: Uitgeverij BOXPress, 's-Hertogenbosch

Contents

1 Introduction **1**
1.1 The nuclear fuel cycle . . . 3
1.2 Weighting schemes . . . 5
1.3 Breeding ratio . . . 11
1.4 Thesis synopsis . . . 14

2 The Continuous Fuel Cycle Model **17**
2.1 Introduction . . . 17
2.2 Theory . . . 20
2.3 Reactor Models . . . 25
2.4 Breeder Reactor Results . . . 27
2.5 Isobreeder Results . . . 33
2.6 Conclusions . . . 44

3 The Double Adjoint Method **47**
3.1 Introduction . . . 47
3.2 Reactivity . . . 48
3.3 Burn-up . . . 50
3.4 Time dependent perturbation theory . . . 51
3.5 Implementation . . . 54
3.6 Testing in a fast spectrum . . . 55
3.7 Testing in a thermal spectrum . . . 57
3.8 Reloading . . . 59
3.9 Reloading a single SFR pin . . . 62
3.10 Reloading a single PWR pin . . . 69
3.11 Breeding ratio . . . 72
3.12 Conclusions . . . 74

4 Application of Coupled Depletion Perturbation Theory 77
4.1 Introduction . . . 77
4.2 Theory . . . 78
4.3 Implementation . . . 86
4.4 Fast system results . . . 89
4.5 Thermal system results . . . 97
4.6 Conclusions . . . 103

5 Waste heat reduction 105
5.1 Introduction . . . 105
5.2 Theory . . . 106
5.3 Method . . . 108
5.4 Results . . . 109
5.5 Conclusions . . . 121

6 Conclusions and Recommendations 125
6.1 Conclusions . . . 125
6.2 Recommendations . . . 127

Bibliography 131

Summary 137

Samenvatting 139

Acknowledgements 143

List of publications 145

Curriculum Vitae 147

Chapter 1

Introduction

The increasing drive for more diverse and sustainable forms of power production has led to a renewed interest in nuclear power. While it does not rely on the combustion of fossil fuels or produce carbon dioxide, nuclear power does consume fuel, typically uranium, and produces radioactive waste. These issues must be considered when nuclear power is proposed as a solution to the existing problems of power production.

The vast majority of reactors currently in operation rely on U-235 for their fuel. This isotope makes up approximately 0.7% of naturally occurring uranium. The remaining material (U-238, with very small amounts of U-234) goes largely unused. Uranium reserves have been estimated to be over 6 million tonnes in the form of identified resources and 10 million tonnes of undiscovered resources (OECD NEA/IAEA, 2010). It is likely that further resources remain to be found, and recovery of uranium from non-conventional sources such as phosphates, black shale, and seawater may become economic with increases in uranium price or new or improved extraction techniques. The rate of uranium usage was around 59 thousand tonnes per year at the end of 2008, and is predicted to increase to between 87 and 138 thousand tonnes by 2035 (OECD NEA/IAEA, 2010). This means that although there is a sufficient supply of uranium available for at the very least the coming decades, it would be prudent to consider improvements to the sustainability of nuclear power production.

Fertile material such as U-238 can be converted into fissile isotopes via neutron capture and decay processes. This process occurs to some extent in all reactors, but a large amount of U-238 is left untouched. Taking full advantage of this conversion would allow all natural uranium to be used for power production. Allowing for the conversion that already occurs and for losses during fuel cycle processes means the fuel cycle efficiency would be improved by a factor of approximately 60 (Waltar et al., 2012). This represents a significant improvement in the sustainability of nuclear power and could extend the lifetime of uranium resources into thousands of years.

The goal of this thesis is to study the improvement of the sustainability of nuclear power by making greater use of uranium resources. Decades of nuclear power production have resulted in large stockpiles of depleted uranium (DU), estimated to be 1.6 million tonnes of uranium metal (tU) at the end of 2005 and increasing annually by around 60000 tU (OECD NEA/IAEA, 2010). A reactor that could maintain operation with an external fuel supply of only depleted uranium could take advantage of this resource. The problem of improving sustainability by making greater use of depleted uranium can be broken up into three issues:

- Can a reactor be designed that operates on a pure depleted uranium feed?
- What are the necessary properties of such a design?
- How far can the waste production of such a design be minimised?

It is clear that if depleted uranium is approximated as a purely fertile material, then a given reactor design can be operated on a pure DU feed if it produces as much or more fissile material as it consumes during operation. The material produced during reactor operation, however, is rarely of the same composition as the material currently present in the reactor, and it is necessary to use some method to compare them. The effects of transmutation must also be considered, as the contribution of a nuclide can change significantly with time and irradiation, the production of Pu-239 from U-238 being a prime example. The main topic of this thesis will therefore be measuring how a nuclide contributes to the behaviour of a reactor, both at the present moment and in the future. Although the techniques in this thesis were developed and applied in the context of depleted uranium usage, they are generic enough to

be used for any similar problem requiring the modelling of nuclide properties and their behaviour over time.

The measurement of the amount of waste produced is not as straightforward as it may initially appear. Although the physical volume of waste produced is an issue, the main limiting factor in waste disposal is the production of heat (Hökmark et al., 2009; U.K. Nirex Ltd., 2004). The more heat produced by a given body of waste, the lower the density of material that can be stored in a given repository space. Reducing the heat produced by the waste therefore effectively reduces the amount of waste as it requires less repository space for disposal. For this reason, the waste limitation work will focus on reducing the heat produced by the waste.

To set the material in the appropriate background, a short description of the stages of the nuclear fuel cycle is provided. The production of fissile material, such as plutonium, from fertile isotopes is discussed. A range of existing schemes to measure the contributions of different isotopes to the criticality of a reactor are reviewed, which are intended to describe the contribution at the moment they are applied and do not allow for changes with time. This is followed by a section on measures of the fuel breeding in a reactor and its associated fuel cycle, which includes both instantaneous and cycle-averaged metrics. Finally an overview of the rest of the thesis is provided.

1.1 The nuclear fuel cycle

The nuclear fuel cycle can be divided into two parts: the in-reactor fuel cycle; and the external fuel cycle. The in-reactor fuel cycle covers the processes that occur while the fuel is being used to produce power in a reactor, while the external fuel cycle includes all the other processes the fuel undergoes. The external fuel cycle can be further divided into front-end processes, that occur before the fuel is irradiated, and back-end processes that take place after it has been irradiated. A brief description of the stages of the uranium-plutonium nuclear fuel cycle will be given, with more detail available from sources such as Cochran and Tsoulfanidis (1999) and the World Nuclear Association (2011).

1.1.1 Nuclear fuel cycle processes

The fuel cycle begins with the **mining** of uranium ore. Once the ore has been recovered, it is sent for **milling** so that it can be separated from the

other material present. The separated uranium ore is usually in the form U_3O_8, known as yellowcake. This compound is chemically stable and can be transported to a **conversion** plant. Here the uranium is converted to UF_6, which is suitable for use in an **enrichment** plant. The uranium is enriched until it contains the desired amount of U-235 and it is then made into UO_2, and goes on to **fuel fabrication**. Once the fuel has been made, it is sent to a reactor for **power production**. After use in a reactor, if a closed fuel cycle is in operation, the spent fuel undergoes **reprocessing**. The uranium recovered from reprocessing can be returned to the enrichment stage, while the plutonium can be sent to the fabrication stage to be combined with uranium in the form of mixed oxide (MOX) fuel. Material recovered during reprocessing that cannot be used in a closed fuel cycle and spent fuel in an open fuel cycle are processed for **waste disposal**. Waste is categorised into different levels such as low level waste (LLW), intermediate level waste (ILW), and high level waste (HLW), and is also produced in several other stages of the nuclear fuel cycle. Figure 1.1 shows a representation of the cycle, including these waste production paths.

1.1.2 Fissile material production

Fissile Pu-239 can be produced from fertile U-238 by neutron capture and allowing time for two β-decays. This process takes place to differing degrees in all reactors with U-238 in their fuel. Pu-239 is likely to fission when it absorbs a neutron, but neutron capture leading to the production of heavier plutonium isotopes also occurs. In general, the longer the irradiation period, the more heavier isotopes are produced. Given the wide range of reactor designs and fuel cycles that have been operated, plutonium stockpiles of many different compositions have built up. The isotopes of plutonium cannot practically be separated by chemical processes, and the small mass difference between e.g. Pu-239 and Pu-240 means that enrichment by physical processes, as used with uranium, is also not practical (Bernstein, 2007). The plutonium compositions must therefore be used with their current isotopic distribution. A similar process is seen in the production of uranium in the thorium-uranium fuel cycle[1]. There are many different approaches to describing the different contributions of these isotopes to reactor behaviour and attempting to quantify the relationship between one isotopic composition and another.

[1]Natural thorium is made up of a single fertile isotope, Th-232. Neutron capture converts this to Th-233, which β-decays to Pa-233 and then fissile U-233.

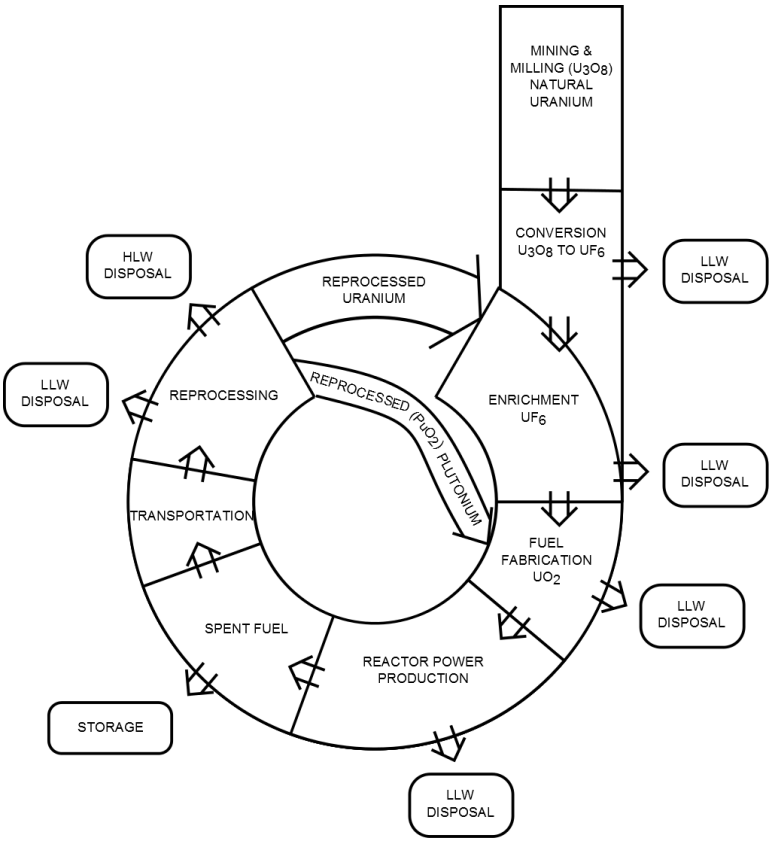

Figure 1.1: Diagram of stages in the nuclear fuel cycle (Cochran and Tsoulfanidis, 1999)

1.2 Weighting schemes

Many different schemes have been used to describe nuclide contributions to reactor criticality. This section will discuss several of these schemes and their associated merits. Any system of numerical weights by nuclide of the kind described here will not fully detail the effects of a nuclide in a given system, as it can only describe first order behaviour. It can however give a good description of the nuclides within these constraints, and allow for a straightforward comparison of different nuclides.

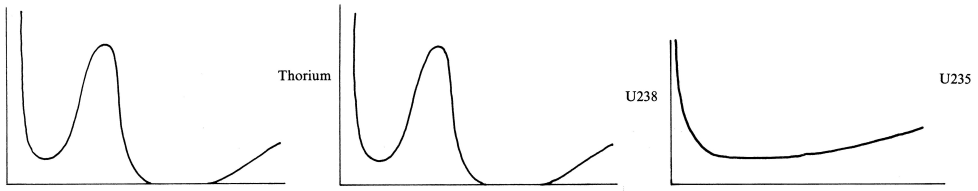

Figure 1.2: Bohr's plots of neutron absorption cross sections against neutron energy for thorium, U-238, and U-235 (Rhodes, 1986)

1.2.1 Fissile isotopes

The earliest scheme for measuring the properties of different nuclides was a simple recognition of the different properties of two uranium isotopes. In 1939, neutron-induced fission had been observed in both uranium and thorium, but would only occur in thorium when fast neutrons were used. Uranium however could be fissioned by both fast and slow neutrons. It was known that naturally occurring thorium was comprised of a single isotope, Th-232. Two isotopes had been found in natural uranium, U-235 and U-238. Niels Bohr realised that the fission behaviour of uranium could be explained by considering the different properties of these two isotopes. U-238 behaves in a similar fashion to Th-232 and, while it can capture thermal neutrons, it can only be fissioned by fast neutrons. U-235 however, given its odd number of neutrons, can be made to fission by slow neutrons as well. Bohr's ideas of the different cross sections of these isotopes are shown in figure 1.2. Understanding the different properties of these different isotopes led to the categorisation of U-235 as fissile, and Th-232 and U-238 as non-fissile.

Once the division between fissile and non-fissile has been made, a numerical weighting scheme follows very simply. Fissile nuclides are given a weight of one and non-fissile nuclides are weighted as zero. For the majority of calculations, the fissile nuclides are considered to be U-235, Pu-239, Pu-241, and the non-fissile ones are U-238, Pu-240, Pu-242. This definition has the advantage of simplicity, but it does not account for the differences in the properties of the fissile nuclides. Pu-241, for example, will usually contribute more to the criticality of a reactor than Pu-239 at a given time. This weighting scheme also does not allow for the effects of the neutron spectrum on how likely a given nuclide is to fission. Fast neutrons can fission the non-fissile actinides, meaning in a fast system the non-fissile nuclides can also provide a significant

contribution to the criticality. Further, no allowance is made for nuclides that are neutron absorbers and have a negative effect on the system criticality.

Other sets of numerical weights based on the fissile/non-fissile distinction have also been used. The definition in Evans (1967) of the British breeding gain, for example, is designed to measure the production of plutonium for use in sustaining a chain reaction. It assigns a value of 1 to Pu-239, 1.5 to Pu-241, and 0.15 to Pu-240 and Pu-242. While these values make some allowance for the different behaviour of the plutonium isotopes, they are only appropriate in systems similar to the one in which they were originally obtained. This scheme also does not generalise well to other nuclides.

1.2.2 Reactivity weighting

A more nuanced weighting can be achieved by considering the properties of a nuclide in the system in which it is irradiated. A brief derivation will be given here, with further discussion available in Adkins (1972) and Van Rooijen (2006). The neutron multiplication of the system can be written as an eigenvalue problem, using the loss and fission operators $\mathbf{L}$, $\mathbf{F}$, the flux ϕ, and eigenvalue λ.

$$(\mathbf{L} - \lambda\mathbf{F})\,\phi = 0 \tag{1.1}$$

The contribution of a nuclide in the one energy group description can then be written in terms of the macroscopic absorption cross section Σ_a, fission cross section Σ_f, and neutrons per fission ν, as $\Sigma_a - \lambda\nu\Sigma_f$. Assuming a critical system, λ is one, meaning the per atom contribution is given using the equivalent microscopic cross sections $\sigma_a - \nu\sigma_f$. Multiplying this value by minus one makes the weights of nuclides that have net neutron production positive, and the weights of net neutron absorbers negative. This defines the reactivity weighting

$$w_\rho = \nu\sigma_f - \sigma_a \tag{1.2}$$

This method requires more information on a nuclide and the system in which it is irradiated. This information is, however, most likely available given that the system is being modelled. It gives a much more detailed picture of how the nuclide contributes to the neutron balance of the system. Each nuclide is weighted according to its individual properties, and the weights can be positive or negative.

The use of the one group approximation in the derivation means that the cross sections used in the reactivity weighting do not capture the full detail of the properties of the nuclide. For example a change in the flux may have different effects on the two cross sections, changing the weight. If a comparison with other weighting systems is carried out, it would be advisable to normalise the weight values by e.g. dividing them all by the weight of Pu-239.

1.2.3 η weighting

Ott (1969) proposed a similar measure based on the η value of certain nuclides.

$$\eta = \frac{\nu\sigma_f}{\sigma_a} \tag{1.3}$$

The intention of using this weighting was to achieve a breeding ratio definition that has a weaker dependence on the fuel composition of the system being studied. This would make the breeding ratio a better description of the properties of the system rather than its current fuel composition. The original proposal suggested using this scheme be used for the four plutonium isotopes: Pu-239; Pu-240; Pu-241; Pu-242; as its intent was to give a better description of plutonium breeding. The weights were normalised to the value of Pu-239, so the weight w_η^i of a nuclide i is

$$w_\eta^i = \frac{\eta_i}{\eta_{49}} \tag{1.4}$$

where 49 represents Pu-239, taking the 4 from its atomic number 94 and the 9 from the nucleon number 239. This notation can be extended to other isotopes, e.g. 40 for Pu-240, and elements, e.g. 28 for U-238. While this weighting scheme can be extended to other nuclides in a relatively straightforward fashion, this does take it beyond its original frame of reference. In particular, the scheme is based on the assumption that U-238 has a zero weight, which would not be the case if it were weighted according to equation (1.4). There is also no allowance in this scheme for negative weights.

1.2.4 Substitutional critical mass weights

Baker and Ross (1963) discovered that the use of weight factors that were proportional to the difference between the reactivity weight of a given plutonium isotope and U-238 resulted in similar values for the critical masses of different

plutonium mixtures. This was used to define the substitutional critical mass weights w_{CM}, which were normalised such that the weight of Pu-239 was equal to 1. The following derivation is based on the one given in Salvatores (1986). In a simplified model of a system fuelled with Pu-239 and U-238, the neutron balance can be written as

$$N_{28}\left(\nu\sigma_f - \sigma_a\right)_{28} + N_{49}\left(\nu\sigma_f - \sigma_a\right)_{49} = DB_m^2 + \Sigma_c \tag{1.5}$$

where D is the diffusion coefficient, B_m^2 is the fixed material buckling and Σ_c represents neutron capture in structural materials. For a similar system fuelled with a mix of plutonium isotopes, the balance equation becomes

$$N'_{28}\left(\nu\sigma_f - \sigma_a\right)'_{28} + \sum_{\mathrm{Pu}} N'_i\left(\nu\sigma_f - \sigma_a\right)'_i = D'B_m^2 + \Sigma'_c \tag{1.6}$$

Assuming that the differences between the two systems are small, the following approximations can be made

$$D \cong D' \tag{1.7a}$$

$$\Sigma_c \cong \Sigma'_c \tag{1.7b}$$

$$\left(\nu\sigma_f - \sigma_a\right)_i \cong \left(\nu\sigma_f - \sigma_a\right)'_i \tag{1.7c}$$

If the number of actinide atoms in the two systems is taken as equal

$$N_{28} + N_{49} = N'_{28} + \sum_{\mathrm{Pu}} N'_i \tag{1.8}$$

then the values in equations (1.5) and (1.6) can be equated, leading to

$$N_{49}\left(w_\rho^{49} - w_\rho^{28}\right) = \sum_{\mathrm{Pu}} N'_i\left(w_\rho^i - w_\rho^{28}\right) \tag{1.9}$$

This allows the substitutional critical mass weights to be defined as

$$w_{\mathrm{CM}}^i = \frac{w_\rho^i - w_\rho^{28}}{w_\rho^{49} - w_\rho^{28}} \tag{1.10}$$

This weighting can be interpreted as the change in the reactivity weighting if an atom of U-238 is removed and an atom of the nuclide in question is substituted in its place, relative to the change caused by using Pu-239 for the

substitution. It has the desired values of 1 for Pu-239 and 0 for U-238. The derivation is predicated on a plutonium fuelled system and the approximation that the differences between the Pu-239 and plutonium isotope mixture fuelled systems are relatively small. It would of course be possible to perform a similar derivation for e.g. a system operating in the thorium-uranium fuel cycle.

1.2.5 Adjoint weighting

If the adjoint flux (Duderstadt and Hamilton, 1976) in a system is found, it can be used to describe how the reactivity will be affected by changes to the system using perturbation theory. This approach can be used to produce a set of weights with a strong theoretical grounding, and which can be reasonably applied to any nuclide in the system. A brief discussion of this approach will be given here, with the full details available in e.g. Ott and Neuhold (1985).

The neutron multiplication eigenvalue problem for a system is written as

$$(\mathbf{L} - \lambda\mathbf{F})\,\phi = 0 \tag{1.11}$$

If a small change is made to the system, giving a new eigenvalue $\lambda' = \lambda + \Delta\lambda$, the change in the eigenvalue can be found by neglecting terms above first order and using the adjoint flux ϕ^*, avoiding the need to re-calculate the behaviour of the perturbed system. Using $\langle , \rangle$ to represent integration over space, energy, and angle

$$\Delta\lambda = \frac{\langle \phi^*, (\Delta\mathbf{L} - \lambda\Delta\mathbf{F})\,\phi \rangle}{\langle \phi^*, \mathbf{F}\phi \rangle} \tag{1.12}$$

This gives the change in the eigenvalue due to the perturbation. It may be that the change in the reactivity is desired instead, but this is simple to determine as

$$\Delta\rho = -\Delta\lambda = \frac{\langle \phi^*, (\lambda\Delta\mathbf{F} - \Delta\mathbf{L})\,\phi \rangle}{\langle \phi^*, \mathbf{F}\phi \rangle} \tag{1.13}$$

The changes in the operators $\mathbf{L}$ and $\mathbf{F}$ due to a change in the composition $\underline{N}$ can be expressed as

$$\Delta\mathbf{L} = \frac{\partial\mathbf{L}}{\partial\underline{N}}\Delta\underline{N} \tag{1.14a}$$

$$\Delta\mathbf{F} = \frac{\partial\mathbf{F}}{\partial\underline{N}}\Delta\underline{N} \tag{1.14b}$$

Setting the value of $\Delta\underline{N}$ to be one atom of the nuclide of interest gives the weight for that nuclide.

This weighting scheme does not suffer many of the drawbacks associated with the previous ones, in that far fewer approximations are made in its derivation. It can be applied to any nuclide in the system, and allows for both positive and negative contributions. It is significantly more work to arrive at the values produced by this scheme, as both the forward and adjoint eigenvalue problems must be solved.

The weighting schemes described here are concerned with measuring the contribution of a nuclide to the criticality of the system at the current point in time. The changes caused by neutron interactions can alter the contribution of a nuclide, for example the production of Pu-239 from U-238 via neutron capture and two β-decays, or the production of fission product poisons. One measure designed to take account of this effect is the w^* weighting proposed by Ott and Borg (1980), which is discussed further in chapter 2. The effects of transmutation on the nuclide contribution to the criticality will form a major part of the rest of this work.

1.3 Breeding ratio

One of the main purposes of assigning weights to different nuclides, and in particular different plutonium isotopes, was to achieve a good definition of the breeding ratio of a system. The breeding ratio is intended to provide a measure of how much fuel a system creates relative to how much it consumes in the process. A brief overview of the breeding ratio, other similar measures and some of the associated issues will be given here. Several other discussions are available, e.g. Waltar et al. (2012), Adkins (1972), Ott and Borg (1977), Salvatores (1986).

The breeding ratio BR of a system at a point in time can be written as

$$BR = \frac{\text{Fuel production rate}}{\text{Fuel consumption rate}} \tag{1.15}$$

The breeding gain BG represents the production of fuel beyond the amount consumed to produce it, and $BG = BR - 1$. If the breeding ratio is less than 1, it is usually referred to as the conversion ratio CR.

An alternative definition of the breeding ratio was given by Baker and Ross (1963), and is known as the U.K. (or British) definition.

$$BR^{\mathrm{UK}} = \frac{\text{Fuel production rate}}{\text{Total fission rate}} \tag{1.16}$$

The difference between this definition and the previous one centres on the fact that not all the nuclides that fission in a reactor are considered to be fuel. The earlier discussion of nuclide weighting schemes shows that there are many ways to define fuel, and the choice of definition can have a significant effect on the value of the breeding ratio.

1.3.1 Time averaged breeding ratio

It is possible to define a value for the breeding ratio that applies to a period of time instead of a single moment. The most common period used is one burn-up cycle. The time averaged value of BR can be found from integrating the rates in equation (1.15) or (1.16) over the time period in question. For solid fuelled reactors operated in distinct burn-up cycles, with stoppages for un-loading and re-loading, this approach may be more useful than the instantaneous one discussed previously. For reactors operated continuously, with on-line reloading such as CANDU or molten salt designs, the instantaneous method may be more appropriate.

1.3.2 Equilibrium breeding ratio

A reactor that breeds fuel from fertile material and is reloaded with the fuel it has bred will tend towards an equilibrium fuel composition over time (Waltar et al., 2012). The behaviour of the instantaneous breeding ratio will be the same in each equilibrium cycle, and the cycle averaged value will be constant. Given that the fuel composition is the same from one cycle to the next in equilibrium, the fuel isotopes are all being produced and consumed at the same rate. In this situation, the choice of weighting scheme becomes unimportant, as any appropriate measure will give the same value for the cycle averaged breeding ratio.

1.3.3 Doubling time

The doubling time is defined as the time required for a breeder reactor to produce enough fuel to start another reactor of the same type. There is

some ambiguity in this description, and a number of definitions have been put forward, of which 2 (Adkins, 1972) or 3 (Waltar et al., 2012) are accepted as standard measures. The four definitions given here comprise the union of those given in Adkins (1972) and Waltar et al. (2012).

- The **simple reactor** doubling time is defined as the time required for a reactor to produce enough fuel to start another reactor of the same type. No allowance is made for the re-use of the fuel before the loading of the new reactor or for losses or delays in the external fuel cycle.

- The **simple system** doubling time also does not allow for the re-use of the fuel, in the same way as the simple reactor doubling time. It does however allow for delays and losses in the external fuel cycle. This means it will usually be longer than the simple reactor doubling time.

- The **compound reactor** doubling time is calculated assuming additional fuel produced is immediately loaded into a reactor of the same type and used to breed more fuel. This makes the amount of available fuel increase at an exponential rate. The compound reactor doubling time is shorter than the simple reactor doubling time.

- The **compound system** doubling time treats the fuel as being re-used in a reactor of the same type, but after going through the external fuel cycle. This means that the effects of any losses or delays are included in the value. This will make the compound system doubling time longer than the compound reactor doubling time, but shorter than the simple system doubling time.

The doubling time value seen in practice would be unlikely to match that given by any of these definitions. It would likely be somewhere between the values of the simple and compound system doubling times. While fuel is not immediately re-used in a system of the same type, it is re-used in closed fuel cycles in the same reactor, instead of being stored until enough has been built up to fuel an entire new reactor. The doubling time nevertheless provides a measure of the breeding capability of a system that takes account of the fissile inventory required to operate the reactor, and this makes it a useful figure to compare different systems.

1.4 Thesis synopsis

This thesis is focussed on the use of adjoint techniques to quantify the contributions of nuclides to reactor behaviour. The use of these measures to compare different fuel compositions is demonstrated by determining the appropriate reloading composition to produce similar reactor behaviour. The following chapters of this thesis treat specific concepts within the topic of quantifying nuclide contributions to reactor behaviour in detail. The contents of the chapters are:

- Chapter 2 describes an existing model (Ott and Borg, 1980) designed to predict the behaviour of fast reactor fuel cycles. The model is examined in the context of applying it to the fuel measurement topic of this thesis. The theory underlying the model is discussed, and it is extended to treat more isotopes and operate under different constraints. The model is tested on breeder and burner systems and the results are discussed. The effects of fuel cycle schemes such as different feed materials, reprocessing strategies and efficiencies are considered.

- Chapter 3 details a model developed to quantify how the material in a reactor at a given time affects its future behaviour. The theory used to develop the model is described and the model is tested on fast and thermal reactor single pin systems. The reloading problem is solved for different reprocessing strategies and feed materials. The necessity of treating the fuel compound material is shown. A definition of breeding ratio that can be applied to non-equilibrium systems is developed. The model is demonstrated to be applicable to the question of quantifying nuclide contributions to the reactor behaviour.

- Chapter 4 covers the theory and implementation of the coupled depletion perturbation method proposed by Williams (1979). This model is studied as a means of removing an approximation made in the previous chapter, and thereby improving the quality and range of application of the results. The method is tested on both fast and thermal systems, over different burn-up periods. The effects on the model of different responses are also studied. The importance of the coupling and how it relates to the response being studied is examined.

- Chapter 5 applies the coupled depletion perturbation method described in chapter 4 to the problem of waste heat reduction. The waste heat worths of nuclides in fast and thermal systems are studied, considering different decay periods and recycling schemes. Equivalent fuel compositions for different plutonium sources are determined and the effects of the different fuels on the waste heat production are calculated.
- Chapter 6 presents the overall conclusions and recommendations of the thesis. The results obtained are reviewed and the implications discussed. Several paths for future research are suggested.

Chapter 2

The Continuous Fuel Cycle Model

2.1 Introduction

The behaviour of reactor fuel composition over multiple burn-up cycles is time consuming to calculate. Approximations such as homogenisation allow the time required to be reduced, in some cases by a very large amount. In a reactor that repeatedly recycles its fuel, the composition tends towards an equilibrium value. Changes over any given cycle are relatively small, making the use of a continuous approximation to the discrete burn-up cycles appear favourable. A continuous model of this type was proposed by Ott and co-workers in a series of papers (e.g. Ott and Borg (1980), Maudlin et al. (1979), Ott et al. (1979), Ott et al. (1981), Ott and Borg (1977), Hanan et al. (1978), Borg (1976)), of which the best summary is Ott and Borg (1980). This chapter re-visits that model and tests its applicability to contemporary fuel cycle issues and explores the possibility of extending the model to make it more useful.

The original form of the continuous fuel cycle model is based around a fast breeder reactor operating on the uranium-plutonium fuel cycle. The reactor produces more fuel than it uses during operation and the excess generated is assumed to be loaded into new reactors of the same type. This process is modelled as continuous by allowing for the existence of fractional reactors, of

a size appropriate to the amount of excess fuel at a given time. The model employs the observation that the majority of the plutonium content of a reactor is made up of the isotopes Pu-239 and Pu-240 and these reach their equilibrium behaviour after relatively few cycles of operation. The isotopes Pu-241 and Pu-242 are also included, although they typically take longer to reach equilibrium, they usually make up a smaller but still significant fraction of the fuel. The composition is used along with an appropriately formulated description of the production and loss rates to create a model that can be solved to predict the equilibrium plutonium composition of the reactor and its associated fuel cycle operations. Once the equilibrium composition and behaviour of the reactor have been determined, the results of continuing the operation of the reactor are known.

The model is based on the construction of the production and loss matrix $\mathbf{C}$, which operates on the composition vector $\underline{N}$. Given that the reactor in the model is breeding its own fuel, the composition is driven towards an equilibrium state. The equilibrium composition $\underline{N}^{\infty}$ is then the fundamental eigenvector of the production and loss matrix, and the fundamental eigenvalue is the asymptotic growth rate γ^{∞}.

$$\mathbf{C}\underline{N}^{\infty} = \gamma^{\infty}\underline{N}^{\infty} \tag{2.1}$$

Provided the matrix $\mathbf{C}$ does not change significantly over the life of the reactor, this allows the composition to be predicted without the need for lengthy burn-up modelling. $\mathbf{C}$ is composed of microscopic reaction rates, which are the products of the microscopic cross sections and the flux. These values can be assumed to be constant provided the compositions of the materials in the reactor do not change significantly and no changes are made to the operation of the reactor (e.g. different power levels). The meaning of the asymptotic growth rate can be understood by considering a system of identical reactors. Any excess fuel that is produced is placed in a fractional reactor of the appropriate size for that amount of fuel. Such a system of breeder reactors would grow as time passes, and once the reactors reach the asymptotic fuel composition, the rate of growth will be γ^{∞}. Obviously this is not an entirely realistic representation, but it does provide some valuable insight. The value of γ^{∞} can be determined in a manner unaffected by changes in the fuel composition (see section 2.2) and, as such, provides a fuel independent means of comparing the breeding capabilities of different reactor designs. For a more detailed discussion of this method of describing reactor growth see Ott and Borg (1977).

The original model studies the uranium-plutonium fuel cycle and uses a composition vector comprised of four plutonium isotopes: Pu-239; Pu-240; Pu-241; Pu-242. These are the main constituents of the plutonium in the reactor fuel and the material bred in the blankets. There is no explicit requirement given to restrict the model to these four isotopes however and, with contemporary reactor fuel cycles considering the recycling of minor actinides, it is reasonable to investigate the addition of more nuclides to the model. The continuous model could then be used to predict the asymptotic composition of such fuel cycles, while still maintaining a decrease in computational expense over fully detailed calculations.

Sustainability is a key issue in contemporary power production. It is generally held that to improve sustainability, all available uranium isotopes should be used for power production, rather than only U-235. Achieving this requires transmuting U-238 to Pu-239 via neutron capture and two β-decays. Traditionally this has been done using breeder reactors, typically sodium cooled, whose neutron surplus allows them to produce more fuel than they consume. This is also the original application of the continuous fuel cycle model.

Breeding excess fuel raises the issue of proliferation, particularly as the plutonium bred in such a system can be of very high quality for weapons production. The solution proposed for this problem is the creation of isobreeders: reactors that convert fertile isotopes to fissile ones at the same rate they consume them. This improves the sustainability of such a system, without running the risk of the spread of weapons-grade plutonium. Designing a system that behaves in this manner requires careful study of the fuel cycle over a significant period of time, to ensure that the rates of production and loss of fuel remain equal even as the fuel composition develops.

The gas cooled fast reactor (GFR) is intended to operate in this fashion, with spent fuel being reprocessed and returned to the reactor until all actinides are fissioned. The design of the reactor has not yet been fixed, and changes to the reactor itself or the associated fuel cycle may well affect the long term behaviour of the system. Given the amount of computational effort needed to study the long term behaviour of the fuel cycle, comprised of many detailed burn-up calculations that must be performed sequentially, it is impractical to propagate the effects of every single design change through a full set of burn-up calculations. Applying the continuous model to an isobreeder such as the GFR may allow the behaviour of the fuel to be studied more quickly and easily.

2.2 Theory

This section provides a summary of the theory involved in the continuous fuel cycle model and its extensions. For a more detailed explanation the interested reader can review the references given.

The production and loss matrix is constructed from the microscopic reaction rates of absorption and capture reactions, along with radioactive decay constants. While there are other processes occurring that can produce or remove isotopes, these are comparatively small and can be neglected without producing serious inaccuracies. The main source of production of Pu-239 is neutron capture in U-238, followed by two β-decays. Neutron capture in each plutonium isotope produces the next isotope in the chain. Assuming all captures in U-238 lead immediately to the production of Pu-239, the balance equations for the isotopes in asymptotic operation can be written as:

$$-\left(\lambda_a^8 + \lambda_d^8\right) N_8^\infty + \xi_8^\infty = 0 \tag{2.2a}$$

$$-\left(\lambda_a^i + \lambda_d^i\right) N_i^\infty + \lambda_c^{i-1} N_{i-1}^\infty + \xi_i^\infty - \kappa_i^\infty - \gamma^\infty N_i^\infty = 0 \tag{2.2b}$$

$$i = 9, 0, 1, 2 \tag{2.2c}$$

The indices 8, 9, 0, 1, 2 refer to U-238, Pu-239, Pu-240, Pu-241, Pu-242 respectively. ξ_i is the rate of feed of isotope i and κ_i the rate of removal. λ_a and λ_c represent microscopic reaction rates for absorption and capture respectively, while λ_d is the decay constant. This results in a set of five equations, expressed in seven unknowns $\underline{N}$, ξ and γ.

2.2.1 Constraints

Two further equations can be added to the system as a pair of constraints on the asymptotic core, one on the total number of actinide atoms, equation (2.3), and the other on the reactivity, equation (2.5). This will result in seven equations expressed in seven unknowns.

$$\sum_{i=8}^{2} N_i^\infty = K_N \tag{2.3}$$

Although in a reactor atoms of these isotopes are being lost due to e.g. fission, the continuous model allows their number to be held constant due to its

treatment of unloading and refuelling as continuous processes. All atoms lost by whatever means are replaced and so the total number is a constant, labelled K_N.

Similarly, the reactivity contribution of the isotopes modelled has a constant value, K_ρ. The contribution of each isotope to the reactivity is measured using the reactivity weight, as discussed in Adkins (1972):

$$w_i^\rho = \nu\sigma_{f_i} - \sigma_{a_i} \tag{2.4}$$

The constraint can then be expressed as:

$$\sum_{i=8}^{2} w_i^\rho N_i^\infty = K_\rho \tag{2.5}$$

The value of K_ρ will not be zero, as this constraint only includes the actinide atoms. Other materials in the reactor such as fission products and structural components will have negative reactivity contributions, which need to be compensated for by the inclusion of positive contributions from the actinides.

The two constraints can be combined to remove U-238 from the set of equations being studied, while still describing the production of Pu-239.

$$\frac{1}{K_N}\sum_{8}^{2} N_i^\infty = 1 \tag{2.6}$$

$$\sum_{8}^{2} w_i^\rho N_i^\infty = \frac{K_\rho}{K_N}\sum_{8}^{2} N_i^\infty \tag{2.7}$$

$$\sum_{8}^{2}\left(w_i^\rho - \frac{K_\rho}{K_N}\right) N_i^\infty = \sum_{8}^{2} b_i N_i^\infty = 0 \tag{2.8}$$

Re-arranging as above to obtain a sum over the isotopes that equals zero allows the value of N_8 to be expressed in terms of the plutonium composition.

$$N_8^\infty = \sum_{9}^{2} -\frac{b_i}{b_8} N_i^\infty = \sum_{9}^{2} \beta_i N_i^\infty \tag{2.9}$$

With a little further re-arrangement, an equation that takes the form of a weighted sum over the plutonium isotopes that is equal to unity can be

achieved. This can then be used to make the inhomogeneous terms in the balance equations homogeneous.

$$\sum_{9}^{2} \beta_i N_i^{\infty} + \sum_{9}^{2} N_i^{\infty} = K_N \tag{2.10}$$

$$\sum_{9}^{2} \left(\frac{1+\beta_i}{K_N} \right) N_i^{\infty} = \sum_{9}^{2} d_i N_i^{\infty} = 1 \tag{2.11}$$

The production of Pu-239 from U-238 can now be described in terms of β_i and a sum over the four plutonium isotopes. The balance equations for the plutonium isotopes can be written:

$$-\left(\lambda_a^9 + \lambda_d^9\right) N_9^{\infty} + \lambda_c^8 \sum_{9}^{2} \beta_i N_i^{\infty} + (\xi_9 - \kappa_9) \sum_{9}^{2} d_i N_i^{\infty} = \gamma^{\infty} N_9^{\infty} \tag{2.12a}$$

$$-\left(\lambda_a^i + \lambda_d^i\right) N_i^{\infty} + \lambda_c^{i-1} N_{i-1}^{\infty} + (\xi_i - \kappa_i) \sum_{9}^{2} d_i N_i^{\infty} = \gamma^{\infty} N_i^{\infty} \tag{2.12b}$$

This formulation is slightly different to that used in Ott and Borg (1980), but it is felt to be clearer. The feed and removal terms have been left separate and explicit, where in the original they were combined, and similarly the neutron absorption and decay terms have been kept separate. The homogeneous equations given above can now be written in the form of equation (2.1).

2.2.2 Isotopic Breeding Worths

The adjoint fuel cycle problem can be obtained from the eigenvalue equation.

$$\mathbf{C}^* \underline{w}^* = \gamma^{\infty} \underline{w}^* \tag{2.13}$$

The fundamental eigenvector of this equation is composed of the isotopic breeding worths. These can be understood as representing the fuel importance for breeding, meaning the contribution of an isotope to the asymptotic critical mass (Hanan et al., 1978).

The breeding worths can also be used in calculating the asymptotic growth rate of the system.

$$\gamma^{\infty} = \frac{(\underline{w}^*, \mathbf{C}\underline{N})}{(\underline{w}^*, \underline{N})} \tag{2.14}$$

Using these values as weight factors allows the asymptotic growth rate to be determined without knowing the asymptotic composition. Using this expression produces a value for the asymptotic growth rate which is stationary to perturbations to the composition (Ott and Borg, 1977).

2.2.3 Additional Nuclides

It is straightforward to extend the composition vector to include plutonium isotopes above Pu-242. The form of the balance equations remains the same. Once elements other than plutonium are considered however, a few extra changes are necessary. Here the effects of including Am-241 will be considered, as it is close to the plutonium isotopes already included in both atomic and mass numbers, is typically the most populous isotope of americium, and provides a good illustration of the changes necessary to include other isotopes in the system.

The main issue in the inclusion of Am-241 is the production path, as it is not a result of neutron capture in lower isotopes, but rather of β-decay of Pu-241. The existing set of equations allows for decay as a loss mechanism, but not for production (beyond the special case of neutron capture in U-238 producing Pu-239). The balance equation must be adjusted to reflect this. The index 51 will be used to refer to Am-241 in the equations.

$$-\left(\lambda_a^{51}+\lambda_d^{51}\right)N_{51}^{\infty}+\lambda_d^1 N_1^{\infty}+\left(\xi_{51}^{\infty}-\kappa_{51}^{\infty}\right)\sum_i d_i N_i^{\infty}=\gamma^{\infty}N_{51}^{\infty} \tag{2.15}$$

It is assumed here that americium is being recycled alongside plutonium, leading to asymptotic growth of the americium content of the fuel.

A generic form of the balance equation for the various nuclides can be written, which covers all possible production paths, rather than simply neutron capture.

$$-\left(\lambda_a^i+\lambda_d^i\right)N_i^{\infty}+\sum_{j\neq i}\lambda_{j\to i}^j N_j^{\infty}+\left(\xi_i^{\infty}-\kappa_i^{\infty}\right)\sum_k d_k N_k^{\infty}=\gamma^{\infty}N_i^{\infty} \tag{2.16}$$

i is the index of the nuclide in question, j represents any nuclide except i, and k all nuclides in the composition vector.

2.2.4 Constant Power Constraint

It can be assumed that the power produced by a given reactor core will be held constant. This should be true not only in asymptotic operation, but throughout the life of the reactor. This is true for both the physical reality and the continuous approximation, unlike the two constraints in the original model, which can only be considered accurate in the asymptotic phase of the continuous description. It can be expressed relatively easily in terms of the microscopic fission reaction rate λ_f^i and the power produced per fission q_i.

$$\sum_i q_i \lambda_f^i N_i = K_Q \tag{2.17}$$

Other constraints can also be envisaged, for example neglecting the differences in the power per fission term to produce a fission rate constraint, or looking at the mass of actinides in the core to give an actinide mass constraint. In each case, the most useful expression gives the value of the constraint in terms of a sum over all the nuclides in the model. Exchanging one of the existing constraints with a new one leads to different forms of d_i and β_i. For two generic constraints, labelled A and B, the derivation would be:

$$\sum_i w_i^A N_i^\infty = K_A \tag{2.18a}$$

$$\sum_i w_i^B N_i^\infty = K_B \tag{2.18b}$$

$$\frac{1}{K_A} \sum_i w_i^A N_i^\infty = 1 \tag{2.19}$$

$$\sum_i w_i^B N_i^\infty - \frac{K_B}{K_A} \sum_i w_i^A N_i^\infty = 0 \tag{2.20}$$

$$\sum_i \left(w_i^B - w_i^A \frac{K_B}{K_A} \right) N_i^\infty = \sum_i b_i N_i^\infty = 0 \tag{2.21}$$

$$N_8^\infty = \sum_{i'} -\frac{b_{i'}}{b_8} N_{i'}^\infty = \sum_{i'} \beta_{i'} N_{i'}^\infty \tag{2.22}$$

$$\sum_{i'} \left(\frac{1+\beta_i}{K_N} \right) N_{i'}^\infty = \sum_{i'} d_{i'} N_{i'}^\infty = 1 \tag{2.23}$$

i' is used here to represent the full set of nuclides except for U-238.

2.3 Reactor Models

It is necessary to compare results from the continuous model to those of full burn-up calculations in order to determine their accuracy. The values used in the continuous model must also be obtained from reactor models. In order to test the continuous model in different reactor scenarios, two models were used, one of a sodium cooled breeder reactor, and the other of a gas cooled fast reactor, intended to operate as an isobreeder.

The models of both systems were created using the SCALE code package (SCALE manual, 2009). The TRITON module of the code was used for burn-up calculations. Where necessary, ex-core decay was determined using the ORIGEN module of the same code.

2.3.1 Sodium Cooled Breeder Reactor

A simplified model of a sodium cooled fast reactor (SFR) was used to test the initial implementation of the continuous model and the additional versions with extra nuclides and different constraints. The model was based on that used by Borg (1976), and is a 1000 MWe oxide fuelled breeder reactor. The reactor is divided into 6 regions, two representing the inner and outer core, two the axial blanket and two the radial blanket. These are surrounded by a steel reflector. The central core was initially loaded with 13.7% Pu-239. The outer core was initially loaded with 15.5% Pu-239. The blankets were started with natural uranium.

2.3.2 Gas Cooled Fast Reactor

The reactor model used for the GFR was based on the design detailed in Girardin et al. (2008). The fuel, clad and coolant within each sub-assembly were homogenised. It was not deemed necessary to use a fully accurate description of the reactor, as the purpose of this work is to investigate the applicability of the continuous model rather than fully detail the long-term composition behaviour of a reactor design.

2.3.3 Reprocessing and Reloading

Reprocessing and reloading of the reactors were assumed to occur instantaneously. In the case of the SFR, the blankets were removed and reprocessed at

the end of each cycle. Fresh blankets were loaded containing only feed material, in the same quantity as used in the previous cycle. Determining the new composition of each core material was more complicated. The constraints from the continuous model were used in calculating the amount of feed material to be added to the reprocessed material to make new fuel. It was assumed that an infinite supply of the feed in question was available, and that the composition of the reprocessed material was not affected by the reprocessing procedure. The feed and reprocessed materials were mixed to produce a new material that had the same number of atoms and reactivity contributions as the one it was replacing.

$$\begin{aligned} F + R &= N \\ w_F^\rho F + w_R^\rho R &= w_N^\rho N \end{aligned} \tag{2.24}$$

F is the amount in atoms of feed material used, R the amount of reprocessed material and N the amount of material used in the reactor in the previous cycle. The reactivity weights are written as w^ρ, and are determined as shown in equation (2.4). The values of F and R can be determined from these equations, allowing the new composition to be found. The growth rate of the reactor was also found using this process, dividing the amount of available reprocessed material by the value of R to determine the number of cores that can be fuelled. Thirty cycles of burn-up calculations were carried out for each set of results. After this number of calculations, asymptotic behaviour is usually well established and there is little to be gained from further modelling. In the case where a different constraint was used in the continuous model, the reloading calculation was changed to use the new constraint also.

Reprocessing losses were modelled in a straightforward fashion. Once the amount of reprocessed material had been determined, a percentage amount equal to the loss factor being used in the model was subtracted. Losses were assumed to occur to all isotopes equally, leaving the composition unchanged and affecting only the total amount of material available.

Values for the actinide waste production by the system were obtained by reading the end of cycle composition from the TRITON output and tracking the amount of material that was not recycled. This was passed into ORIGEN for a decay calculation of the same length as the reactor burn-up cycle. After this, the waste produced in the new cycle was added to that already being modelled. This process was repeated over the full 30 cycles. The production of waste was only followed for Pu, Np, Am and Cm, meaning that the curium

recycling strategy effectively produced no waste. For the models that did produce waste, the mass lost to the waste stream could be replaced by feed material. The loss of reactivity cannot be made up in this fashion however. While this is not an entirely realistic model, it allows the waste production of each reprocessing strategy to be compared.

2.4 Breeder Reactor Results

2.4.1 Composition Evolution

The predictions from the continuous model were compared to the results of the TRITON calculations. The evolution of the fuel composition over the burn-up calculations is shown in figure 2.1. The dashed lines give the average values over each cycle. These results show that, as expected, the fuel composition did tend towards an equilibrium value, and that this state is reached within a realistic number of cycles.

It is evident that as the composition changes, the cross sections and fluxes in the reactor will change, affecting the production and loss matrix. This in turn will affect the predictions of the equilibrium composition from the continuous model. Figure 2.2 shows how the prediction of the equilibrium composition from the continuous model changes over thirty cycles, with the values given in relative terms to those of the thirtieth cycle. The values from the continuous model are compared to those from the TRITON calculations in figure 2.3. The results have been normalised to the value at the end of the thirtieth cycle of TRITON calculations to allow for a good comparison.

Figure 2.2 shows that the predictions changed over the cycles, starting off with some significant differences to the final value, and tending towards it. The accuracy of the prediction also appears to be related to the atomic mass of the isotope in question, with the values for Pu-239 being quite accurate throughout and those for Pu-242 starting off considerably different to the final value. The predictions do not move smoothly towards their final value, this is caused by statistical variations in the TRITON results, due to the use of Monte Carlo methods to determine the flux in the core. The initial value for Pu-239 is closer to the equilibrium value than those of the other isotopes, and this initial effect is less pronounced for that isotope.

The comparison of the predicted values to those seen during the evolution

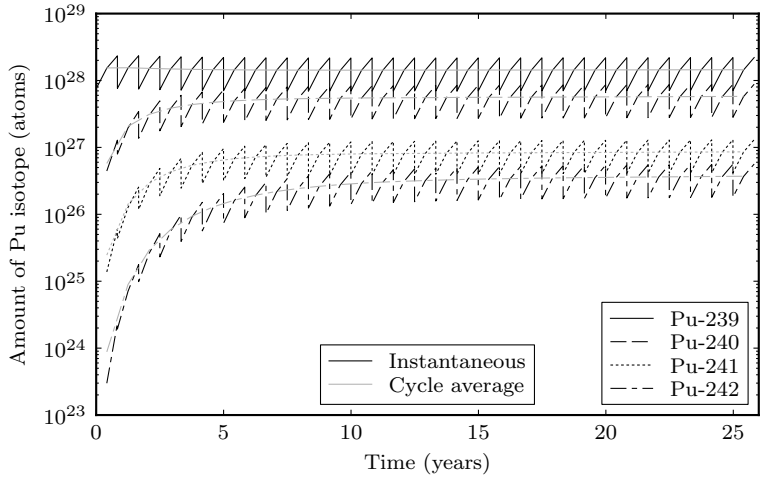

Figure 2.1: Evolution of plutonium composition over 30 cycles comparing values throughout the cycle with cycle averages

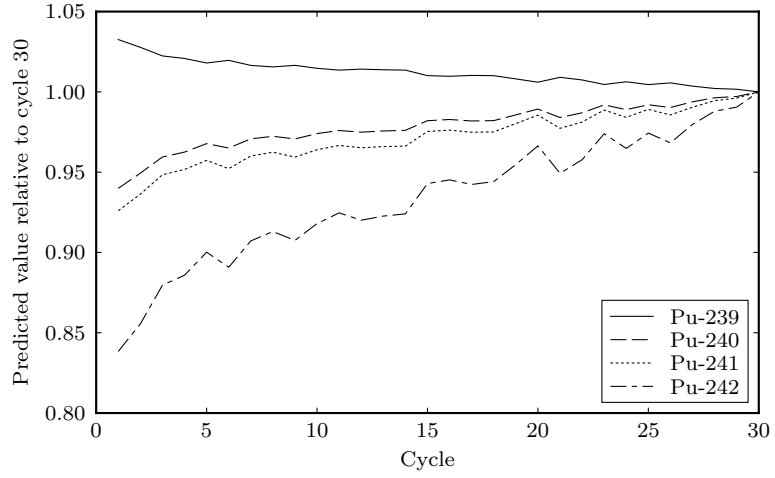

Figure 2.2: Continuous model predictions of equilibrium composition relative to the value at cycle 30

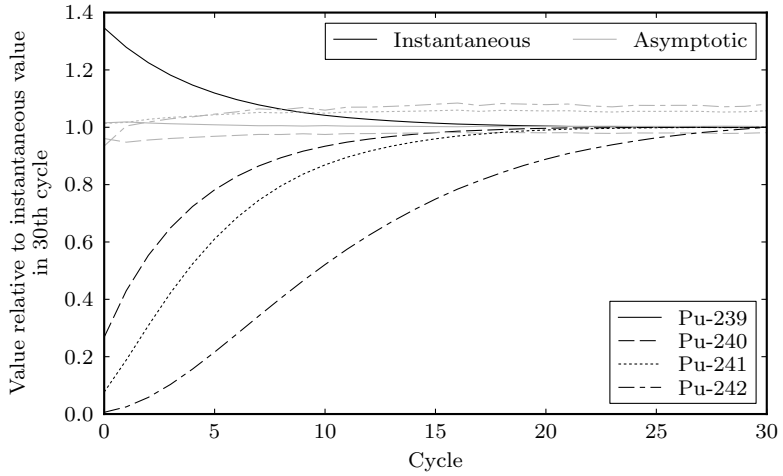

Figure 2.3: Comparison of composition and predicted values for asymptotic composition relative to the value at the 30th cycle

of the fuel in figure 2.3 shows that the predictions are quite accurate. The actual fuel composition tended towards that predicted and appeared to stabilise around those values. The statistical variations seen in figure 2.2 are not visible here, due to the different scale of the y-axis.

2.4.2 System Growth Rate

The growth rate of the system as a whole can also be predicted from the continuous model and compared to that seen in the TRITON calculations. The burn-up model showed the system moving towards an asymptotic composition, eventually increasing the amount of each nuclide at the same rate. Figure 2.4 shows the asymptotic growth of each isotope and how the different isotopes tend towards the same growth rate with time. The more populous ones reach the asymptotic rate sooner than the less populous ones. The equilibrium composition is clearly established within the thirty cycles studied.

The growth rate of the system can be found from the eigenvalue problem. In combination with the isotopic breeding worths from the adjoint problem, it is possible to predict the asymptotic growth rate using a non-asymptotic

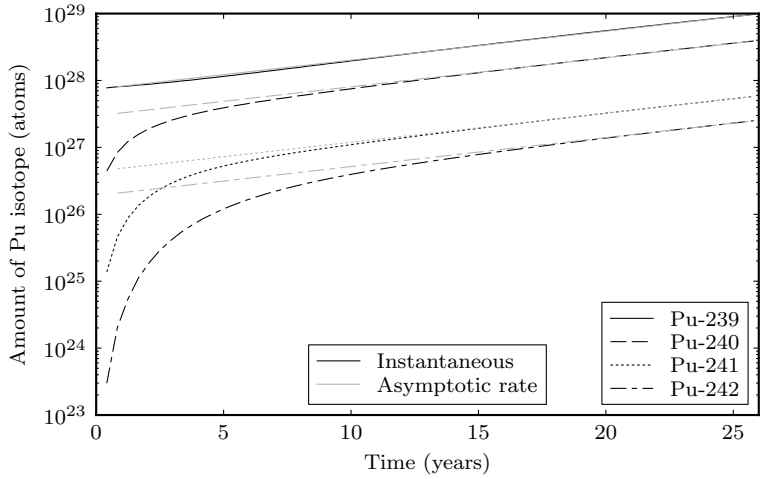

Figure 2.4: Evolution of plutonium inventory in a system of breeder reactors

fuel composition. A comparison of the predicted asymptotic growth rates from each cycle and the growth rate seen in that cycle is shown in figure 2.5.

Initially the instantaneous and predicted asymptotic rates are significantly different. The system moves towards asymptotic behaviour with time and the difference decreases as the asymptotic prediction stabilises and the instantaneous value tends towards the true asymptotic value. It can be seen that after a number of cycles the asymptotic growth rate prediction stays relatively stable. The value found is close to that seen in the instantaneous case for the thirtieth cycle. The prediction does not improve further with time however.

2.4.3 Isotopic Breeding Worths

The isotopic breeding worths were found from the continuous model for each of the thirty cycles modelled. The results are shown in figure 2.6. The values are normalised so that the value for Pu-239 is one, meaning it remains constant across all cycles. The figure shows that the worths change significantly in the earliest cycles, but as the system moves towards asymptotic operation the worths tend towards constant values. Pu-241 has the highest worth, slightly above that of Pu-239, which is to be expected given the fission cross sections

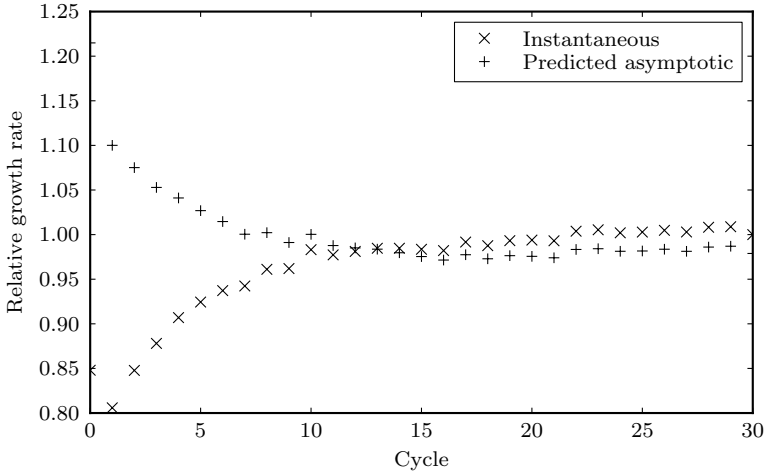

Figure 2.5: Comparison of instantaneous and predicted asymptotic growth rates relative to the 30th cycle instantaneous value

of these isotopes. Pu-240 has a much higher worth than Pu-242, which stems from its role in the production of Pu-241, allowing it to contribute to the future criticality of the system.

2.4.4 Additional Nuclides

The isotope Am-241 was added to the system described by the continuous model in order to test how easily the system could be extended. This isotope was chosen as it is a significant concern in the fuel cycle, due to its relatively fast production from the decay of Pu-241. Only one isotope was added in order to provide a straightforward test of extending the nuclide vector and so that the effects due to the additional isotope can be seen clearly from a comparison to the previous results. A set of TRITON calculations in which plutonium and americium were recycled was also performed. The values from these calculations were compared to the predictions from the continuous model. The composition predictions over thirty cycles are shown in figure 2.7.

The predictions of the asymptotic composition remain fairly constant throughout the thirty cycles. The results for plutonium isotopes were quite good,

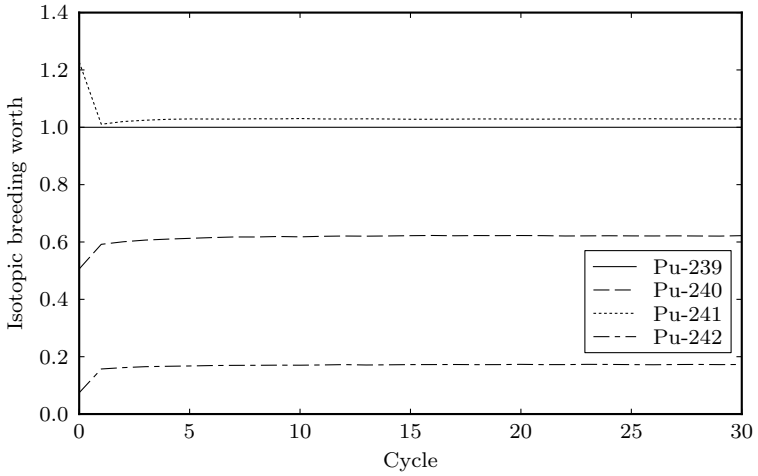

Figure 2.6: Evolution of isotopic breeding worths over 30 cycles

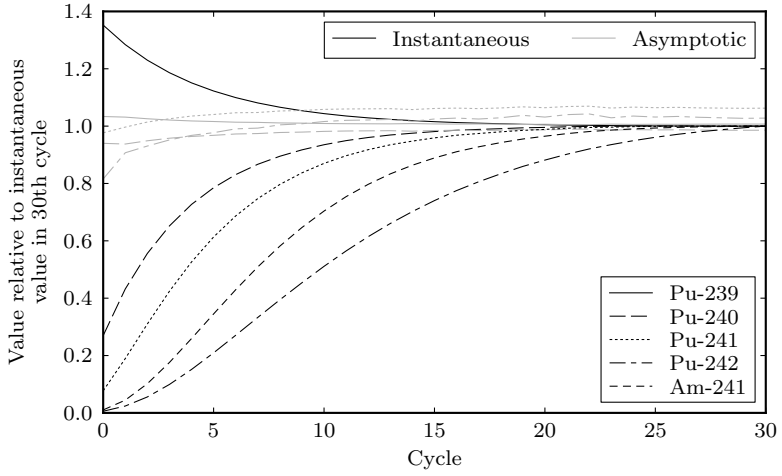

Figure 2.7: Evolution of composition and predictions of asymptotic composition including Am-241 (the asymptotic Am-241 value cannot be seen due to the large difference between it and the instantaneous value)

differing from the values of the thirtieth cycle by a few percent at most. The results for americium were significantly worse, with the prediction from the thirtieth cycle being $3.7\times10^{-6}\%$ compared to the actual figure of $3.9\times10^{-3}\%$, a difference large enough that the asymptotic prediction cannot be seen in figure 2.7. This may be due to the model not including pathways for the production of Am-241 such as neutron capture in Am-240 or electron capture in Cm-241, although the main route of production via the decay of Pu-241 was present. Without usable values for Am-241, there was little point in including higher isotopes, as the incorrect value would have had a knock-on effect.

2.4.5 Constant Power Constraint

The two constraint equations play an important role in the set-up of the continuous model. The power produced by a core will be held constant during operation, so this constraint applies even during the transition phase of the reactor's life, while the actinide number and reactivity constraints only apply once in asymptotic operation. The constant power constraint was substituted into the continuous model in place of the reactivity constraint. This new model was used to predict the asymptotic composition of the fuel from thirty cycles of calculations of a plutonium recycling system with a pure U-238 feed. The TRITON code uses a constant power approximation in its calculations, so no changes were required to model this.

The two sets of results were very similar, differing only slightly for the first few cycles and being in close agreement thereafter. While this means the constant power constraint may be used in the model without negatively affecting the results, there is also no improvement in their quality. It is possible that if the reloading of the TRITON model was not determined using the reactivity constraint, the constant power constraint would have a more pronounced effect.

2.5 Isobreeder Results

Having tested the continuous model with a breeder reactor, as in its original formulation, it was then used to predict the behaviour of the gas cooled fast reactor described in section 2.3.2. The intention was to see how well the continuous model could be used with an isobreeder system. Determining the reloading of the GFR model in the manner previously described however did

not lead to isobreeder behaviour. The constraints from the continuous model were used unchanged in order to give an accurate comparison between the results from TRITON and the continuous model. Although the model was started assuming one reactor, fractions of reactors were not modelled as the system decreased in size. A whole core was studied in each cycle and the resulting material balance was multiplied by the appropriate quantity.

2.5.1 Recycling Additional Actinides

Several modelling runs were carried out with different actinide recycling behaviour. The default for comparison is recycling only plutonium. Three further sets of calculations were performed for reactors recycling additional actinides. Each scheme is referred to by the recycled isotope that distinguishes it from the previous one, given in brackets in the list below.

1. Plutonium (Pu)
2. Plutonium, neptunium (Np)
3. Plutonium, neptunium, americium (Am)
4. Plutonium, neptunium, americium, curium (Cm)

Recycling of fission products was not considered, as they are not taken into account in the continuous model. The recycling of uranium was also not considered, as an effectively infinite supply of uranium feed material is assumed. In addition, no isotopic separation was considered in the recycling calculations. The results of these calculations are shown in table 2.1. The Pu-239 row, for example, shows that as more actinides are recycled, the amount of Pu-239 in the fuel at the end of the 30th cycle decreases, although it remains the most populous isotope of those studied. The recycling of additional actinides shifts the fuel composition away from plutonium and towards the higher actinides, as would be expected. The higher amounts of Pu-238 present as more actinides are recycled are a result of α-decay from Cm-242. The recycling of neptunium has a relatively small effect on the fuel composition, due to the small amount of neptunium seen in the system. Reprocessing americium has a larger effect, more than doubling the amount of Am-241 and Am-243 seen in the fuel. Reprocessing curium has a small effect on the fuel composition, although any significant amount of curium in the fuel raises questions about

Table 2.1: Percentage atomic composition of fuel at end of 30th cycle

Element	Isotope	Reprocessing strategy			
		Pu	Np	Am	Cm
Pu	238	0.4445	0.6775	1.8927	1.9795
	239	46.397	46.387	43.481	43.554
	240	39.844	39.587	37.731	36.929
	241	5.8853	5.8348	5.4969	5.3483
	242	5.3304	5.2552	6.0544	5.5021
	243	0.0001	0.0001	0.0001	0.0001
	244	0.0006	0.0006	0.0006	0.0006
Np	237	0.1431	0.3247	0.3372	0.3343
	238	0.0001	0.0003	0.0003	0.0003
	239	0.0566	0.0562	0.0500	0.0508
Am	241	1.0398	1.0317	2.1873	2.0799
	242	0.0003	0.0003	0.0006	0.0006
	242m	0.0211	0.0208	0.1060	0.0997
	243	0.6182	0.6092	1.7813	1.5975
Cm	242	0.0549	0.0543	0.1231	0.1177
	243	0.0026	0.0025	0.0086	0.0135
	244	0.1482	0.1452	0.6772	1.5762
	245	0.0109	0.0106	0.0639	0.3917
	246	0.0005	0.0005	0.0039	0.2976
	247	0.0000	0.0000	0.0002	0.0572
	248	0.0000	0.0000	0.0000	0.0658

fuel manufacturing due to the issues of neutron radiation and heat production (Pillon et al., 2003).

The waste produced during operation of the Pu, Np and Am strategies is shown in table 2.2. The Cm strategy is not shown, as it effectively produces no waste, as described earlier. The results show that the recycling of additional actinides decreases the amount of waste produced, but at the cost of the creation of larger amounts of higher actinides such as curium. This can be seen clearly in the americium recycling strategy, which results in much larger amounts of all the curium isotopes.

The radiotoxicity of the waste resulting from the different strategies over time was calculated using the values in ICRP (1994) and is shown in figure 2.8. There is very little difference between the Pu and Np strategies, the radiotoxicity of the Np strategy waste is slightly lower than that of the Pu strategy waste, but they behave in very much the same fashion as the waste decays. The waste from the Am strategy has a lower radiotoxicity than the other two at all times, although the difference is small in some places. The Am strategy produces significantly less waste than the Pu or Np strategies, although it has a higher curium content, which forms an important part of the radiotoxicity. The results show that the reduction in the amount of waste is more than enough to offset the high radiotoxicity per atom of the waste that is produced.

The growth rate of the system is also affected by altering the recycling strategy. The effects of these changes are shown in figure 2.9. The difference from recycling neptunium alongside plutonium is relatively small, due to the minimal amount of neptunium in the system. Once americium was included the system growth rate decreased. The majority of the americium was in the forms of Am-241 and Am-243, which have negative weights in the reactivity constraint equation, leading to the decrease in the number of reactors in the system. Curium has a large positive weight, and moved the system back to higher numbers than those seen for plutonium recycling alone.

2.5.2 Effects of Different Feed Materials

There are a number of materials that can be used to replace actinide atoms removed from the system by fission or reprocessing. The original continuous model considered a feed of pure U-238, neglecting the effects of other isotopes

Table 2.2: Amounts of waste (kg) after 30 cycles of operation with different recycling strategies

Element	Isotope	Reprocessing strategy		
		Pu	Np	Am
Th	230	0.0027	0.0027	0.0054
U	233	0.0043	0.0017	0.0000
	234	18.720	18.390	38.550
	235	0.0928	0.0073	0.0068
	236	0.5665	0.5612	2.5660
	238	0.0001	0.0001	0.0000
Np	237	216.28	107.10	0.0105
	238	0.0042	0.0000	0.0000
	239	2.0157	0.0004	0.0000
Pu	238	25.360	24.610	51.540
	239	41.960	4.8610	4.1670
	240	82.130	80.400	405.70
	241	0.0086	0.0084	0.0570
	242	0.9431	0.9301	0.0192
Am	241	876.91	860.66	0.1624
	242	0.0132	0.0132	0.0000
	242m	12.368	12.066	0.0000
	243	511.64	501.19	0.0102
	244	0.0003	0.0003	0.0000
	244m	0.0002	0.0002	0.0000
Cm	242	2.3592	2.3483	5.7495
	243	0.4336	0.4180	1.5332
	244	15.902	15.372	88.455
	245	5.9579	5.8195	40.004
	246	0.2163	0.2117	1.8552
	247	0.0061	0.0060	0.0609
	248	0.0002	0.0002	0.0019
Total		1813.9	1635.0	640.45

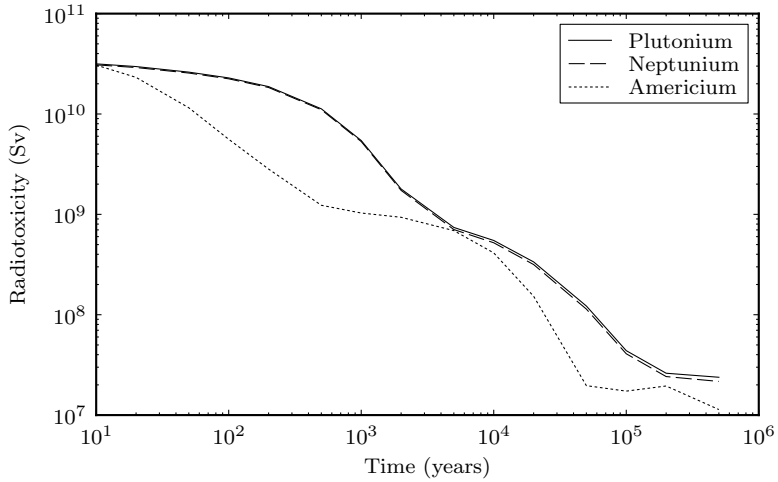

Figure 2.8: Radiotoxicity of waste produced by 30 cycles of operation with different recycling strategies

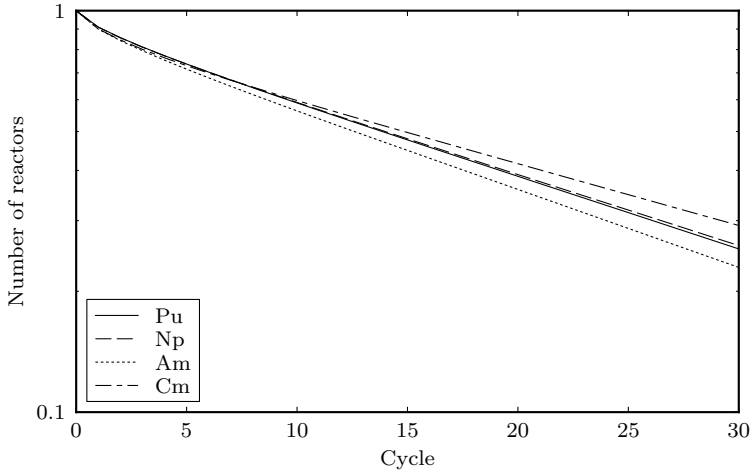

Figure 2.9: Changes to system growth rate with recycling of additional elements

Table 2.3: Feed material compositions

Feed	Label	Composition	
Uranium 238	U8	U-238	100%
Depleted uranium	DU	U-235	0.25%
		U-238	99.75%
Natural uranium	NU	U-234	0.005%
		U-235	0.711%
		U-238	99.284%

such as U-234 and U-235. The effects of depleted and natural uranium feeds are also considered here. Other feed materials such as LWR spent fuel are not investigated, although this work may be carried out in the future.

While the differences in the compositions of the three feeds are small, the addition of fissile material in the form of U-235 is a serious consideration. The proliferation resistance of the design may be affected if switching from depleted to natural uranium feed leads to the production of excess plutonium. The extra fissile material can also affect the composition of material produced over many cycles of the core. The plutonium compositions seen after 30 cycles of the different feeds detailed in table 2.3 are given in table 2.4.

The increased amounts of U-234 and U-235 in the feed slightly alter the balance of the plutonium composition over the course of many cycles. With the move from pure U-238 to depleted uranium and then to natural uranium, the Pu-239 content of the fuel increased. The amounts of the other three plutonium isotopes all decreased, by a larger amount following the change from depleted to natural uranium than from U-238 to depleted uranium. The larger difference between the compositions of these feed materials appears to be the reason for this. In particular the additional U-235 in the feed material means the feed has a higher reactivity contribution and less plutonium is required. The lower amount of plutonium in the fuel means less of each higher isotope is produced. The growth rate of the system was also affected by the different feeds. The behaviour is shown in figure 2.10. The changes are relatively straightforward, with the inclusion of greater amounts of fissile material in the form of U-235 making it possible to run a larger number of reactors.

Table 2.4: Plutonium composition after 30 cycles with different feed materials

Feed	Plutonium composition (%)			
	Pu-239	Pu-240	Pu-241	Pu-242
U8	47.608	40.884	6.0388	5.4694
DU	48.263	40.504	5.9717	5.2615
NU	49.432	39.820	5.8452	4.9027

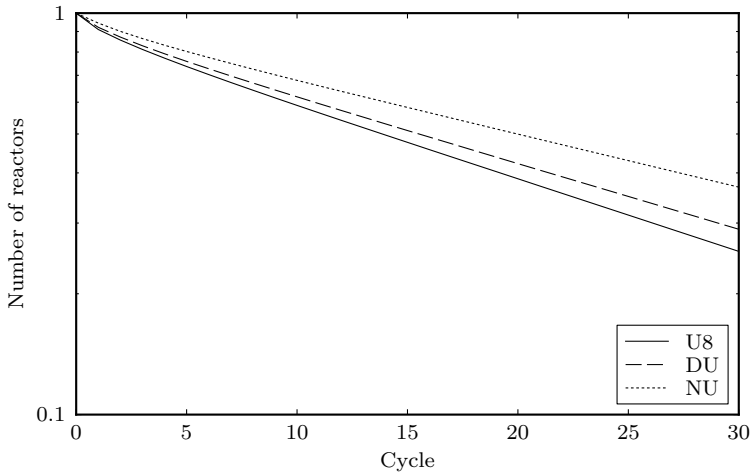

Figure 2.10: Changes to system growth with different feed materials

2.5.3 Effects of Reprocessing Losses

The impacts of reprocessing losses on the behaviour of the GFR were also studied. Losses of 0.1%, 1% and 10% were model led for a plutonium recycling system (PUREX can achieve 99.9% separation of uranium and plutonium, while the figure is lower for other, less developed processes (Silverio and de Queiroz Lamas, 2011)). All isotopes were assumed to be subject to equal loss rates as their chemical behaviours were considered to be identical.

The main impact of these losses was on the growth rate of the system. Given that each plutonium isotope was lost at the same rate, the decreased amount

Table 2.5: Fraction of original reactors that can be refuelled after initial cycle at different reprocessing losses

Loss rate (%)	Fraction of reactors refuelled
0	0.9104
0.1	0.9095
1	0.9013
10	0.8193

of fuel served only to decrease the number of reactors that could be fuelled with that material. This in turn reduces the growth rate of the system. These results can be seen in table 2.5.

2.5.4 Continuous Model Results

Applying the continuous model to the results produced by the TRITON calculations allows the efficacy of the model to be determined. The values for the model, such as the microscopic reaction rates, were found from the TRITON output files. There are three key results produced by the continuous model: asymptotic composition prediction; asymptotic growth rate; isotopic breeding worths.

Asymptotic composition prediction

The asymptotic composition was predicted from the fundamental eigenvector of the production and loss matrix that describes the system. Values for the elements of the production and loss matrix can be determined from any of the TRITON calculations. Values from the later cycles will of course be closer to those of the asymptotic state, so can be expected to produce better results.

Figure 2.11 shows how the plutonium composition of the reactor fuel changes over 30 cycles, using the model of a plutonium recycling, U-238 fed reactor. It also gives the predictions of the asymptotic composition from each of those cycles. It can be seen that the prediction of the asymptotic composition does not change greatly after the first ten cycles. This means only a few cycles worth of calculations are necessary to produce a prediction that is unlikely to improve further. The accuracy of the prediction is good for Pu-239, but worse

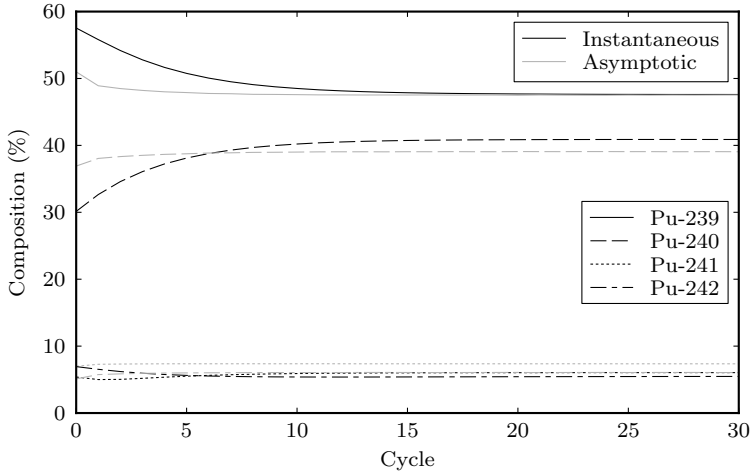

Figure 2.11: Composition evolution and asymptotic predictions over 30 cycles

for the other three plutonium isotopes. The errors are of a few percent on each of the isotopes.

The other fuel cycle strategies described earlier in this chapter were also examined with the continuous model. The results were very similar to those above in all cases, with the continuous model producing poor predictions of the behaviour of the isobreeder-style system. This suggests that the accuracy of the values found is either inherent in the model or a result of applying it to a system with the negative growth seen here. Given that the model provided reasonable results when applied to a breeder reactor as described earlier, it is more likely the problem comes from applying the method to negative growth systems.

Asymptotic growth rate

The fundamental eigenvalue of the production and loss matrix problem predicts the asymptotic growth rate of the system. This prediction can be compared to the growth rate of the system at any time after asymptotic operation has been reached. Once again the true values and the predicted asymptotic values have been calculated and compared, shown in figure 2.12.

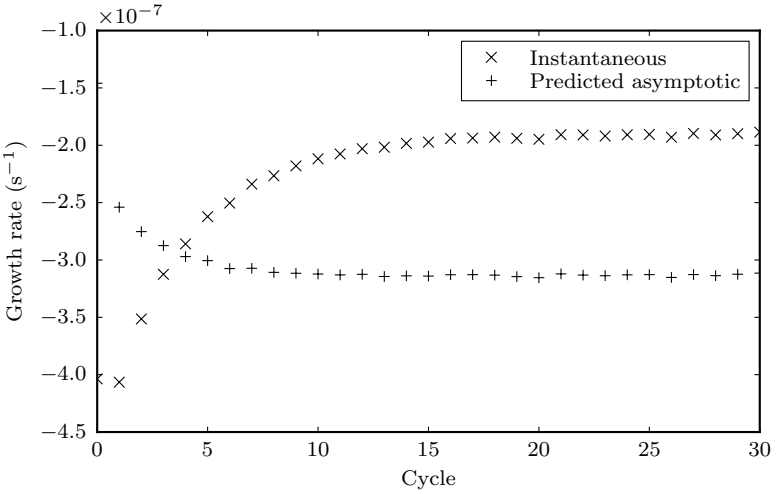

Figure 2.12: Instantaneous growth rate and asymptotic prediction over 30 cycles relative to instantaneous value in the 30th cycle

The predictions of the asymptotic growth rate were quite poor, in the same manner as the composition prediction. This pattern was seen for all variations of the GFR fuel cycle studied.

Isotopic breeding worths

The isotopic breeding worths are found from the fundamental eigenvector of the adjoint problem of the continuous model. They can be used to evaluate the importance of a given isotope to the asymptotic criticality (Hanan et al., 1978). They are normalised such that the value for Pu-239 from the thirtieth cycle is one.

The values of the isotopic breeding worths for the default fuel cycle strategy are shown in figure 2.13. The values reached a constant level after only a few cycles. Pu-239 and Pu-241 have very similar values. These isotopes are well known as having a positive contribution to the criticality of a core. Pu-241 is usually described as more reactive than Pu-239, here the values are similar because the continuous model describes how the nuclide will contribute to the reactivity in the future, rather than at the present moment. Neutron capture

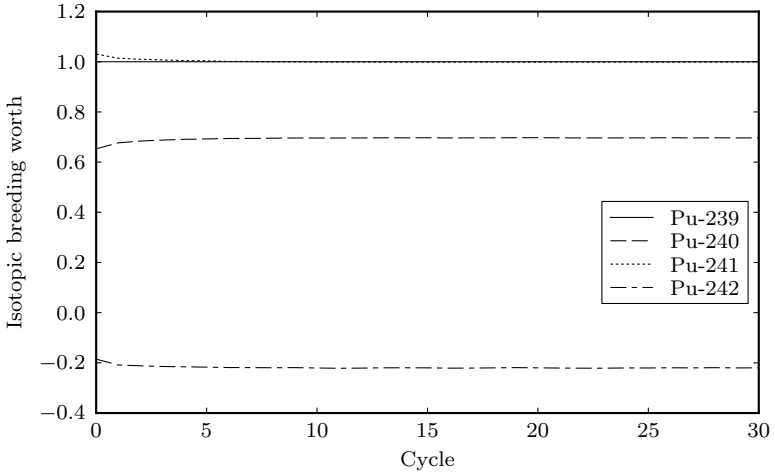

Figure 2.13: Evolution of isotopic breeding worths over 30 cycles

in Pu-239 is still likely to lead to a positive contribution, given that Pu-240 can become Pu-241 with relative ease. Neutron capture in Pu-241 does not show this style of behaviour, so the contribution would be lower than that seen from a simple consideration of criticality. Further, Pu-241 decays to Am-241, which tends to have a low reactivity weighting, lowering the value of Pu-241. The value for Pu-240 is higher than it would be as an instantaneous value, reflecting this ability to produce Pu-241. The negative value for Pu-242 stems from its low contribution to the criticality of the core and the low chance of it producing an isotope that does contribute.

2.6 Conclusions

The continuous model was used in the study of fuel cycles of fast breeder reactors. The approximations made allowed values such as the asymptotic composition to be estimated without the use of a full burn-up study. The values found for the asymptotic composition are a reasonable estimate when compared to those from full burn-up calculations. They are not completely accurate however, and cannot replace detailed analysis when precise values are required. The predictions of the rate at which the system expands asymptotically (γ^{∞})

are of similar accuracy as the composition predictions, but are subject to the same caveats.

Extending the model by including Am-241 gave inaccurate results for the extra nuclide. The accuracy of the predictions of the plutonium composition remained unchanged. The values found for the americium were much worse and cannot be considered useful. It is possible this is due to some of the production and loss paths for this isotope (e.g. production from Cm-241) not being included in the model. This is difficult to check however, as it would mean including additional nuclides, which would then have further production and loss paths that would need to be included, compounding the problem.

The inclusion of the constant power constraint in place of the reactivity constraint had little effect on the quality of the results. While this means there is no issue preventing the use of the constant power constraint, there is also little to be gained. Possibly a system with larger shifts in fuel reactivity from cycle to cycle would produce more interesting results.

Applying the constraints from the continuous model to the GFR design used here resulted in a system with negative growth. This was not the intended isobreeder behaviour, but in order to provide a good comparison between the two sets of results, it was considered necessary to continue the use of these constraints.

The different fuel cycle strategies that were investigated had a range of effects on the fuel behaviour in the GFR. The changes due to reprocessing losses were the most straightforward, with less available plutonium, the system decreased in size faster. Increasing the reprocessing losses simply increased the rate at which the system shrank. Recycling of additional actinides affected the composition of the fuel and the growth rate of the system. The composition shifted towards the higher actinides as they were recycled along with the plutonium. The largest change was seen with the recycling of americium, which had a considerable effect on the balance of isotopes in the system. This also had a significant effect on the waste produced by the system, decreasing the total mass by a large amount, but also greatly increasing the amount of curium in the waste. The recycling of neptunium had a relatively small effect, and that of curium chiefly changed the amount of Cm-244 seen in the fuel. Recycling the higher actinides decreased the radiotoxicity of the waste, with larger reductions occuring as more actinides were recycled.

Altering the feed material used for the system also changed the fuel composition. Increasing the amount of isotopes other than U-238, specifically U-234 and U-235, moved the asymptotic fuel composition such that it contained more Pu-239 and less of the other three isotopes considered.

Using the continuous model on this system gave mixed results, with composition prediction giving reasonable values, but growth rate prediction showing significant errors across the whole time period that was examined. This was true for all variations of the GFR fuel cycle that were modelled. The values for the isotopic breeding worths appear reasonable, with the Pu-239 and Pu-241 values being very close, and a significant difference between the worths of Pu-240 and Pu-242 to allow for the breeding of Pu-241 from Pu-240.

From these results, it can be concluded that the continuous model can only be of limited use for fuel cycle studies of the GFR. While the composition prediction may be used for a rough evaluation of the asymptotic fuel make-up of a given design, it does not provide highly accurate results. This means it cannot reasonably be used to evaluate the effects of relatively small changes such as recycling neptunium alongside plutonium. The growth rate predictions cannot be relied upon. For accurate and detailed results, the continuous model cannot replace full burn-up calculations.

2.6.1 Recommendations

There is much work that could still be done on the continuous fuel cycle model. The cause of the problems when Am-241 was included in the model are still unknown. The accuracy of the model in predicting the behaviour of a breeder system with different feed materials and reprocessing strategies could also be tested. The problems encountered in applying the continuous model to the negative growth GFR would need to be resolved before it could be usefully applied to such systems.

Chapter 3

The Double Adjoint Method

3.1 Introduction

The contribution of a given isotope to the reactivity can be determined using the forward and adjoint fluxes (Ott and Neuhold, 1985). This allows the effects of different isotopes to be compared. The problem becomes more complicated when the effects of transmutation are considered. For example, Pu-240 may contribute less to the reactivity of a hypothetical system than Pu-239 at a given time, but may capture a neutron and become Pu-241, which has a higher contribution. This issue can be resolved by using the forward and adjoint transmutation problems along with the reactivity contributions determined with the forward and adjoint fluxes. An alternative approach would be to solve the forward transmutation problem repeatedly for systems with small perturbations, but this would come at a heavy computational cost.

A coupled neutron-nuclide depletion perturbation theory has previously been described (Williams, 1979). While this theory gives a complete picture of the development of the neutron and nuclide fields over the burn-up cycle (and indeed can be extended to multi-cycle (White, 1980)), there are certain problems with its implementation. In particular the adjoint flux shape problem must be solved with the inclusion of source term. This requires the code used to have been specially adapted to this task. These adaptations have been made for one and two dimensional problems in the SCALE code system (Jessee et al.,

2009), but not for three dimensional ones. The existing three dimensional code can still be used, provided care is taken to allow for the effects that arise from neglecting the coupling between the flux and the composition.

The double adjoint method is based on using the contribution of a nuclide to the reactivity, determined using the forward and adjoint fluxes, as the source for the adjoint transmutation problem. This allows the contributions of nuclides to the reactivity at a later point in time to be determined. Using this method to determine the contribution of the beginning of cycle composition to the end of cycle reactivity, and looking also at the beginning of cycle reactivity allows the appropriately formulated reloading problem to be solved.

First, the theory underlying the double adjoint method will be described, covering determining the contribution to the reactivity, and forward and adjoint transmutation. This is followed by details of the implementation of the method and its testing in fast and thermal systems. Then the double adjoint method is used to determine the reloading of such systems. The effects of the fuel compound used, in this case oxide fuels, are discussed. Reloading calculations in which neptunium and americium are recycled alongside plutonium are studied. The effects of neglecting the coupling between the composition and the flux are considered. Finally a breeding ratio definition is described and used to describe the behaviour of systems with different feed materials and reprocessing strategies.

3.2 Reactivity

The forward and adjoint fluxes, ϕ and ϕ^*, can be used to measure the contribution of a variable to the reactivity. The critical eigenvalue λ can be expressed in terms of the flux and the neutron production $\mathbf{P}$ and loss $\mathbf{L}$ operators.

$$\mathbf{L}\phi = \lambda \mathbf{P}\phi \tag{3.1}$$

Further, the effect of a perturbation to the system on λ can be found using the expression (Williams, 1986):

$$\frac{\Delta\lambda}{\lambda} = \frac{\langle \phi^*, (\Delta\mathbf{L} - \lambda\Delta\mathbf{P})\,\phi \rangle}{\lambda \langle \phi^*, \mathbf{P}\phi \rangle} \tag{3.2}$$

where Δ is used to represent a small change in the relevant variable. This can be re-arranged to give the effect of a perturbation on the value of the

multiplication factor k, accurate to first order.

$$\frac{\Delta k}{k} = \frac{\left\langle \phi^*, \left(\frac{1}{k}\Delta\mathbf{P} - \Delta\mathbf{L}\right)\phi \right\rangle}{\left\langle \phi^*, \frac{\mathbf{P}}{k}\phi \right\rangle} \tag{3.3}$$

The effect on the loss operator of a perturbation in a variable α, of which the loss operator is a function, can be written in first order terms as:

$$\Delta\mathbf{L} = \frac{\partial\mathbf{L}}{\partial\alpha}\Delta\alpha \tag{3.4}$$

and similarly for the production operator. For changes in the composition $\underline{N}$, the effect on the multiplication factor becomes

$$\frac{\Delta k}{k} \simeq \frac{\left\langle \phi^*, \left(\frac{1}{k}\frac{\partial\mathbf{P}}{\partial\underline{N}}\Delta\underline{N} - \frac{\partial\mathbf{L}}{\partial\underline{N}}\Delta\underline{N}\right)\phi \right\rangle}{\left\langle \phi^*, \frac{\mathbf{P}}{k}\phi \right\rangle} \tag{3.5}$$

3.2.1 TSUNAMI

The process of determining the relationship between the multiplication factor and the composition is automated in SCALE in the TSUNAMI module (SCALE manual, 2009). It is described as "a SCALE control module that facilitates the application of sensitivity and uncertainty analysis theory to criticality safety analysis". The output generated by a TSUNAMI run includes a table of sensitivity coefficients by nuclide, which can be used to determine the effects of a change in the composition on the multiplication factor. The sensitivity S_i of k to nuclide N_i, which describes the change in k for a given change in N_i, is

$$S_i = \frac{N_i}{\Delta N_i} \cdot \frac{\Delta k}{k} \tag{3.6}$$

As before, this is only accurate to first order and so can only treat small perturbations. This expression can be re-arranged to give the worth of an isotope, the effect of an absolute instead of relative change in the value of N_i.

$$\Delta k = \left(S_i \frac{k}{N_i}\right)\Delta N_i = w_i \Delta N_i \tag{3.7}$$

The composition N_i is described in TSUNAMI and TRITON in terms of atom densities, measured in atoms per barn-cm. Given that the multiplication factor is unit-less the worths w_i are determined in units of barn-cm per atom. Since these values are used either comparatively or as a product with the atom densities, there is no need to convert to a more conventional unit. These values will be used to measure the contribution of each nuclide to the reactivity.

3.3 Burn-up

The composition of the fuel changes during burn-up, which in turn affects reactor properties such as the multiplication factor. If the value of k drops below one at any point, the reactor will stop operating. It is therefore not enough to ensure that the reactor is critical at start-up, instead it must be critical at all points during the burn-up cycle. Burn-up tends to decrease the value of k so this requirement can be approximated by ensuring the reactor is critical at the end of cycle. There are some systems, typically operated on natural uranium, in which reactivity increases in the early stages of the cycle as extra fissile material is bred and then decreases later on as the bred material is burnt. In these systems the end of cycle multiplication factor is usually the lowest value of any point in the cycle, meaning this approximation remains reasonable. The previous section describes how the effect of the composition on the reactivity can be determined at a given time. Here the effect of the composition on itself at a later point in time will be discussed.

The evolution of fuel composition can be an involved process, as there are many different paths for the production and loss of different isotopes. Typically, the beginning of cycle (BOC) fuel composition is known and the composition at later times is calculated from that. For small changes in the BOC composition, the resulting changes to the composition at a later time, e.g. the end of cycle (EOC), can also be found from the adjoint burn-up problem. Solving the problem in this fashion avoids the need to carry out a full burn-up calculation for every change made to the initial composition. It can, however, only give the change to the end of cycle composition in terms of a single response for each adjoint problem solved.

The burn-up problem can be written as

$$\mathbf{C}\underline{N} = \frac{\partial}{\partial t}\underline{N} \tag{3.8}$$

$\mathbf{C}$ is referred to as the transmutation matrix, and its components are the microscopic reaction rates of the transmutation processes occurring due to neutron interactions and radioactive decay. The BOC composition is known and can be used in this problem to determine the EOC composition. The composition may be different at different locations in the reactor, which would require a separate burn-up problem for each different composition.

3.3.1 TRITON

The forward burn-up problem can be solved in SCALE. For a three-dimensional problem, the TRITON module is used, which determines the flux in the reactor using the Monte Carlo based KENO criticality solver, also in the SCALE code package (SCALE manual, 2009). This means there is an uncertainty associated with the values found for the multiplication factor. The inputs for TRITON and TSUNAMI are quite similar, making it straightforward to convert from one to the other. Once the end of cycle composition has been found using TRITON, TSUNAMI can be used to determine the sensitivities of the end of cycle composition.

3.4 Time dependent perturbation theory

The adjoint method can be used to determine the effects of perturbations on time dependent problems such as the burn-up problem, in a manner similar to that used for the reactivity earlier. The discussion here follows that given in Williams (1986), with some minor notational variations. Burn-up is a linear initial value problem. An external source term $\underline{Q}$ can be included in the problem to represent input quantities, making equation (3.8) into

$$\mathbf{C}\underline{N} = \frac{\partial}{\partial t}\underline{N} - \underline{Q} \tag{3.9a}$$

$$0 \leq t < t_F \tag{3.9b}$$

$$\underline{N}\,(t=0) = \underline{N}_0 \tag{3.9c}$$

The response R can be written as

$$R = \langle \underline{h}, \underline{N} \rangle \tag{3.10}$$

with $\underline{h}$ the vector response function and the brackets representing integration over all independent variables. If, for example, the response of interest was the amount of Pu-239, $\underline{h}$ would consist of a 1 in the Pu-239 component and 0 in all others. If $\underline{h}$ is a final time response function, it can be written using the Kronecker delta δ

$$\underline{h} = \underline{h}_F \delta\,(t - t_F) \tag{3.11}$$

and R becomes a final time response

$$R\,(t_F) = [\underline{h}_F, \underline{N}\,(t_F)] \tag{3.12}$$

with the square brackets now indicating integration over all independent variables except time.

The problem at hand is how to determine the change in the response caused by a perturbation in the initial composition. The original formulation in equation (3.9a) can be re-written to change the initial condition to a homogeneous one.

$$\mathbf{C}\underline{N} = \frac{\partial}{\partial t}\underline{N} - \underline{N}_0\delta\left(t\right) - \underline{Q} \tag{3.13a}$$

$$\underline{N}\left(t=0\right) = 0 \tag{3.13b}$$

Changes to the initial condition $\underline{N}_0$ can instead be treated as changes in the source term $\underline{Q}$.

If the source term is perturbed to a value $\underline{Q}' = \underline{Q} + \Delta\underline{Q}$, e.g. if the initial composition is altered, then the burn-up equation describing the system becomes

$$\mathbf{C}\underline{N}' = \frac{\partial}{\partial t}\underline{N}' - \underline{Q}' \tag{3.14a}$$

$$\underline{N}'\left(t=0\right) = 0 \tag{3.14b}$$

The response functional is also changed to

$$R' = R + \Delta R = \left\langle \underline{h}, \underline{N}' \right\rangle \tag{3.15}$$

3.4.1 Adjoint problem

The adjoint equation for this type of time dependent problem can be written as

$$\mathbf{C}^*\underline{N}^* = -\frac{\partial}{\partial t}\underline{N}^* - \underline{Q}^* \tag{3.16a}$$

$$0 \leq t < t_F \tag{3.16b}$$

$$\underline{N}^*\left(t=t_F\right) = 0 \tag{3.16c}$$

Setting $\underline{Q}^*$ to an appropriate value allows the properties of the adjoint to be used advantageously

$$\underline{Q}^* = \frac{\partial R}{\partial \underline{N}} = \underline{h} \tag{3.17}$$

If R is a final time response

$$\frac{\partial R}{\partial \underline{N}} = \underline{h}_F \delta\left(t - t_F\right) \tag{3.18}$$

This can be used to re-express the adjoint problem for final time responses only as

$$\mathbf{C}^* \underline{N}^* = -\frac{\partial}{\partial t}\underline{N}^* \tag{3.19a}$$

$$\underline{N}^*\left(t = t_F\right) = \left.\frac{\partial R}{\partial \underline{N}}\right|_{t_F} = \underline{h}_F \tag{3.19b}$$

Taking the inner product of $\underline{N}^*$ with equation (3.14a) and of $\underline{N}'$ with equation (3.19a) and subtracting the second from the first gives

$$\left\langle \underline{N}, \frac{\partial}{\partial t}\underline{N}' \right\rangle + \left\langle \underline{N}', \frac{\partial}{\partial t}\underline{N}^* \right\rangle = \left\langle \underline{N}, \underline{Q}' \right\rangle - \left\langle \underline{N}', \underline{h} \right\rangle \tag{3.20}$$

The left hand side of this equation can be shown to be equal to zero due to the homogeneous initial and final conditions applied to $\underline{N}'$ and $\underline{N}^*$. This leaves

$$\left\langle \underline{N}^*, \underline{Q}' \right\rangle = \left\langle \underline{N}', \underline{h} \right\rangle = R' \tag{3.21a}$$

$$\Delta R = \left\langle \underline{N}^*, \Delta \underline{Q} \right\rangle \tag{3.21b}$$

This produces a relationship between a change in the source and the resulting change in the response. For a change in the initial composition

$$\Delta \underline{Q} = \Delta \underline{N}_0 \delta\left(t\right) \tag{3.22}$$

$$\Delta R = \left[\underline{N}^*\left(t = 0\right), \Delta \underline{N}_0\right] \tag{3.23}$$

It should be noted that this derivation does not include the effects of changing the initial composition on the transmutation matrix $\mathbf{C}$. It is possible to describe these changes, as in Williams (1979), but this work was designed not to use that approach.

3.4.2 Reactivity as the response

The end of cycle reactivity is the response under scrutiny. In order to express it in the form used in equation (3.12), it is necessary to create a vector describing

the contribution of the nuclides in the composition at t_F to the end of cycle reactivity. This vector, labelled $\underline{w}$, is made up of the nuclide worths determined using the end of cycle composition and the forward and adjoint fluxes, the w_i in equation (3.7). This means that equation (3.19a) must be solved using $\underline{w}$ as the final time condition in equation (3.19b).

$$\mathbf{C}^* \underline{N}^* = -\frac{\partial}{\partial t} \underline{N}^* \tag{3.24a}$$

$$\underline{N}^* (t = t_F) = \underline{w} \tag{3.24b}$$

Solving this problem gives the value of $\underline{N}^* (t = 0)$, allowing equation (3.23) to be solved for a given value of $\Delta \underline{N}_0$. This solution gives the effect of a perturbation of the beginning of cycle composition on the end of cycle reactivity.

The components of $\underline{w}$ are determined using the EOC composition. Perturbations of the BOC composition affect the EOC values, meaning they can also change the values that make up $\underline{w}$. If, for example, a change is made that produces an EOC composition which provides more moderation, then the EOC neutron spectrum will be softer. This will increase the values of most cross sections, changing the reactivity worths. These worths vary only slowly with changes of this kind, and as such these effects have been neglected here. Similarly, higher order effects have been neglected due to their small contributions.

3.5 Implementation

In order to determine the effect of the BOC composition on the EOC reactivity, a three step method is used.

1. The forward burn-up problem is calculated using TRITON.
2. The worths of the EOC composition are found using TSUNAMI.
3. The worths are used as the source for the adjoint burn-up problem, which is solved using a purpose-built Python code.

The adjoint burn-up code employs the VODE routine (Brown et al., 1989) as implemented in the SciPy package (Jones et al., 2001–) to solve the differential

equations. The code reads composition and flux values from the TRITON output of the forward problem and cross section data from the associated ORIGEN libraries. These data are used to produce the components of the adjoint transmutation matrix.

The transmutation matrix is approximately 2000 by 2000 elements and this problem can be computationally intensive to solve. To improve the performance of the code, the Cython language (Behnel et al., 2011) was used to carry out the numerically demanding parts of the calculation. An option was built into the adjoint burn-up code to use only those isotopes above a given ORIGEN identification number, to decrease the work necessary to solve the problem if desired. The default value for this cut-off was set to 890000, meaning that only isotopes of actinium and heavier elements were included in the calculation. This reduced the time needed to run the adjoint burn-up code by a factor of approximately 10. Even when all the isotopes are included in the calculation however, the time taken is in the order of minutes, meaning the time to solve the whole problem remains dominated by the solution of the forward burn-up problem.

TSUNAMI provides worths for the isotopes present in the EOC composition. There may be nuclides that are not present at the end of cycle, but which affected the reactivity at an earlier time. The reactivity worths of these isotopes could optionally be estimated in the adjoint burn-up code by using the one group reactivity approximation, $\nu\sigma_f - \sigma_a$ (Salvatores, 1986), where ν is the number of neutrons produced per fission, σ_f the microscopic fission cross section, and σ_a the microscopic absorption cross section. Including these values in the calculations did not result in large changes, with the final result differing by no more than 0.01% in most cases.

3.6 Testing in a fast spectrum

The double adjoint method was tested on a model of a single sodium cooled fast reactor (SFR) pin in an infinite lattice. The pin design was based on the information on the European Fast Reactor (EFR) given in IAEA (2006). The fuel used was a mixed oxide, the composition of which was determined by mixing depleted uranium containing 0.25% U-235 and plutonium from PWR spent fuel after 43000 MW d/t burn-up (Nuclear Decommissioning Authority, 2008). The pin was depleted using TRITON and the BOC and

Table 3.1: Sample worths for isotopes at BOC, EOC, and BOC contributions to EOC reactivity in a fast system

Element	Isotope	Worth (barn-cm/atom)		
		BOC	EOC	BOC to EOC
U	235	185.51	195.05	139.04
	238	-23.459	-22.642	-13.876
Pu	238	118.70	126.17	117.61
	239	242.91	252.73	189.75
	240	12.670	15.592	34.080
	241	371.50	384.00	243.66
	242	-1.2628	1.0090	-2.7975

EOC sensitivities and worths were calculated with TSUNAMI. The EOC worths were then used as the source for the burn-up adjoint to determine the contribution of the BOC composition to the EOC reactivity. Sample values of the worths for the beginning-of-cycle, end-of-cycle, and from the adjoint burn-up problem are given in table 3.1, labelled BOC, EOC, and BOC to EOC respectively. The results show that the evolution of the fuel over the burn-up cycle can produce significant changes in the values of the worths. They also show that the effects of transmutation and decay can mean that the value of the BOC composition contribution to the EOC reactivity can be significantly different to the BOC or EOC worths. For example, Pu-240 has comparable BOC and EOC worths. The BOC to EOC worth of Pu-240 is significantly higher than either, however, reflecting the fact that over the course of the cycle a Pu-240 atom may absorb a neutron and become Pu-241, which has a much larger contribution to the reactivity at a given point in time.

3.6.1 Comparison with perturbed forward calculations

In order to see how well the worths from the double adjoint method predict the effects of changing the BOC composition on the EOC reactivity, the predictions were compared to perturbed forward calculations. The quantities of two isotopes, U-238 and Pu-239, were altered in steps of 1% up to plus and minus 10%. These two isotopes were chosen as they are the most populous actinides in the single pin model and can be considered as the most important.

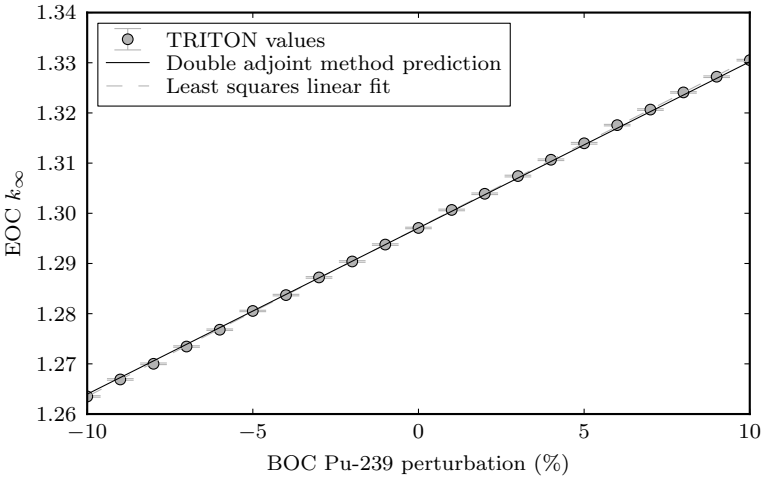

Figure 3.1: Variation of EOC k_∞ behaviour with BOC Pu-239 perturbation in a fast system compared to prediction from double adjoint method

TRITON was used to perform burn-up calculations on models with these perturbed compositions and the results compared to those predicted by the double adjoint method.

The variation of EOC k_∞ with perturbations of the amount of Pu-239 at BOC is shown in figure 3.1 and U-238 in figure 3.2. Least squares linear fits to the values from the perturbed calculations are also shown for purposes of comparison with the double adjoint values. Predictions of the change are good for small perturbations, particularly for Pu-239.

3.7 Testing in a thermal spectrum

The spectrum and reaction rates in a thermal system vary more with burn-up than those of a fast system, due to effects such as the production of isotopes with high thermal neutron absorption cross sections. This means that the errors caused by neglecting changes in the spectrum resulting from changes in the initial composition are likely to be more noticeable in a thermal system. In order to test this, a model of a single PWR pin in an infinite lattice was created and studied in a similar fashion to the previous fast system model.

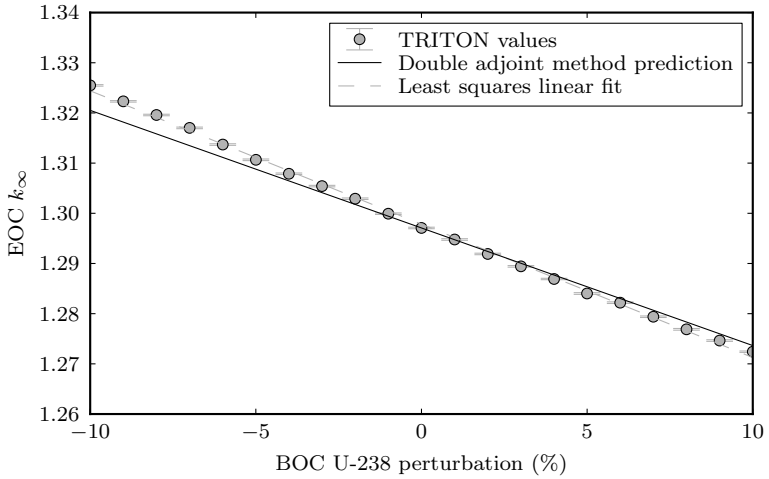

Figure 3.2: Variation of EOC k_∞ behaviour with BOC U-238 perturbation in a fast system compared to prediction from double adjoint method

The pin was made of oxide fuel and contained in Zircaloy cladding with light water as the coolant. The fuel itself was a mixed oxide made up of depleted uranium (with 0.25% U-235) and plutonium with the composition given for Magnox fuel following 3000 MW d/t burn-up (Nuclear Decommissioning Authority, 2008). Depletion calculations were carried out using TRITON, and sensitivities determined using TSUNAMI, as previously.

Table 3.2 shows the reactivity worths of some isotopes in the thermal system at the beginning and end of the burn-up cycle, as well as the contribution of isotopes at the beginning of the cycle to the end of cycle reactivity. Comparing these values with those in table 3.1 shows some differences between the two systems. The fissile isotopes U-235, Pu-239, and Pu-241 have relatively large positive values in both cases. The non-fissile isotopes show much larger differences, with their worths being much lower in the thermal system. This is to be expected as they cannot be fissioned by thermal neutrons, meaning they will contribute less to the reactivity. Combined with the increase in capture cross section due to low neutron energy this means e.g. Pu-240 has a negative weight as it detracts from the reactivity instead of adding to it.

Table 3.2: Sample worths for isotopes at BOC, EOC, and BOC contributions to EOC reactivity in a thermal system

Element	Isotope	Worth (barn-cm/atom)		
		BOC	EOC	BOC to EOC
U	235	119.53	181.29	143.86
	238	-8.5071	-6.2004	-5.0655
Pu	238	-280.27	-262.96	-206.55
	239	181.70	310.52	130.03
	240	-615.37	-512.26	-249.58
	241	478.87	638.72	288.52
	242	-543.97	-433.77	-450.89

3.7.1 Comparison with perturbed forward calculations

Once again, the amounts of Pu-239 and U-238 in the initial composition were perturbed by values up to plus and minus 10% and the resulting EOC k_∞ values compared to the predictions from the double adjoint method. The results are shown in figures 3.3 and 3.4. The figures show that the results for the thermal system are much less accurate than for the fast system. This is believed to be caused by the larger changes in the reaction rates during burn-up seen in thermal systems. Altering the initial composition leads to a different set of initial reaction rates, which means the changes to the composition due to burn-up are also different. In the fast system, the reaction rates are almost constant during burn-up and are not affected by changes in the composition to the same extent. Indirect effects such as resonance self shielding are also affected when the composition is changed, and again these effects are smaller in a fast system.

3.8 Reloading

In a fast system, fuel left at the end of a burn-up cycle can be reprocessed and returned to the reactor until it is fissioned. Those atoms that are removed by fission or during reprocessing must be replaced by an external feed material. The composition of the material at the end of the cycle is of course different to that at the beginning. In order to reload the reactor with the appropriate

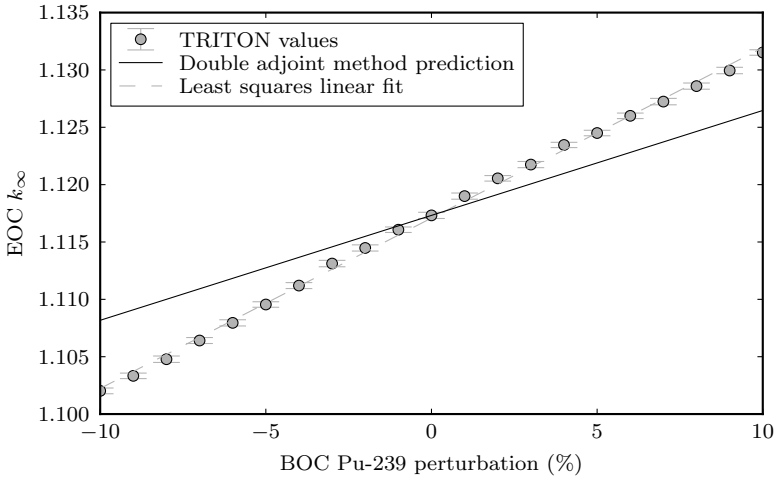

Figure 3.3: Variation of EOC k_∞ behaviour with BOC Pu-239 perturbation in a thermal system compared to prediction from double adjoint method

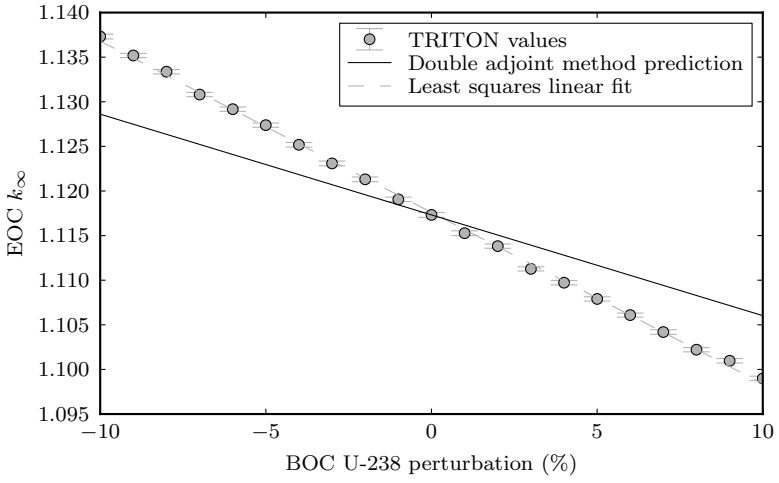

Figure 3.4: Variation of EOC k_∞ behaviour with BOC U-238 perturbation in a thermal system compared to prediction from double adjoint method

amount of reprocessed material, it is necessary to have some method to compare fuel of different compositions. Specifically, the reloading is determined by mixing appropriate amounts of two materials of fixed composition, the feed and the reprocessed materials. This means two methods of comparison are required to solve the pair of simultaneous equations posed by this problem.

3.8.1 Reactivity contribution

The first requirement of fuelling a reactor is to make sure it is critical at the beginning of cycle. It is therefore necessary to determine the contribution of each nuclide in the composition to the reactivity. This is done using the forward and adjoint fluxes to determine the worth of each nuclide. This provides the first set of weights, which are organised as a vector $\underline{w}_B$ for the reloading calculation.

Once the reactor has been made critical, it is necessary to ensure it remains critical throughout the burn-up cycle. The multiplication factor typically trends downwards during burn-up, meaning it is sufficient to ensure that the reactor is critical at the end of cycle to meet this condition. The double adjoint method can be used to determine the contribution of the beginning of cycle composition to the end of cycle reactivity. This provides the second set of weights, $\underline{w}_E$ for the reloading calculation.

3.8.2 Reloading calculation

The composition of the reloaded fuel is made up of a combination of reprocessed material and feed material. Given that the compositions of these two materials are fixed, the variables that define the composition of the reloaded fuel are the amounts of each of the two materials. The amount and composition of each of the feed and reprocessed materials can be separated and written as $F\underline{\hat{N}}_F$ and $R\underline{\hat{N}}_R$ respectively, where $\underline{\hat{N}}$ represents the composition normalised such that its components sum to unity. The reloaded fuel composition $\underline{N}_L$ can then be written as

$$\underline{N}_L = F\underline{\hat{N}}_F + R\underline{\hat{N}}_R \tag{3.25}$$

The values to be determined by the reloading calculation are F and R. They are found by using the BOC and EOC reactivity contributions of the BOC composition, labelled $\underline{w}_B$ and $\underline{w}_E$ respectively. Taking the inner product of these weights with the feed and reprocessed material compositions, and

ensuring that the contributions to the BOC and EOC reactivity are the same as they were in the previous cycle allows the values of F and R to be determined.

$$\underline{w}_i \cdot \underline{N}_P = F\big(\underline{w}_i \cdot \hat{\underline{N}}_F\big) + R\big(\underline{w}_i \cdot \hat{\underline{N}}_R\big) \quad i = B, E \tag{3.26}$$

This will result in a fuel reloading that gives the same multiplication factors at the beginning and end of the burn-up cycle as were seen in the previous cycle. This is not the same as ensuring the system remains critical throughout the cycle. It is assumed that the original reactor design was such that the reactor was able to operate for the whole length of the burn-up cycle, and that any excess reactivity at the beginning or end of the cycle was included in the design deliberately. As discussed previously, the lowest value of the multiplication factor is typically at the end of cycle, so matching this value should lead to a system that is critical for the entire cycle length.

3.9 Reloading a single SFR pin

The single pin model developed earlier was used to test the reloading calculation method outlined above. The reprocessed material was chosen to have the same composition as the plutonium in the pin at the end of the original burn-up cycle and the feed material used was depleted uranium with 0.25% U-235. The double adjoint code was run for both the actinides only and the all isotopes problems. The compositions found are shown in table 3.3, along with the original composition. The reloaded compositions differ significantly from the original one, both in the concentrations of each isotope present and the total amount of isotopes used. The all isotopes problem includes oxygen, so it is possible to allow for the effect on the reactivity of changing the amount in the composition. This is not true for the actinides only problem, and the actinide total row shows that the amount of oxygen used is not equal to two oxygen atoms for every actinide atom in the fuel, as would be the case in a realistic fuel composition.

3.9.1 Effects of oxide fuel

In order to allow for the effects of the oxide fuel, the adjoint transmutation code was altered to include oxygen in the problem, even if it was excluded using the cut-off value described earlier. Solving the actinides only problem with this new code gave a composition that was significantly different to the

Table 3.3: Original and reloaded BOC compositions of SFR single pin model

Element	Isotope	Density (atoms/barn-cm)		
		Original	Actinides only	All isotopes
O	16	4.05×10^{-2}	4.05×10^{-2}	3.37×10^{-2}
U	235	4.23×10^{-5}	2.88×10^{-5}	3.48×10^{-5}
	238	1.69×10^{-2}	1.15×10^{-2}	1.39×10^{-2}
Pu	236	0	5.37×10^{-11}	7.85×10^{-11}
	237	0	3.59×10^{-10}	5.25×10^{-10}
	238	6.65×10^{-5}	3.30×10^{-5}	4.83×10^{-5}
	239	1.75×10^{-3}	1.11×10^{-3}	1.62×10^{-3}
	240	8.01×10^{-4}	5.04×10^{-4}	7.38×10^{-4}
	241	4.89×10^{-4}	2.24×10^{-4}	3.27×10^{-4}
	242	2.06×10^{-4}	1.30×10^{-4}	1.90×10^{-4}
	243	0	4.91×10^{-9}	7.18×10^{-9}
	244	0	4.06×10^{-10}	5.94×10^{-10}
Actinide total		2.03×10^{-2}	1.35×10^{-2}	1.69×10^{-2}

one produced without allowing for the effects of oxygen. In order to explore the effects of the oxide fuel on the reloading calculation, three compositions were considered. The first, labelled "None", is shown in table 3.3 under the heading "Actinides only". The second uses the same actinide composition as the first, but has the amount of oxygen appropriate to that number of actinide atoms. It is labelled "Appropriate", and is shown in table 3.4. The third is from the solution of the actinides only problem with oxygen included and is labelled "Adjoint", and is also shown in table 3.4. The results of depletion calculations on these different BOC compositions are shown in figure 3.5.

The efficacy of the double adjoint method in reproducing k_∞ behaviour is clear, as is the effect of altering the amount of oxygen in the system. When the actinide reloading is calculated without considering the effects of oxygen on the reactivity, and leaving the amount of oxygen unchanged from that in the original, the reloaded pin follows the behaviour of the original closely. If the amount of oxygen is changed to the amount appropriate to the new actinide loading, the results deteriorate significantly. Correcting the reloading

Table 3.4: Reloading compositions of SFR single pin making different allowances for use of oxide fuel

Element	Isotope	Density (atoms/barn-cm)		
		None	Appropriate	Adjoint
O	16	4.05×10^{-2}	2.70×10^{-2}	3.67×10^{-2}
U	235	2.88×10^{-5}	2.88×10^{-5}	3.80×10^{-5}
	238	1.15×10^{-2}	1.15×10^{-2}	1.52×10^{-2}
Pu	236	5.37×10^{-11}	5.37×10^{-11}	8.44×10^{-11}
	237	3.59×10^{-10}	3.59×10^{-10}	5.64×10^{-10}
	238	3.30×10^{-5}	3.30×10^{-5}	5.20×10^{-5}
	239	1.11×10^{-3}	1.11×10^{-3}	1.75×10^{-3}
	240	5.04×10^{-4}	5.04×10^{-4}	7.93×10^{-4}
	241	2.24×10^{-4}	2.24×10^{-4}	3.52×10^{-4}
	242	1.30×10^{-4}	1.30×10^{-4}	2.04×10^{-4}
	243	4.91×10^{-9}	4.91×10^{-9}	7.72×10^{-9}
	244	4.06×10^{-10}	4.06×10^{-10}	6.38×10^{-10}

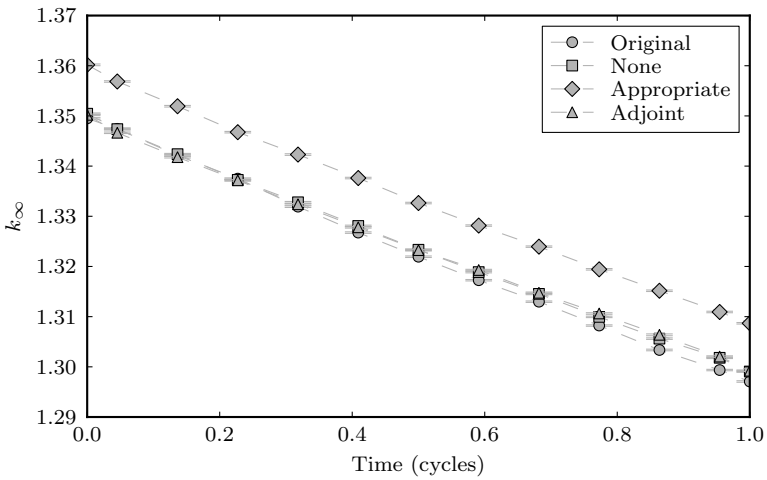

Figure 3.5: k_∞ behaviour of original pin and reloaded pins with different oxygen calculations

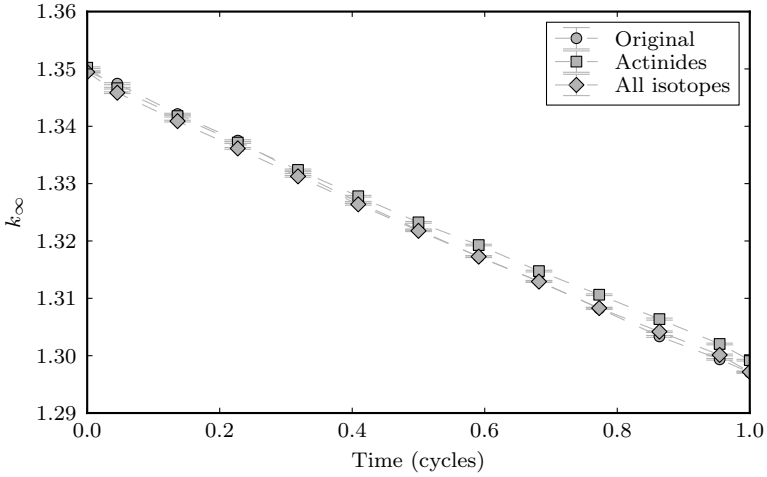

Figure 3.6: k_∞ behaviour of original pin and different reloading compositions

calculation for the effect of oxygen restores the quality of the results. For practical applications, the oxygen corrected model is to be preferred, as it is the best approximation of reality. A similar technique could be applied to other fuel compounds, such as carbides, nitrides, or metallic alloys.

The results of the actinides only with adjoint oxygen reloading and the all isotopes reloading are shown in figure 3.6 along with the original k_∞ behaviour. It can be seen that all three systems show very similar behaviour. The results of the actinides only solution are slightly worse than those of the all isotopes problem, but the variation is small. It is worth remembering that the double adjoint method is only designed to produce matching multiplication factors at the beginning and end of the cycle. The similar behaviour during the cycle is expected due to the similarities between the three compositions, but they are not required to act in this fashion.

3.9.2 Recycling additional actinides

It may be desirable to recycle additional actinides, such as neptunium or americium, alongside plutonium. The introduction of these elements into the reloading calculation represents a significant change in the composition. While

Table 3.5: Compositions of reloaded fuel pin with americium recycling

Element	Isotope	Density (atoms/barn-cm)	
		Actinides only	All isotopes
O	16	3.61×10^{-2}	3.22×10^{-2}
U	235	3.72×10^{-5}	3.31×10^{-5}
	238	1.49×10^{-2}	1.3294×10^{-2}
Pu	236	8.34×10^{-11}	7.60×10^{-11}
	237	5.58×10^{-10}	5.08×10^{-10}
	238	5.14×10^{-5}	4.68×10^{-5}
	239	1.73×10^{-3}	1.57×10^{-3}
	240	7.84×10^{-4}	7.14×10^{-4}
	241	3.48×10^{-4}	3.17×10^{-4}
	242	2.02×10^{-4}	1.84×10^{-4}
	243	7.63×10^{-9}	6.95×10^{-9}
	244	6.31×10^{-10}	5.75×10^{-10}
Am	241	1.99×10^{-5}	1.81×10^{-5}
	242	9.46×10^{-9}	8.62×10^{-9}
	242m	1.84×10^{-7}	1.68×10^{-7}
	243	9.55×10^{-6}	8.69×10^{-6}
	244	1.75×10^{-10}	1.59×10^{-10}
	244m	1.02×10^{-10}	9.28×10^{-11}

the absolute amount of either element is likely to be small, in relative terms any increase from a value of zero is a large difference. The oxygen corrected double adjoint method was used to calculate the reloading of the SFR pin when americium was recycled with plutonium and when neptunium was also included. The compositions used were again taken from the end of the original burn-up cycle. The calculations were carried out for both the actinides only and all isotopes cases. The resulting fuel compositions are given in table 3.5 for the fuel with americium and table 3.6 for the fuel with americium and neptunium. The k_∞ behaviour of the pin reloaded with americium included is shown in figure 3.7 and with americium and neptunium in figure 3.8. The graphs show that the k_∞ behaviour of the reloaded pins is very close to that of the original pin. Despite the inclusion of actinides not previously in the

Table 3.6: Compositions of reloaded fuel pin with americium and neptunium recycling

Element	Isotope	Density (atoms/barn-cm)	
		Actinides only	All isotopes
O	16	3.52×10^{-2}	3.08×10^{-2}
U	235	3.63×10^{-5}	3.16×10^{-5}
	238	1.45×10^{-2}	1.26×10^{-2}
Np	235	8.61×10^{-14}	7.71×10^{-14}
	236	1.51×10^{-11}	1.35×10^{-11}
	237	3.21×10^{-6}	2.87×10^{-6}
	238	4.58×10^{-9}	4.10×10^{-9}
	239	4.10×10^{-6}	3.67×10^{-6}
Pu	236	8.18×10^{-11}	7.33×10^{-11}
	237	5.47×10^{-10}	4.90×10^{-10}
	238	5.04×10^{-5}	4.51×10^{-5}
	239	1.69×10^{-3}	1.52×10^{-3}
	240	7.69×10^{-4}	6.89×10^{-4}
	241	3.41×10^{-4}	3.05×10^{-4}
	242	1.98×10^{-4}	1.77×10^{-4}
	243	7.48×10^{-9}	6.70×10^{-9}
	244	6.19×10^{-10}	5.54×10^{-10}
Am	241	1.95×10^{-5}	1.75×10^{-5}
	242	9.28×10^{-9}	8.31×10^{-9}
	242m	1.81×10^{-7}	1.62×10^{-7}
	243	9.36×10^{-6}	8.39×10^{-6}
	244	1.71×10^{-10}	1.54×10^{-10}
	244m	9.99×10^{-11}	8.95×10^{-11}

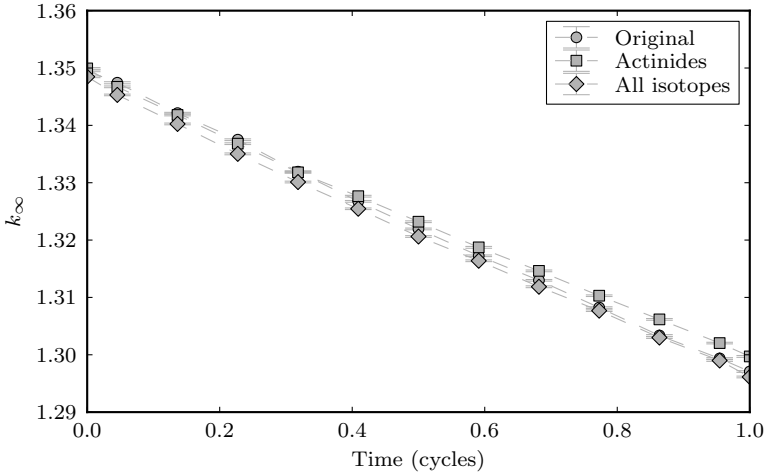

Figure 3.7: k_∞ behaviour in fuel pin reloaded with Pu and Am

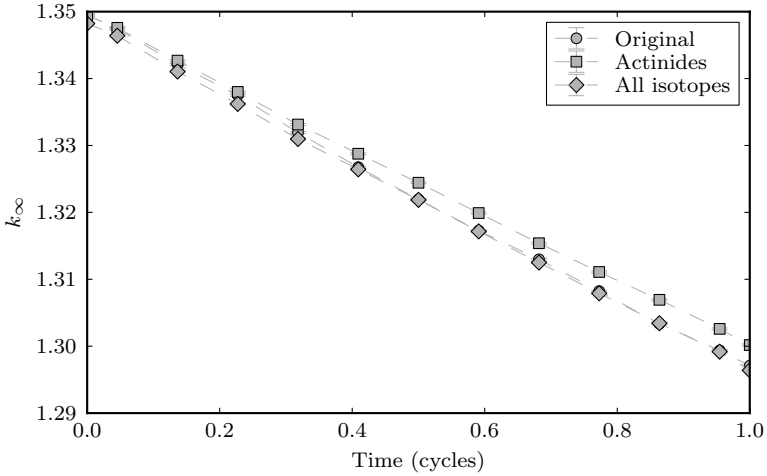

Figure 3.8: k_∞ behaviour in fuel pin reloaded with Pu, Am, and Np

composition, the double adjoint method provides good results in this type of scenario.

3.10 Reloading a single PWR pin

The double adjoint method was also used to calculate the reloading of the PWR pin described previously in order to test its efficacy in thermal systems. Given that the predictions compared poorly to the perturbed forward calculations, the reloading calculation was not expected to be as accurate as for the SFR pin case.

The oxygen effect corrected method was used to determine the reloading of the PWR pin. The plutonium composition at the end of the original burn-up cycle was used for the reloading, and was mixed with depleted uranium. While multi-recycling of plutonium in a thermal system is not yet practised, it serves as a reasonable problem to examine the differences between the fast and thermal systems. The adjoint burn-up code was run for both the all isotopes and actinides only cases. In order for the ODE solver to handle the all isotopes problem it was necessary to increase the relative tolerance by two orders of magnitude. This increased the errors in the results by a similar margin, as the allowed relative error was now significantly larger than the absolute error and dominated the inaccuracy in the values found. The reloaded compositions from both cases are given in table 3.7, along with the original composition.

The k_∞ behaviour of the original and reloaded pins are shown in figure 3.9. The results are different to those seen in the fast system, the actinides only solution provides a close match to the original behaviour, while the all isotopes solution differs significantly. The difference worsens as the cycle progresses, suggesting the problem lies in the BOC to EOC weights and not the BOC weights. This is to be expected as the BOC weights for both the all isotopes and actinides only solutions are read from the same TSUNAMI output, so which isotopes are included in the adjoint transmutation problem does not affect these values.

To investigate the differences in the actinides only and all isotopes problems in thermal systems, the behaviour of the nuclide worths in the system was studied. The adjoint transmutation problem was run repeatedly, using each isotope in turn as the cut-off value. This showed how the worths change as more nuclides are included in the problem. The values of the worths for three

Table 3.7: Original and reloaded PWR pin compositions

Element	Isotope	Composition		
		Original	Actinides only	All isotopes
O	16	4.65×10^{-2}	3.62×10^{-2}	3.83×10^{-2}
U	235	5.81×10^{-5}	4.33×10^{-5}	4.38×10^{-5}
	238	2.23×10^{-2}	1.73×10^{-2}	1.75×10^{-2}
Pu	236	0	1.62×10^{-12}	3.41×10^{-12}
	237	0	4.31×10^{-12}	9.11×10^{-12}
	238	8.79×10^{-7}	8.93×10^{-7}	1.89×10^{-6}
	239	7.03×10^{-4}	4.98×10^{-4}	1.05×10^{-3}
	240	1.49×10^{-4}	1.86×10^{-4}	3.93×10^{-4}
	241	2.37×10^{-5}	6.40×10^{-5}	1.35×10^{-4}
	242	2.64×10^{-6}	7.80×10^{-6}	1.65×10^{-5}
	243	0	1.67×10^{-9}	3.53×10^{-9}
	244	0	6.69×10^{-11}	1.41×10^{-10}
	246	0	1.01×10^{-17}	2.14×10^{-17}

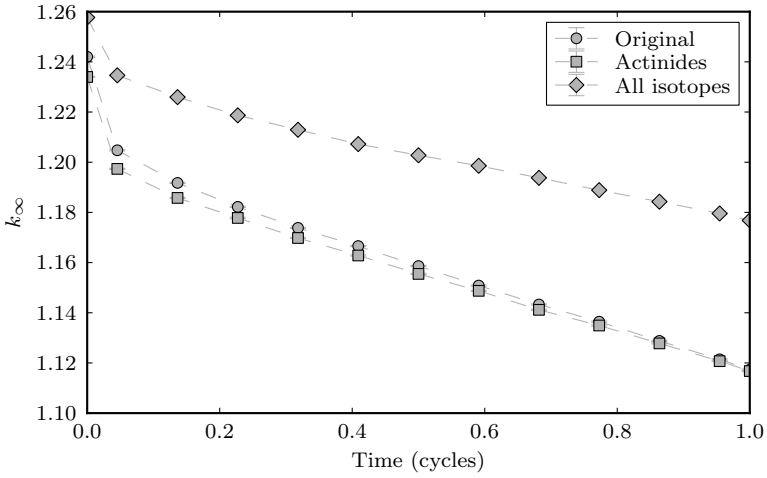

Figure 3.9: k_∞ behaviour of original and reloaded PWR pins

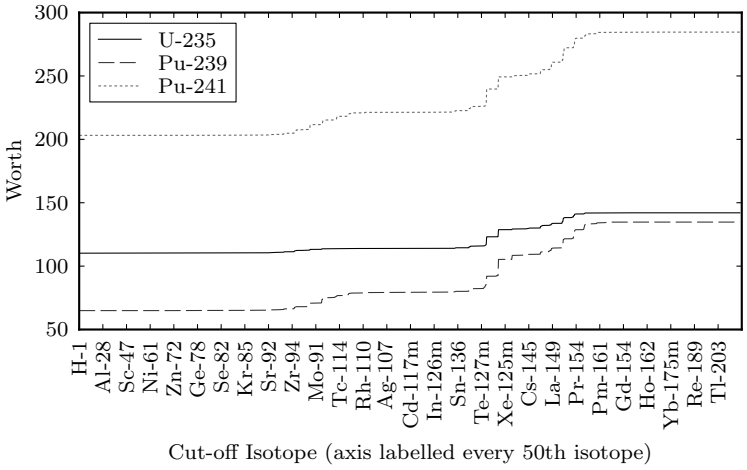

Figure 3.10: Worth behaviour in sample fissile isotopes with different nuclides in adjoint transmutation problem

fissile isotopes, U-235, Pu-239, and Pu-241 are shown in figure 3.10, and those of three non-fissile isotopes, U-238, Pu-240, and Pu-242, in figure 3.11.

The plots show that the worths of the fissile isotopes change significantly as more nuclides are included in the problem, while those of the non-fissile isotopes remain largely unchanged. Moving from the right to the left in the plots (that is adding more nuclides to the problem), there are two groups of isotopes in which the worths decrease, separated by an group showing very little change. These two groups correspond to the peaks in the fission product yield behaviour of a thermal system. It is to be expected that including the negative reactivity worths of the fission products decreases the worths of the fissile isotopes, as they are responsible for the creation of the fission products during the burn-up cycle. This effect can also be seen in the worth of Pu-240, which also decreases as the fission products are included, although by a smaller amount than the worths of the fissile isotopes. Given that the worths of the non-fissile isotopes are not affected as strongly by the inclusion of additional isotopes, the balance of the feed and reprocessed materials determined by the reloading calculation shifts, leading to the behaviour seen in figure 3.9.

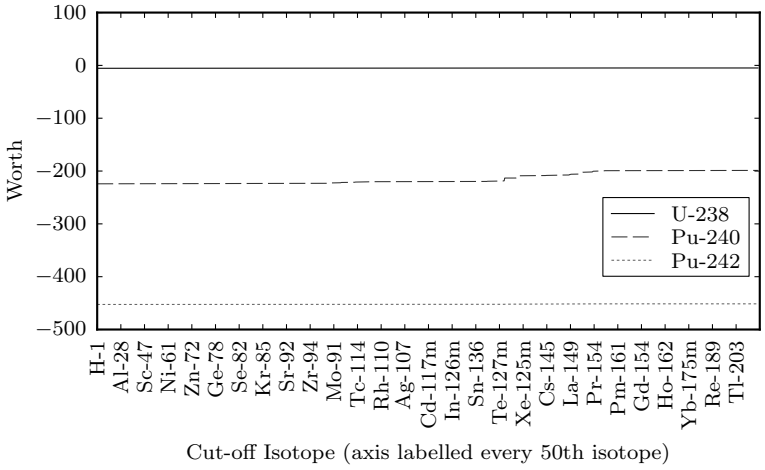

Figure 3.11: Worth behaviour in sample non-fissile isotopes with different nuclides in adjoint transmutation problem

This behaviour is a reflection of the fact that the indirect effects of altering the composition are not allowed for in the double adjoint method. Fission products alter the flux and therefore the one group cross sections in a reactor, particularly in thermal systems. The values used in the double adjoint method do not change as more isotopes are included in the problem and the results deteriorate accordingly. This problem is not seen in the fast system due to the negligible effects of fission products in such systems. On this evidence, the double adjoint method can be used for both fast and thermal systems, provided appropriate care is taken over these indirect effects.

3.11 Breeding ratio

No discussion of this kind would be complete without considering how the double adjoint method relates to the breeding ratio, BR. It is relatively simple to calculate the value of BR for a system by dividing the amount of reprocessed material by the amount required to re-fuel the system.

$$BR = \frac{\sum \underline{N}_R}{R} \tag{3.27}$$

Table 3.8: Value of breeding ratio determined with the double adjoint method in fast and thermal systems with different feed materials

Feed	Fast	Thermal
DU	1.036	1.035
NU	1.059	1.278
RU	1.031	1.032

This assumes that the amount of reprocessed material is the limiting factor in the re-fuelling, and that enough feed material is available to supply any number of systems. Note that as the value of R is affected by the compositions of both the feed and reprocessed materials, BR changes with different feeds. Values of BR for the fast and thermal systems discussed previously are given in table 3.8, which shows the effects of depleted, natural, and reprocessed uranium (labelled DU, NU, and RU respectively) on the value of the breeding ratio.

The values of BR given here are all larger than one, indicating breeding systems, but this value applies only to the current cycle. The amount of actinides in the fuel decreases significantly after the reloading, meaning more reloaded pins can be created from the material taken from the previous pin. After going through several cycles, the amount of fuel used would be expected to remain similar between cycles and the value of BR would decrease. The different feed materials have a significant effect on the breeding ratio, particularly with the use of natural uranium in the thermal system. The amount of U-235 in the NU feed is larger than in the other two feeds, and its weights have absolute values two orders of magnitude higher than U-238 (see table 3.2), which is the main constituent of all the feed materials. This means the NU feed is able to displace some of the reprocessed material, making it possible to reload more systems from the same amount of material. This effect is not seen in the fast system, where the smaller cross sections make it necessary to use a much larger amount of fissile material in the fuel. The use of NU feed in the fast system does not free up a large enough amount of reprocessed material to allow much more fuel to be created.

Altering which elements are included in the reprocessing can also affect the breeding ratio of a system. Values of BR for the fast system recycling

Table 3.9: Value of breeding ratio determined with the double adjoint method in fast systems with different reprocessing schemes

Pu	Am	Np
1.036	1.041	1.059

plutonium (Pu), plutonium and americium (Am), and plutonium, americium, and neptunium (Np) are given in table 3.9. In these cases, increasing the amount of material reprocessed leads to an increase in the breeding ratio. If one of the recycled elements had a predominantly negative contribution to the reactivity, it might also be possible to decrease the breeding gain by reprocessing it.

This definition of breeding ratio has several important features. It can be accurately applied to non-equilibrium cycles, unlike many of the existing definitions, discussed in e.g. Adkins (1972); Ott and Borg (1977). The inclusion of the feed material means the value found is a more accurate representation of the fuel produced, but is also specific to the chosen feed. The value of the breeding ratio can be affected by the feed material, as shown previously. Allowing for the effects of the oxygen used in making the fuel compound is also important, given that the amount of feed and reprocessed material, and hence the amount of oxygen, in the fuel can vary from cycle to cycle.

3.12 Conclusions

A method was described to determine the contributions of the composition to the system reactivity at a later point in time. It is based on a combination of the reactivity and time adjoints. It was tested in fast and thermal systems. The results for the fast system were good, and those for the thermal system were less accurate. The reloading calculation for the SFR pin produced a model with a new composition that showed very similar reactivity behaviour to that seen in the original. The reloading of the thermal pin produced good results in the actinides only case, but poor ones in the all isotopes case. Neglecting the indirect effects in the double adjoint method gives inaccurate results as the fission products cause large changes in the behaviour of thermal systems.

The breeding ratio definition follows from the reloading calculation. Different

feed materials can have a significant effect on the breeding ratio, particularly in thermal systems, although care must be taken to allow for shifts in the total amount of fuel used.

The double adjoint method lends itself to the solution of the reloading problem described previously, that is the appropriate balance of feed and reprocessed materials to reproduce the behaviour of the original system. It can further be used to describe the effects of including various isotopes in the system, giving a more nuanced picture than that provided by a simple reactivity adjoint calculation. The allowance for the fuel compound, oxygen in the cases described above, is also important, as it affects the relative contributions of the different isotopes. The breeding ratio definition that follows from the double adjoint method makes allowance for the inclusion of the feed material, which is often missing in existing definitions. It can also be applied to non-equilibrium burn-up cycles, an advantage over many other measures.

The double adjoint method can be useful, provided care is taken to ensure it is applied only in appropriate situations. It allows the contributions of nuclides in the composition to the reactivity at a later point in the cycle to be evaluated. There is no requirement that the beginning and end of cycle are the chosen times. Other points in the cycle could be chosen, as either alternatives or in addition to those already used, if for example the reloading was to be calculated from more than two materials. Systems in which the reactivity does not simply decrease with time, such as those that show an initial increase, could be modelled with the inclusion of extra points. Other constraints, such as the use of a fixed number of actinide atoms, could be included in a similar fashion.

Chapter 4

Application of Coupled Depletion Perturbation Theory

4.1 Introduction

The first application of perturbation theory methods was the modelling of celestial mechanics by Newton, and later Euler and Clairaut (Boccaletti and Pucacco, 1998). They have since been applied to a range of subjects in both physics and chemistry (Fernández, 2001). Fundamentally it is concerned with determining the effects of small changes (perturbations) on the behaviour of a system with a known reference state. Several perturbation theory techniques have been applied to reactor analysis, and Williams (1986) provides a review of these methods.

The double adjoint method (chapter 3) assumes that the coupling between the flux and the composition in the reactor can be neglected over the burn-up period. This assumption can negatively affect the results in systems in which there is a strong relationship between the evolution of the composition and the flux. The coupled depletion perturbation theory (DPT) described by Williams (1979) allows for the relationship between these two components, meaning it should be possible to determine accurate values for the contributions of all

nuclides in a given system, instead of the restricted set used for the thermal system in chapter 3.

The implementation of the coupled DPT method is significantly different to that of the double adjoint method. In order to allow for the coupling between the flux and the composition, some additional information, such as the multi-group transmutation matrix, is needed for the model. In particular, it is necessary to solve an adjoint eigenvalue problem including a source term, a capability that is not currently present in most reactor modelling codes.

A full description of coupled depletion perturbation theory will be given. The implementation of the model will then be discussed, followed by the results produced by the code. Different neutron spectra and adjoint responses will be considered. The goal of the research is to test how well the coupled depletion perturbation theory can be implemented with existing reactor modelling software and to use the results found in the reloading problem described in chapter 3.

4.2 Theory

The description of coupled DPT given here will follow that given in the original paper by Williams (1979), which is recommended to the interested reader. There will be some minor variation in the notation used, with the aim of adding clarity to the explanation. Further discussion can be found in Williams (1986), and a generalised approach that allows changes and additions to the physics of the problem, such as the inclusion of heat transfer, without requiring it to be reformulated is presented in Stripling et al. (2013).

The composition of the material in a reactor at location $\underline{r}$ and time t is described by the vector $\underline{N}(\underline{r},t)$, whose components $N_i(\underline{r},t)$ represent the amount of nuclide i at that position and time. The neutron flux ϕ is dependent on position, time, direction $\hat{\underline{\Omega}}$, and energy E. These variables form a seven-dimensional space labelled ρ. The nuclide transmutation equation can be written

$$\frac{\partial}{\partial t}\underline{N}(\underline{r},t) = [\phi(\rho)\mathbf{R}(\sigma)]_{\hat{\underline{\Omega}},E}\underline{N}(\underline{r},t) + \mathbf{D}\underline{N}(\underline{r},t) + \underline{C}(\underline{r},t) \tag{4.1}$$

where $\mathbf{R}$ is the transmutation cross section matrix, whose components are the production and loss cross sections $\sigma(\underline{r},E)$ of the various neutron induced

transmutation mechanisms. **D** is the transmutation decay matrix, made up of the decay constants λ of the decay transmutation processes. $\underline{C}$ represents all external sources of nuclides, such as control rod movement or chemical shim. The square brackets $[\ldots]_{\underline{\hat{\Omega}},E}$ represent integration of their contents over direction and energy. The transmutation operator **M** can be defined as

$$\mathbf{M} = [\phi(\rho)\mathbf{R}(\sigma)]_{\underline{\hat{\Omega}},E} + \mathbf{D} \tag{4.2}$$

which makes the transmutation equation

$$\frac{\partial}{\partial t}\underline{N}(\underline{r},t) = \mathbf{M}(\rho)\underline{N}(\underline{r},t) + \underline{C}(\underline{r},t) \tag{4.3}$$

The behaviour of the neutron flux is determined from the neutron transport equation

$$\begin{aligned}\frac{1}{v}\frac{\partial}{\partial t}\phi(\rho) + \hat{\Omega}\cdot\nabla\phi(\rho) + \underline{N}(\underline{r},t)\cdot\underline{\sigma_t}(\underline{r},E)\phi(\rho)\\ = \underline{N}(\underline{r},t)\cdot\left[\underline{\sigma_s}(\underline{r},E',\hat{\Omega}'\rightarrow E,\hat{\Omega})\phi(\rho') + (1-\beta)\frac{\chi(E)}{4\pi}\underline{\nu\sigma_f}(E')\phi(\rho')\right]_{E',\hat{\Omega}'}\\ + \sum_i \chi_{Di}(E)\lambda_i d_i(\underline{N})\end{aligned} \tag{4.4}$$

where v is the neutron speed, $\underline{\sigma_{t,s,f}}$ are cross section vectors for total, scattering, and fission interactions respectively, β is the yield of all precursors per fission neutron, $\underline{\nu}$ is the neutrons produced per fission, $\chi(E)$ is the prompt neutron fission spectrum, χ_{Di} is the delayed neutron fission spectrum for precursor group i, λ_i is the decay constant for precursor group i, and $d_i(\underline{N})$ is the precursor concentration of group i. The components of the vectors $\underline{\nu}$ and $\underline{\sigma}$ correspond to those of the composition $\underline{N}$.

The Boltzmann operator $\mathbf{B}[\underline{N}(\underline{r},t),\underline{\sigma}(\underline{r},E)]$ can be used to re-write the transport equation as

$$\frac{1}{v}\frac{\partial}{\partial t}\phi(\rho) = \mathbf{B}(\underline{N},\underline{\sigma})\phi(\rho) + \sum_i \chi_{Di}(E)\lambda_i d_i(\underline{N}) \tag{4.5}$$

The fission rate in the system is held constant. This has been described as a constant power constraint, but as no allowance is made for the power produced

per fission, the fission rate description is more accurate. The P notation is maintained for ease of comparison to the original formulation. The constraint is expressed as

$$P = \left[\underline{N}(\underline{r},t)\cdot\underline{\sigma}_f(\underline{r},E)\phi(\rho)\right]_{\underline{r},\hat{\underline{\Omega}},E} \tag{4.6}$$

Equation (4.5) can be simplified by assuming the flux only changes slowly with time, which means the term on the left-hand side of the equation can be considered to be zero. The timescales over which reactor burn-up is studied are significantly longer than those of delayed neutron transients, and it can be assumed that the reactor is critical and the precursors are in a steady state, as the timescales used in burn-up problems are significantly longer than those seen in precursor transients. Changing the prompt fission spectrum to

$$\chi(E) = (1-\beta)\chi(E) + \sum_i \beta_i \chi_{Di}(E) \tag{4.7}$$

means equation (4.5) can be reduced to

$$\mathbf{B}\phi = 0 \tag{4.8}$$

This, in turn, can be re-written in terms of neutron production $\mathbf{F}$ and loss $\mathbf{L}$ operators and the fundamental eigenvalue λ.

$$(\mathbf{L} - \lambda\mathbf{F})\phi = 0 \tag{4.9}$$

4.2.1 The quasi-static approximation

To simplify the burn-up problem, it is assumed that the flux can be split into shape and amplitude functions, in the same fashion as in the point-kinetics equations.

$$\phi(\rho) = \Phi(t)\psi(\underline{r},\hat{\underline{\Omega}},E) \tag{4.10}$$

The shape function ψ can be found from equation (4.9), which for time interval τ of the quasi-static approximation is written

$$\big(\mathbf{L}(\underline{N}_\tau) - \lambda\mathbf{F}(\underline{N}_\tau)\big)\psi_\tau(\underline{r},\hat{\underline{\Omega}},E) = 0 \tag{4.11}$$

and $\psi_\tau$is normalised such that its integral over the whole system is unity.

$$\left[\psi_\tau(\underline{r},\hat{\underline{\Omega}},E)\right]_{\underline{r},\hat{\underline{\Omega}},E} = 1 \tag{4.12}$$

The value of Φ can then be determined from the fission rate constraint.

$$\Phi(t) = \frac{P}{\left[\underline{N}(\underline{r},t)\cdot\underline{\sigma}_f(\underline{r},E)\psi(\underline{r},\hat{\underline{\Omega}},E)\right]_{\hat{\underline{\Omega}},E,V}} \tag{4.13}$$

where V represents the volume of the system. In a typical calculation, the values of Φ and ψ are determined at the beginning of a time interval and then treated as constant for the duration of the interval. The burn-up of the system can then be determined by finding the flux shape and amplitude for a given interval, depleting the composition with those values, and repeating this process for the appropriate number of time intervals.

$$\frac{\partial}{\partial t}\underline{N}(\underline{r},t) = \Phi_\tau \mathbf{R}_\tau \underline{N}(\underline{r},t) + \mathbf{D}\underline{N}(\underline{r},t) + \underline{C}(\underline{r},t) \qquad t_\tau^+ < t < t_{\tau+1}^- \tag{4.14}$$

t_τ^- and t_τ^+ represent the times immediately before and after the boundary of time interval τ.

4.2.2 Sensitivity theory

The goal of sensitivity analysis is to predict how the system will respond to changes of the input parameters. The response of the system is described using a functional

$$R = R\left(\Phi, \underline{N}, \underline{h}\right) \tag{4.15}$$

$\underline{h}$ is the vector response function and represents the reactor behaviour being studied. For example if the response was the amount of plutonium at the end of the burn-up cycle, the components of $\underline{h}$ would be one for the plutonium isotopes and zero for all others at the end of the period being studied.

For some parameter α, the sensitivity of R to changes in α is

$$\frac{\delta R}{R} = \left(S(\rho)\frac{\delta\alpha}{\alpha}(\rho)\right) + \text{higher order terms} \tag{4.16}$$

where $S(\rho)$ is the sensitivity coefficient. If the value of $\delta\alpha$ is small, then the first order term dominates. R can be expanded as a Taylor series about the

original value.

$$R' \cong R + \left(\frac{\partial R}{\partial \alpha}\right)\delta\alpha + \left(\frac{\partial R}{\partial \underline{N}}\right)\frac{d\underline{N}}{d\alpha}\delta\alpha + \left(\frac{\partial R}{\partial \phi}\right)\frac{d\phi}{d\alpha}\delta\alpha \tag{4.17}$$

$$\frac{\delta R}{R} \cong \frac{\alpha}{R}\left(\frac{\partial R}{\partial \alpha} + \frac{\partial R}{\partial \underline{N}}\frac{d\underline{N}}{d\alpha} + \frac{\partial R}{\partial \phi}\frac{d\phi}{d\alpha}\right)\frac{\delta\alpha}{\alpha} \tag{4.18}$$

$$S(\rho) = \frac{\alpha}{R}\left(\frac{\partial R}{\partial \alpha} + \frac{\partial R}{\partial \underline{N}}\frac{d\underline{N}}{d\alpha} + \frac{\partial R}{\partial \phi}\frac{d\phi}{d\alpha}\right) \tag{4.19}$$

This gives the sensitivity coefficient $S(\rho)$ in terms of R, α, $\underline{N}$ and ϕ. The derivatives of $\underline{N}$ and ϕ with respect to α are found from the coupled neutron transport, burn-up, and constant fission rate equations described earlier.

4.2.3 Adjoint quasi-static burn-up

The derivation of the coupled adjoint equations is performed using a variational technique, of the kind detailed in Pomraning (1967) and Stacey (1974). The quasi-static equations (4.11), (4.12), (4.13), and (4.14) are used as constraints on the response. The functional K is defined by combining the response and the quasi-static equations in the form of Lagrange multipliers.

$$\begin{aligned}
&K[\underline{N}, \psi_\tau, \Phi_\tau, \alpha, \lambda, \underline{h}] \\
&= R[\underline{N}, \psi_\tau, \Phi_\tau, \underline{h}] + \sum_{\tau=0}^{T}\Bigg\{\int_{t_\tau^+}^{t_{\tau+1}^-}\Bigg[\underline{N}^*(\underline{r},t)\left([\psi_\tau \mathbf{R}]_{E,\hat{\underline{\Omega}}}\Phi_\tau + \mathbf{D} - \frac{\partial}{\partial t}\right)\underline{N}(\underline{r},t) \\
&\quad + \underline{C}(\underline{r},t)\Bigg]_V dt - \left[\Gamma^*(\rho)\left(\mathbf{L}(\underline{N}_\tau) - \lambda_\tau \mathbf{F}(\underline{N}_\tau)\right)\psi_\tau(\rho)\right]_{\hat{\underline{\Omega}},E,V} \\
&\quad - P_\tau^*\left([\psi_\tau \underline{\sigma}_f \underline{N}_\tau]_{\hat{\underline{\Omega}},E,V}\Phi_\tau - P_\tau\right) - a_\tau\left([\psi_\tau]_{\hat{\underline{\Omega}},E,V} - 1\right)\Bigg\}
\end{aligned} \tag{4.20}$$

where T is the number of time intervals used in the problem, $\underline{N}_\tau = \underline{N}(\underline{r}, t_\tau)$, and $\underline{N}^*(\underline{r},t)$, $\Gamma_\tau^*(\rho)$, P_τ^*, and a_τ are Lagrange multipliers representing the quasi-static equations. It can be seen that if $\underline{N}$, ψ_τ, and Φ_τ are exact solutions to the coupled equations then $K = R$.

If the perturbed state K' is expanded about the unperturbed state K and

terms above first order are neglected then

$$K' = K + \frac{\partial K}{\partial \alpha}\delta\alpha + \frac{\partial K}{\partial \underline{N}}\delta\underline{N} + \frac{\partial K}{\partial \underline{h}}\delta\underline{h} + \sum_{\tau}\left(\frac{\partial K}{\partial \psi_\tau}\delta\psi_\tau + \frac{\partial K}{\partial \Phi_\tau}\delta\Phi_\tau + \frac{\partial K}{\partial \lambda_\tau}\delta\lambda_\tau\right) \tag{4.21}$$

If the partial derivatives of K with respect to $\underline{N}$, ψ_τ, Φ_τ, and λ_τ can be made equal to zero then

$$\delta R = \frac{\partial K}{\partial \alpha}\delta\alpha + \frac{\partial K}{\partial \underline{h}}\delta\underline{h} \tag{4.22}$$

$$\frac{\delta R}{R} = \frac{\alpha}{R}\left(\frac{\partial K}{\partial \alpha} + \frac{\partial R}{\partial \underline{h}}\frac{\partial \underline{h}}{\partial \alpha}\right)\frac{\delta\alpha}{\alpha} \tag{4.23}$$

$$S(\rho) = \frac{\alpha}{R}\left(\frac{\partial K}{\partial \alpha} + \frac{\partial R}{\partial \underline{h}}\frac{\partial \underline{h}}{\partial \alpha}\right) \tag{4.24}$$

This makes the value of S comparatively simple to determine, so the focus of the problem is shifted to the partial derivatives in equation (4.21) that were taken as equal to zero earlier. First the derivative of K with respect to Φ_τ

$$\frac{\partial K}{\partial \Phi_\tau} = \frac{\partial R}{\partial \Phi_\tau} + \int_{t_\tau^+}^{t_{\tau+1}^-}\left[\underline{N}^*, [\psi_\tau \mathbf{R}]_{\underline{\hat{\Omega}},E}\,\underline{N}\right]_V dt - P_\tau^*\left[\psi_\tau \underline{\sigma}_f \cdot \underline{N}_\tau\right]_{\underline{\hat{\Omega}},E,V} \tag{4.25}$$

This gives the value of P_τ^* as

$$P_\tau^* = \frac{\int_{t_\tau^+}^{t_{\tau+1}^-}\left[\underline{N}^*, [\psi_\tau \mathbf{R}]_{\underline{\hat{\Omega}},E}\,\underline{N}\right]_V dt + \frac{\partial R}{\partial \Phi_\tau}}{\left[\psi_\tau \underline{\sigma}_f \cdot \underline{N}_\tau\right]_{\underline{\hat{\Omega}},E,V}} \tag{4.26}$$

Next the derivative with respect to ψ_τ is considered.

$$\frac{\partial K}{\partial \psi_\tau} = \left[\frac{\partial R}{\partial \psi_\tau} - \left(\mathbf{L}^* - \lambda_\tau \mathbf{F}^*\right)\Gamma_\tau^* - P_\tau^*\Phi_\tau \underline{\sigma}_f \cdot \underline{N}_\tau + \Phi_\tau \int_{t_{\tau+}}^{t_{\tau+1}^-} \underline{N}^* \mathbf{R} \underline{N} dt - a\right] \tag{4.27}$$

where the commutative properties of the adjoint operators $\mathbf{L}^*$ and $\mathbf{F}^*$ have been used to re-arrange the equation. To make the equation vanish, it can be formulated as a generalised eigenvalue problem

$$\left(\mathbf{L}^* - \lambda_\tau \mathbf{F}^*\right)\Gamma_\tau^* = Q_\tau^* \tag{4.28}$$

where

$$Q_\tau^* = \frac{\partial R}{\partial \psi_\tau} + \Phi_\tau \int_{t_\tau^+}^{t_{\tau+1}^-} \underline{N}^* \mathbf{R} \underline{N} dt - \Phi_\tau P_\tau^* \underline{\sigma}_f \cdot \underline{N}_\tau - a_\tau \tag{4.29}$$

Equations (4.28) and (4.29) require that the flux shape and adjoint source be orthogonal

$$[\psi_\tau Q_\tau^*]_{\underline{\hat{\Omega}},E,V} = 0 \tag{4.30}$$

From this requirement it follows that

$$a_\tau = \left[\psi_\tau \frac{\partial R}{\partial \psi_\tau}\right]_{\underline{\hat{\Omega}},E,V} - \Phi_\tau \left[\frac{\partial R}{\partial \Phi_\tau}\right]_{\underline{\hat{\Omega}},E,V} \tag{4.31}$$

Typically this will mean that a_τ is zero, e.g. if R is bilinear in ψ_τ and Φ_τ or is a bilinear ratio.

The derivative with respect to λ_τ is

$$\frac{\partial K}{\partial \lambda_\tau} = [\Gamma_\tau^* \mathbf{F} \psi_\tau]_{\underline{\hat{\Omega}},E,V} \tag{4.32}$$

and setting this term to zero means Γ_τ^* must be orthogonal to the fission source at $t = t_\tau$. There must therefore not be any contamination of Γ_τ^* with the fundamental solution of the homogeneous equation. If Γ_p^* is a particular solution of equation (4.28) and is orthogonal to the fundamental solution of the homogeneous equation ϕ_h^*, then $\Gamma_p^* + b\phi_h^*$ is also a solution of equation (4.29) for any value of b. Equation (4.32) solves this problem by making b equal to zero and therefore $\Gamma_\tau^* = \Gamma_p^*$.

The removal of the partial derivative of K with respect to $\underline{N}$ is more involved than the other cases. Assuming a change of $\delta\underline{N}$ in $\underline{N}$ leads to a change of δK in K

$$\begin{aligned}\delta K(\delta \underline{N}) = &\left[\frac{\partial R}{\partial \underline{N}}, \delta \underline{N}\right]_\rho + \sum_{\tau=1}^{T} \Bigg\{ \int_{t_\tau^+}^{t_{\tau+1}^-} \left[\delta \underline{N} \left([\psi_\tau \mathbf{R}^*]_{\underline{\hat{\Omega}},E} \Phi_\tau + \mathbf{D}^* + \frac{\partial}{\partial t} \right) \underline{N}^* \right]_V dt \\ &- \left[\underline{N}_{\tau+1}^{*-} \delta \underline{N}_{\tau+1}^- - \underline{N}_\tau^{*+} \delta \underline{N}_\tau^+\right]_V - \left[\delta \underline{N}_\tau \left[\Gamma_\tau^* \frac{\partial}{\partial \underline{N}_\tau} (\mathbf{L} - \lambda_\tau \mathbf{F}) \psi_\tau\right]_{\underline{\hat{\Omega}},E}\right]_V \\ &- P_\tau^* \Phi_\tau \left[\delta \underline{N}_\tau \left[\psi_\tau \underline{\sigma}_f\right]_{\underline{\hat{\Omega}},E}\right]_V \Bigg\}\end{aligned} \tag{4.33}$$

This expression can be made equal to zero through several steps. The first two terms on the right hand side can be removed if

$$\Phi_\tau \left[\psi_\tau \mathbf{R}^*\right]_{\underline{\hat{\Omega}},E} \underline{N}^* + \mathbf{D}^* \underline{N}^* = -\frac{\partial}{\partial t}\underline{N}^* - \left[\frac{\partial R}{\partial \underline{N}}\right]_{\underline{\hat{\Omega}},E} \text{ for } t_\tau^+ < t < t_{\tau+1}^- \quad (4.34)$$

This can be re-written in a form similar to the burn-up equation

$$\mathbf{M}^* \underline{N}^* + \underline{C}^* = -\frac{\partial}{\partial t}\underline{N}^* \quad (4.35)$$

with $\underline{C}^*$ defined as

$$\underline{C}^* = \left[\frac{\partial R}{\partial \underline{N}}\right]_{\underline{\hat{\Omega}},E} \quad (4.36)$$

This describes the behaviour of $\underline{N}^*$ within the time interval, but not at the boundaries of the intervals. The boundary behaviour can be determined from the other terms in equation (4.33), and by taking advantage of the continuity of $\underline{N}$ over the time boundaries.

$$\sum_{\tau=1}^{T}\left[\delta\underline{N}_\tau \left\{\underline{N}_\tau^{*+} - \left[\Gamma_\tau^* \frac{\partial}{\partial \underline{N}_\tau}\left(\mathbf{L} - \lambda_\tau \mathbf{F}\right)\psi_\tau\right]_{\underline{\hat{\Omega}},E} - \Phi_\tau P_\tau^* \left[\psi_\tau \underline{\sigma}_f\right]_{\underline{\hat{\Omega}},E}\right\} - \delta\underline{N}_{\tau+1}\underline{N}_{\tau+1}^{*-}\right]_V \quad (4.37)$$

The terms containing $\delta\underline{N}_\tau$ can be removed, except at $t = 0$ and $t = t_f$ by allowing the value of $\underline{N}^*$ to be discontinuous at the boundary and requiring

$$\begin{aligned}\underline{N}^*(\underline{r}, t_\tau^-) &= \underline{N}^*(\underline{r}, t_\tau^+) - \left[\Gamma^* \frac{\partial}{\partial \underline{N}_\tau}(\mathbf{L} - \lambda\mathbf{F})\psi_\tau + \Phi_\tau P_\tau^* \underline{\sigma}_f \psi_\tau\right]_{\underline{\hat{\Omega}},E} \\ &= \underline{N}^*(\underline{r}, t_\tau^+) - \left[\Gamma_\tau^* \underline{\beta}_\tau + P_\tau^* \underline{\Pi}_\tau\right]_{\underline{\hat{\Omega}},E} \end{aligned} \quad (4.38)$$

where

$$\underline{\beta}_\tau = \frac{\partial}{\partial \underline{N}_\tau}\left(\mathbf{L} - \lambda_\tau \mathbf{F}\right)\psi_\tau \quad (4.39)$$

$$\underline{\Pi}_\tau = \Phi_\tau \underline{\sigma}_f \psi_\tau \quad (4.40)$$

and the components of $\underline{\beta}$ and $\underline{\Pi}$ correspond to those of $\underline{N}$.

The term containing $\delta\underline{N}_f$ can be removed if the final time condition is fixed as

$$\underline{N}^*(\underline{r}, t_f) = 0 \tag{4.41}$$

Equations (4.26), (4.28), (4.35), (4.38), and (4.41) form the adjoint coupled system for an arbitrary response. In many cases, the response of interest is a value at a specified time, typically t_f.

$$R = R\left[\underline{N}_f, \underline{h}\right] = R\left[\underline{N}(\underline{r}, t)\delta(t - t_f), \underline{h}\right] \tag{4.42}$$

In such cases, the adjoint source term becomes a fixed final condition and the adjoint system can be simplified.

$$\underline{C}^*(\underline{r}, t) = 0 \quad t < t_f \tag{4.43}$$

$$\underline{N}_f^* = \frac{\partial R}{\partial \underline{N}_f} \quad t = t_f \tag{4.44}$$

$$\frac{\partial R}{\partial \Phi_\tau} = \frac{\partial R}{\partial \psi_\tau} = 0 \quad t = t_\tau \tag{4.45}$$

4.2.4 Procedure

The adjoint problem is solved starting from t_f and ending at t_0. Equation (4.35) is solved using the appropriate values of $\underline{N}_f^*$ and $\underline{C}_f^*$. The value of P_{T-1}^* can then be determined with equation (4.26) by combining the values found for $\underline{N}^*$ and the information from the forward problem. This allows the value of Q_{T-1}^* to be calculated using equation (4.29), which can then be used in turn to find Γ_{T-1}^* from equation (4.28). The change in $\underline{N}^*$ at the boundary of the time interval can then be found from equation (4.38). This process can be repeated until $t = 0$ is reached.

4.3 Implementation

The coupled DPT model derived by Williams (1979) was built as a combination of modules from the SCALE code package (SCALE manual, 2009) and a purpose built code. The custom code was written in Python, with use of the NumPy (Oliphant, 2006) and SciPy modules (Jones et al., 2001–), the Cython language (Behnel et al., 2011) for the numerically intensive work, and Matplotlib (Hunter, 2007) for plotting.

4.3.1 The forward problem

Once a model had been built for study, the first stage was to solve the forward depletion problem. Calculations were run using both the TSUNAMI and TRITON modules of SCALE. The TSUNAMI run provided the flux shape ψ, fundamental eigenvalue λ, and multi-group cross sections for the nuclides in the initial composition, while the TRITON run gave single group transmutation cross sections for a much wider range of nuclides. These two calculations were performed at the start of each time interval. 238 energy groups were used, and those values with energy dependence were represented in the code as vectors with a component value for each group.

Although TRITON performs a burn-up calculation, these results were not used in the coupled DPT implementation. The theory developed earlier is suited for use with the quasi-static approximation, but not for the predictor-corrector method employed by TRITON. The method used by TRITON is a variant of the quasi-static method, in which the flux is held constant over a given time interval, but is determined using the composition in the middle of the time interval, which is found using the flux from the previous time step (or from the beginning of the burn-up cycle for the first interval). The forward burn-up problem was therefore solved according to the method in the coupled DPT model, using the one group cross sections produced by TRITON and the VODE solver (Brown et al., 1989) available in the SciPy package (Jones et al., 2001–).

4.3.2 The adjoint problem

The source vector $\underline{h}$ was determined appropriately according to the response being studied. For example, when studying the end of cycle (EOC) criticality response, the worths found from an EOC TSUNAMI calculation were used for the source components. Once the source had been formulated, the adjoint burn-up problem was solved in the same manner as the forward burn-up problem. Once the behaviour of $\underline{N}^*$ throughout the time interval had been determined, it was used along with $\underline{N}$ for the appropriate interval to find the value of P^*. The integral in equation (4.26) was approximated using Romberg's method (Romberg, 1955).

The determination of the adjoint source Q^* relies on the multi-group transmutation matrix $\mathbf{R}$. These values are not available from the TRITON or

TSUNAMI calculations. TRITON works with one group transmutation cross sections, while TSUNAMI gives multi-group cross sections for neutron production and loss processes, instead of nuclide transmutation cross sections. TSUNAMI produces cross sections only for those nuclides present in the system at the time, so values are not available for any nuclide not present at the start of the time interval, but produced during it, such as a fission product.

The multi-group cross section data were approximated using a combination of the values produced by TRITON and TSUNAMI. If data were available for a given nuclide from TSUNAMI, then these were used in the multi-group transmutation matrix. If no data were available, then the value was approximated as the one group value. For some processes only some of the necessary data were available, such as the production of a fission product from an actinide initially present in the system. Here the fission cross section of the actinide was known, but the yield of the fission product from fission of that actinide in that energy group was not. The yield was approximated using the ratio of the one group production of that nuclide to the sum of all the one group production processes of all nuclides from fission of the original actinide. The values for neutron capture and other processes were determined in a similar fashion.

This approximation will cause some inaccuracy in the results of the coupled DPT model. The values of Q^* will be affected, and they in turn will affect the values of Γ^*. This means the inaccuracies will be seen in the adjustment of the values of $\underline{N}^*$ at the time interval boundary, from equation (4.38). The nuclides that are present in the system from the start will be modelled with more accuracy than those that are produced during the burn-up period, and this means the quality of the results will depend on the response being studied. Responses that are expressed mainly or completely in terms of the nuclides initially present in the system can be expected to give better results than those with large contributions from nuclides produced during burn-up.

Once the value of Q^* had been found, it was used as the source in a generalised eigenvalue calculation in XSDRN. The value of Γ^* was read from the XSDRN output file. The components of $\underline{\beta}$ and $\underline{\underline{\Pi}}$ were found from the cross sections produced by TSUNAMI at the beginning of the time interval. These were then used to find the new value of $\underline{N}^*$ as in equation (4.38). This process can then be repeated over the next time interval in the adjoint problem.

Table 4.1: BOC nuclide worths for 30 days of burn-up from coupled and uncoupled DPT compared to those found from perturbed forward calculations

Nuclide	Worth (per 10^{24} atoms)		
	Perturbed forward	Uncoupled DPT	Coupled DPT
U-235	7.18	7.29	7.30
U-238	-0.448	-0.481	-0.484
Pu-239	8.50	8.66	8.67
Pu-240	0.772	0.783	0.783
Pu-241	13.0	13.2	13.2
Pu-242	0.180	0.196	0.195

4.4 Fast system results

4.4.1 End of cycle criticality response

Once the code had been written, it was first tested on a model of a sodium cooled fast reactor mixed oxide (MOX) fuel pin in an infinite lattice. The model was subjected to 30 days of burn-up, which was modelled with one time interval, and the response studied with the coupled DPT method was the end of cycle criticality. This burn-up period was chosen as a reasonable compromise between loss of accuracy due to the quasi-static approximation and computational load. The results were compared to those found from perturbed forward calculations, which were performed for U-235, U-238, Pu-239, Pu-240, Pu-241, Pu-242, with the beginning of cycle (BOC) amount of each nuclide being perturbed in steps of 1% up to values of $\pm 5\%$. A graph of the results for Pu-239 is shown in figure 4.1, and the coupled and uncoupled DPT values for each nuclide can be found in table 4.1, along with values extrapolated from the perturbed forward calculations with a least squares fit. The worths are given in units of per 10^{24} atoms, as the measurement of the criticality has no unit. The results in table 4.1 show that the DPT values are comparable to those from the perturbed forward calculations. There are differences between the different methods, with the gap between either of the DPT results and the perturbed forward ones being larger than the gap between the two sets of DPT results. The differences in the values may be due to the approximation of the multi-group transmutation matrix, or could be caused by the re-calculation

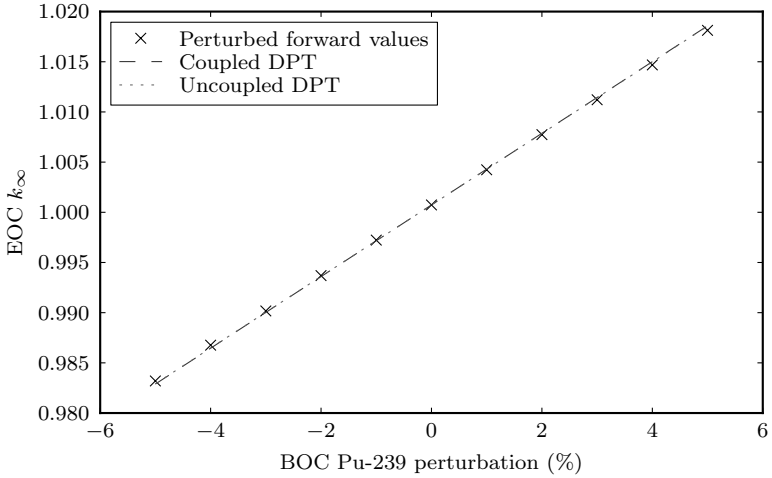

Figure 4.1: Comparison of EOC criticality values from forward calculations with perturbed initial composition and predictions from coupled DPT for Pu-239 after 30 days of burn-up

of the EOC criticality for each of the perturbed cases, instead of determining the value by using the worths. The DPT results are still reasonable estimates of the contribution of a BOC nuclide to the EOC criticality however. It is important to remember that the DPT results were found by performing one adjoint calcuation, while the perturbed forward ones were found from several additional calculations for each nuclide.

4.4.2 Increased burn-up period

The small difference between the two sets of DPT results is due in part to the short burn-up time. The longer the burn-up period, the more the composition changes and the greater the effect on the flux. Another set of calculations was performed with a burn-up period of 300 days, using one time interval. Using only one interval for this length of burn-up is unlikely to produce physically accurate results, as the quasi-static approximation becomes less appropriate over longer time periods. It does however show the effect of coupling in the DPT model, as the difference between the coupled and uncoupled results becomes more pronounced with time. The results for Pu-239 are shown in

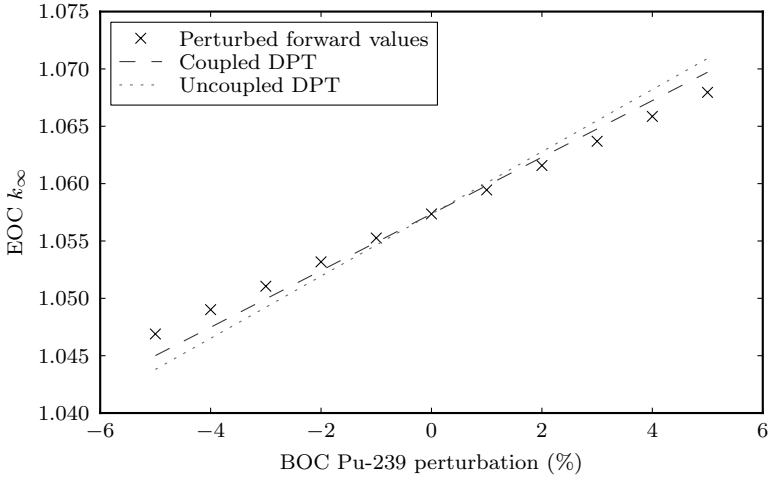

Figure 4.2: Comparison of EOC criticality values from perturbed forward calculations and predictions from coupled DPT for Pu-239 after 300 days of burn-up

figure 4.2, and for the full set of six nuclides in table 4.2. The difference between the coupled and uncoupled version is larger after the longer burn-up period. The coupled value is closer than the uncoupled one to that found from the forward calculations except for the case of U-238. Pu-240 shows a large difference between the perturbed forward and DPT values. It is likely that this has been caused by the long burn-up period changing the behaviour of the forward calculations beyond what can be predicted by the DPT method. The non-fissile nature of Pu-240 combined with its propensity to produce fissile Pu-241 could explain the scale of the difference.

The differences between the DPT values and those from the perturbed forward calculations could arise from several sources. Changes to the initial composition affect not only the value of $\underline{N}_0$, but also the initial flux shape and amplitude. While the coupling allows for changes to the flux, the cross sections are also affected and this is not included in the coupled model. This alters the transmutation matrix, making the comparison between the perturbed forward and adjoint problems less accurate. A possible solution to this problem is the DPT model proposed in Downar (1992) that allows for the burn-up dependense

Table 4.2: BOC nuclide worths for 300 days of burn-up from coupled and uncoupled DPT compared to those found from perturbed forward calculations

Nuclide	Worth (per 10^{24} atoms)		
	Perturbed forward	Uncoupled DPT	Coupled DPT
U-235	3.64	5.31	4.59
U-238	-0.232	-0.288	-0.343
Pu-239	5.12	6.59	6.00
Pu-240	1.13	0.986	0.844
Pu-241	6.55	9.38	8.46
Pu-242	0.0388	0.108	7.62×10^{-3}

of the cross sections. The approximation of the multi-group transmutation cross sections may have given inaccurate values for the source in the generalised adjoint problem, leading to issues with the determination of the behaviour of $\underline{N}^*$ at the time boundary. It is also possible that the worths that form the source for the adjoint problem were not determined to sufficient accuracy to solve the problem well. Further, the solver used for the problem may have struggled with what is a very stiff matrix.

4.4.3 Fixed response worths

To examine the possibility that the re-calculation of the EOC criticality was the cause of the differences between the perturbed forward and DPT values, the worths used as the source for the adjoint calculation were used to find the response seen in the perturbed forward calculations. Instead of finding the criticality response by performing a TSUNAMI calculation at the end of the burn-up cycle, the response was determined by taking the inner product of the adjoint source $\underline{h}$ and the EOC composition $\underline{N}_f$. Having determined the response with this method, a least squares fit was used to determine a worth for each nuclide. The values for the two burn-up periods are shown in table 4.3.

Comparing the values in table 4.1 and 4.3, it can be seen that the fixed response worths have had a relatively small effect on the results found for the perturbed forward calculations. The changes from using the fixed response worths improve the match between the perturbed forward and DPT calculations.

Table 4.3: BOC nuclide worths for 30 and 300 days of burn-up from perturbed forward calculations with fixed response worths

Nuclide	Worth (per 10^{24} atoms)	
	30 days	300 days
U-235	7.18	3.70
U-238	-0.484	-0.234
Pu-239	8.56	5.12
Pu-240	0.773	1.12
Pu-241	13.0	6.57
Pu-242	0.183	-0.0383

The values from the 300 day burn-up period, shown in tables 4.2 and 4.3, generally improve the match between the forward and adjoint results, but the difference remains considerable. The result for Pu-242 is particularly bad.

From these results, it can be concluded that some of the difference between the perturbed forward and DPT results can be attributed to changes of the response worths. While fixing the response worths improved the results, it did not produce a close fit for the whole set of nuclides tested. The differences in the long burn-up period results may stem from the inaccuracies inherent in performing the burn-up calculation using a single time step. The short burn-up calculation does not suffer from the same problems, but still shows some differences. To study the issue further, a simplified response was used, and the effects of changes in the transmutation matrix were studied.

4.4.4 End of cycle Pu-239 response

The response being studied was changed to the end of cycle amount of Pu-239 in order to simplify the problem. This also has the effect of removing the need for an additional TSUNAMI run at the end of the cycle, so any changes in the worths could be discounted.

To test how well the solver was handling the transmutation matrix, the results of the adjoint problem were compared to those produced by running the perturbed forward problem without changing the matrix components from the reference calculation. That is, the components of $\underline{N}$ were varied, while $\mathbf{M}$ was

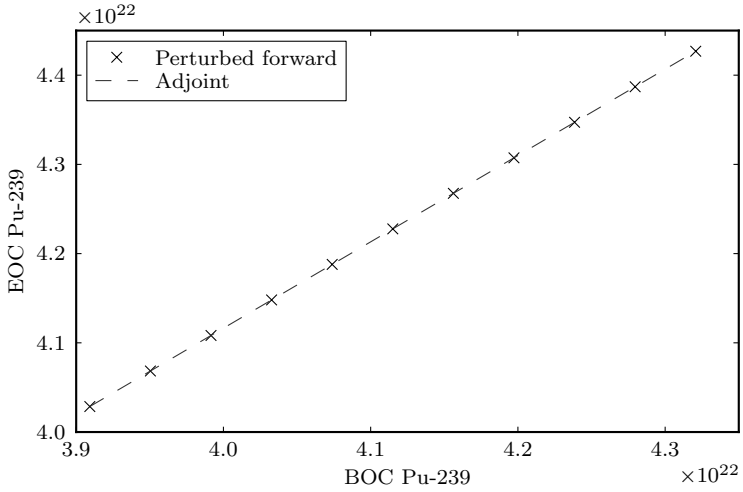

Figure 4.3: Comparison of results from adjoint and perturbed forward calculations of EOC Pu-239 response to BOC Pu-239 amount with constant transmutation matrix

kept constant. This should produce very good agreement between the adjoint and perturbed forward results, and removes the need for the coupling between the neutron and nuclide fields. The results for the variation of BOC Pu-239 are shown in figure 4.3, and the values from the adjoint and perturbed forward test nuclides are given in table 4.4. It can be seen that the adjoint values are in good agreement with those from the perturbed forward calculations. The only difference is in the values for U-235, and is small compared to the worths, which are themselves the smallest of the set. From this it was concluded that the solver was handling the transmutation matrix well despite its stiffness.

Once the transmutation matrix was allowed to vary with the changes in the initial composition, the importance of the coupling in the DPT model could be seen. Table 4.5 shows the coupled and uncoupled DPT worths for the EOC Pu-239 response, along with the value found from a fit to the perturbed forward calculations. These results show the strong effect the coupling can have, with changes of several orders of magnitude being seen in some worths, e.g. U-235. The forward burn-up results with perturbed BOC U-235 amounts also show a much stronger effect with the coupling included, as shown in figure

Table 4.4: BOC nuclide worths for EOC Pu-239 with constant transmutation matrix

Nuclide	Worth (per atom)	
	Perturbed forward	Adjoint
U-235	2.21×10^{-10}	2.20×10^{-10}
U-238	3.48×10^{-3}	3.48×10^{-3}
Pu-239	9.68×10^{-1}	9.68×10^{-1}
Pu-240	3.32×10^{-6}	3.32×10^{-6}
Pu-241	6.53×10^{-8}	6.53×10^{-8}
Pu-242	2.08×10^{-9}	2.08×10^{-8}

Table 4.5: BOC nuclide worths for EOC Pu-239 response from adjoint and perturbed forward calculations

Nuclide	Worth (per atom)		
	Perturbed forward	Uncoupled DPT	Coupled DPT
U-235	-1.88×10^{-2}	2.20×10^{-10}	-1.74×10^{-2}
U-238	2.97×10^{-3}	3.48×10^{-3}	2.66×10^{-3}
Pu-239	9.52×10^{-1}	9.68×10^{-1}	9.53×10^{-1}
Pu-240	-2.88×10^{-3}	3.29×10^{-6}	-3.14×10^{-3}
Pu-241	-2.37×10^{-2}	6.16×10^{-8}	-2.26×10^{-2}
Pu-242	-2.26×10^{-3}	2.08×10^{-8}	-2.16×10^{-3}

4.4, making the comparison between the fit and the adjoint more meaningful.

The heavier plutonium isotopes also show significant differences between the coupled and uncoupled values, with sign changes in the worths of Pu-240, Pu-241, and Pu-242. The flux-related effects produce much larger changes in the production of Pu-239 over the course of the cycle than the transmutation effects.

The results show that the differences between the perturbed forward and adjoint worths are related to the changes in the transmutation matrix as the composition is altered. When the matrix is held constant the results from the forward and adjoint calculations were in close agreement. Given

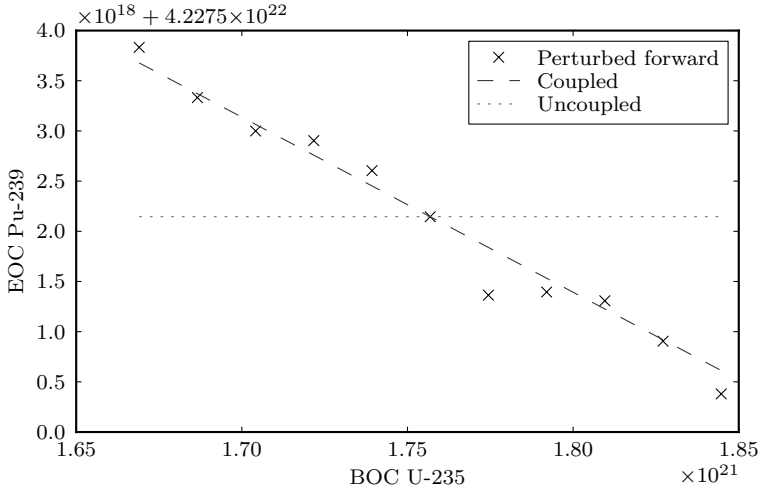

Figure 4.4: Comparison of results from coupled and uncoupled adjoint with perturbed forward calculations of EOC Pu-239 response to BOC U-235 amount

how the coupling improves the results, particularly with the EOC Pu-239 response, it can be concluded that the values produced by the coupled model as implemented can be considered to be reasonably accurate.

4.4.5 Reloading calculation

The fast pin model was reloaded using plutonium with the same isotopic make up as the EOC plutonium in the model after one burn-up period of 30 days, mixed with depleted uranium. The new composition was determined using the method described in chapter 3. The short burn-up period meant that there was only a small difference in the composition of the plutonium in the original and reloaded systems. The compositions used are shown in table 4.6.

Once the reloading composition had been determined, the reloaded system was depleted over a burn-up period of 30 days and the BOC and EOC k_∞ values of the original and reloaded systems were compared, as shown in table 4.7.

Although the match between the two sets of k_∞ values is not perfect, the difference is very small. The change in k_∞ over the burn-up period is also very

Table 4.6: Original and reloaded fast pin fuel compositions

Nuclide	Density (atoms/b-cm)	
	Original	Reloaded
O-16	3.36×10^{-2}	3.28×10^{-2}
U-235	3.79×10^{-5}	3.70×10^{-5}
U-238	1.51×10^{-2}	1.48×10^{-2}
Pu-236	4.47×10^{-11}	4.38×10^{-11}
Pu-237	2.99×10^{-10}	3.08×10^{-10}
Pu-238	2.75×10^{-5}	2.59×10^{-5}
Pu-239	8.88×10^{-4}	8.82×10^{-4}
Pu-240	4.20×10^{-4}	4.08×10^{-4}
Pu-241	1.86×10^{-4}	1.75×10^{-4}
Pu-242	1.08×10^{-4}	1.05×10^{-4}
Pu-243	4.09×10^{-9}	7.07×10^{-9}
Pu-244	3.38×10^{-10}	3.70×10^{-10}

Table 4.7: Original and reloaded fast pin BOC and EOC k_∞ values

Time	k_∞	
	Original	Reloaded
BOC	0.9956	0.9952
EOC	1.0007	1.0004

similar for the two compositions. These results indicate that the coupled DPT worths can produce accurate new compositions when used in the reloading calculation.

4.5 Thermal system results

Thermal systems have stronger effects connecting the flux and the composition, as burn-up produces isotopes such as Xe-135 that have very high neutron capture cross sections at thermal energies and have a significant effect on the flux. To test how well these effects were modelled, the coupled DPT method

Table 4.8: BOC nuclide worths for EOC criticality response of a thermal system from perturbed forward, coupled, and uncoupled DPT calculations

Nuclide	Worth (per 10^{24} atoms)		
	Perturbed forward	Uncoupled DPT	Coupled DPT
U-235	3.16	2.92	3.01
U-238	-0.148	-0.189	-0.189
Pu-239	4.56	4.04	4.28
Pu-240	-9.64	-9.42	-9.34
Pu-241	10.7	10.2	10.5
Pu-242	-10.9	-10.7	-10.6

was applied to a PWR MOX fuel pin in an infinite lattice. The responses used were the end of cycle criticality and the end of cycle Pu-239 amount.

4.5.1 End of cycle criticality response

The EOC criticality after 30 days of burn-up was calculated as described previously, and the results produced by the adjoint model were compared to those from perturbed forward calculations for the six nuclides U-235, U-238, Pu-239, Pu-240, Pu-241, Pu-242. The worths from the forward calculations were determined using least squares fits to the results of the perturbed calculations. The coupled and uncoupled DPT results are shown in table 4.8 along with the values produced by the fit to the perturbed forward calculations. Figure 4.5 shows the results of changing the amount of Pu-239 in the initial composition.

The results for the thermal system show only small variations between the coupled and uncoupled values. The inclusion of the coupling produces a slight improvement in the set of values found.

4.5.2 Increased burn-up period

The calculation was repeated with the burn-up period increased to 300 days. This produced a larger change in the composition and made the effect of the coupling in the DPT model more pronounced. The results of this calculation are shown in table 4.9, and a comparison of the coupled and uncoupled values

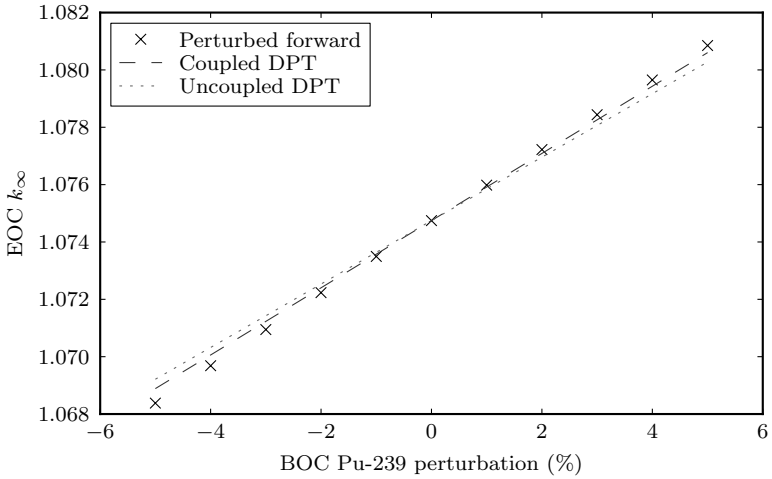

Figure 4.5: Comparison of results from coupled and uncoupled adjoint with perturbed forward calculations of EOC criticality response to BOC Pu-239 amount after 30 days of burn-up in a thermal system

to the perturbed forward results from changes to the initial Pu-239 amount is shown in figure 4.6. The inclusion of the coupling results in only small differences in the worths found from the DPT calculation. The values are generally improved by its inclusion, but differences between the DPT values and those seen from the perturbed forward results remain.

4.5.3 End of cycle Pu-239 response

The behaviour of the thermal system when the EOC Pu-239 amount was the chosen response was also studied. The burn-up period was taken to be 30 days. The results are shown in table 4.10, and a graph of the effects of changing the BOC Pu-239 amounts is shown in figure 4.7. There are significant differences between the values found using the perturbed forward, coupled and uncoupled DPT methods. The coupling improves the accuracy of the DPT values in the cases shown, by orders of magnitude for some. Most of the coupled values still differ from the forward ones by a considerable margin. It appears that the larger the effect of the coupling, the more pronounced the difference between the forward and adjoint values. This suggests that the

Table 4.9: BOC nuclide worths for EOC criticality response of a thermal system after 300 days of burn-up from perturbed forward, coupled, and uncoupled DPT calculations

Nuclide	Worth (per 10^{24} atoms)		
	Perturbed forward	Uncoupled DPT	Coupled DPT
U-235	3.54	2.66	2.93
U-238	-0.130	-0.135	-0.140
Pu-239	4.69	2.28	2.47
Pu-240	-6.47	-5.71	-5.74
Pu-241	8.21	6.21	6.40
Pu-242	-10.5	-9.37	-9.34

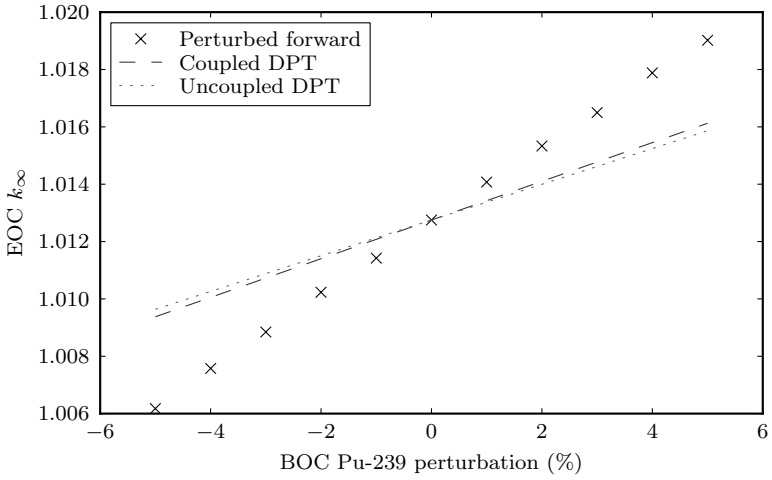

Figure 4.6: Comparison of results from coupled and uncoupled adjoint with perturbed forward calculations of EOC criticality response to BOC Pu-239 amount after 300 days of burn-up in a thermal system

Table 4.10: BOC nuclide worths for EOC Pu-239 response of a thermal system after 30 days of burn-up from perturbed forward, coupled, and uncoupled DPT calculations

Nuclide	Worth (per atom)		
	Perturbed forward	Uncoupled DPT	Coupled DPT
U-235	1.11×10^{-2}	2.85×10^{-11}	5.09×10^{-4}
U-238	3.33×10^{-4}	4.28×10^{-4}	4.26×10^{-4}
Pu-239	9.90×10^{-1}	9.04×10^{-1}	9.10×10^{-1}
Pu-240	3.95×10^{-3}	5.59×10^{-7}	5.03×10^{-5}
Pu-241	3.50×10^{-2}	1.51×10^{-8}	1.26×10^{-3}
Pu-242	1.25×10^{-3}	5.03×10^{-8}	4.46×10^{-5}

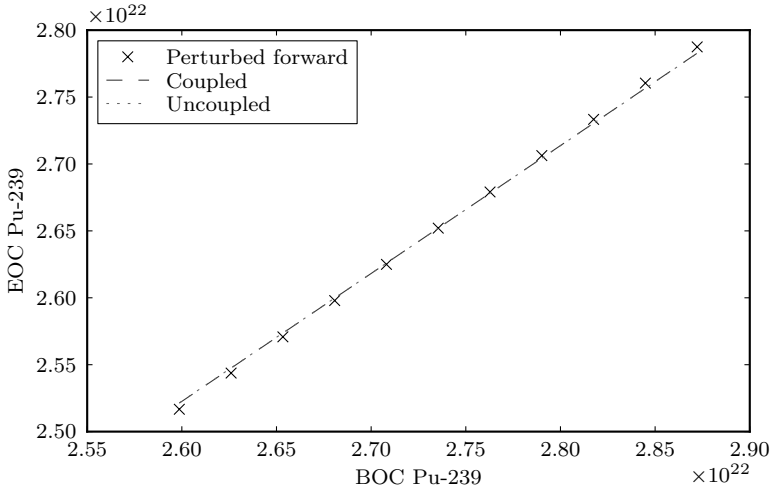

Figure 4.7: Comparison of results from coupled and uncoupled adjoint with perturbed forward calculations of EOC Pu-239 response to BOC Pu-239 amount in a thermal system after 30 days of burn-up

Table 4.11: Original and reloaded thermal pin fuel compositions

Nuclide	Density (atoms/b-cm)	
	Original	Reloaded
O-16	3.62×10^{-2}	3.55×10^{-2}
U-235	4.33×10^{-5}	4.25×10^{-5}
U-238	1.72×10^{-2}	1.69×10^{-2}
Pu-236	1.62×10^{-12}	1.59×10^{-12}
Pu-237	4.31×10^{-12}	4.13×10^{-12}
Pu-238	8.93×10^{-7}	8.88×10^{-7}
Pu-239	4.98×10^{-4}	4.86×10^{-4}
Pu-240	1.86×10^{-4}	1.90×10^{-4}
Pu-241	6.40×10^{-5}	6.68×10^{-5}
Pu-242	7.80×10^{-6}	8.46×10^{-6}
Pu-243	1.67×10^{-9}	1.44×10^{-9}
Pu-244	6.69×10^{-11}	7.41×10^{-11}
Pu-246	1.01×10^{-17}	7.71×10^{-18}

determination of the coupling values should be investigated to improve the results, given the approximations made in determining the coupling effect and the accuracy of the solutions found with a constant transmutation matrix.

4.5.4 Reloading calculation

The thermal system was reloaded in the same fashion as the fast system, described in section 4.4.5. The original and reloaded compositions are shown in table 4.11.

The k_∞ values of the original and reloaded systems are given in table 4.12. The differences between the k_∞ values in original and reloaded systems are very small. While it may be possible to reduce them even further with improved values for the worths from the DPT calculations, the gain in accuracy would likely be small. Refinements of this sort may be necessary over longer burn-up periods however. Using the coupled DPT model allows the worths to be determined from the full set of nuclides in the adjoint burn-up problem, as opposed to the restricted set used for the thermal system in chapter 3.

Table 4.12: Original and reloaded thermal pin BOC and EOC k_∞ values

Time	k_∞	
	Original	Reloaded
BOC	1.1072	1.1066
EOC	1.0748	1.0738

4.6 Conclusions

The coupled depletion perturbation theory proposed in Williams (1979) was implemented as a combination of SCALE codes and custom software. The model was tested in fast and thermal systems, with the end of cycle criticality and Pu-239 amounts chosen as the responses studied for perturbations of the initial actinide composition. Both systems were run for short (30 days) and long (300 days) burn-up periods, to examine how the effect of the neutron-nuclide coupling changes with time.

The results of applying the coupled model to the fast system showed that the choice of response has a large effect on the importance of the coupling. The relative changes in the worths of the criticality response were much smaller than those of the Pu-239 response. The increased burn-up period led to a larger difference between the coupled and uncoupled values, as was expected. The coupled results were generally more accurate than the uncoupled ones. Using the adjoint source vector to calculate the response for the perturbed forward values instead of an additional TSUNAMI run improved the comparison between the perturbed forward and DPT results. This implies that some of the differences between the two sets of values can be attributed to changes in the behaviour of the system that are not represented in the DPT model, such as differences in the cross section values. The behaviour of the solver was also examined, with the transmutation matrix being held constant to ensure that the adjoint problem was being solved accurately. The results showed a good match between the forward and adjoint values, meaning the solver was handling the problem well. The reloading problem was solved for the system with the 30 day burn-up period and the reloaded system showed behaviour very similar to that of the original system.

The work on the thermal system produced results similar to those seen for

the fast system. The inclusion of the coupling in the DPT calculation generally improved the results when compared to the perturbed forward values. The effect was small in some cases, often significantly smaller than the difference between the values found from the forward and adjoint approaches. This behaviour was seen in both the criticality and Pu-239 responses. The reloading calculation produced good results, with the k_∞ values of the original and reloaded systems matching closely. The reloading was determined using the full set of nuclides, an improvement over the restricted set used for the thermal system in chapter 3.

The implementation of the coupled DPT method worked well, producing good values for both responses studided. The compositions determined in the reloading calculations duplicated the behaviour of their original systems to a high degree of accuracy. There remains room for improvement of the implementation of the model. The inaccuracies seen in some of the values produced may be the result of approximations in the coupling calculation. In particular, the treatment of the multi-group transmutation matrix could be improved, if the data were available for use. If a full custom code were built to solve the problem, a closer integration of the DPT code with the criticality and burn-up routines could be achieved. Further, the theory behind the method could be re-visited with the goal of using a predictor-corrector method of the kind employed in TRITON.

Chapter 5

Waste heat reduction

5.1 Introduction

The most widely accepted solution for the disposal of high level radioactive waste is the use of geological repositories (Chapman and Hooper, 2012). The waste is processed to turn it into a form that will be stable over long timescales. It can then be placed in the repository and left to decay.

While no geological repository is currently in full operation, projects are underway in several locations (ERDO, 2011). The siting and construction of a repository is a challenging process, for both technical and political reasons. Given this limited availability, it is important to make full use of the available repository space. The loading of a repository is limited by the heat produced by the radioactive waste (Hökmark et al., 2009; U.K. Nirex Ltd., 2004). The less heat produced by the waste, the more of it can safely be stored in a given space.

The work in this chapter will focus on the reduction of heat produced by waste resulting from the use of plutonium and uranium mixed oxide fuel. Reducing the heat produced by the waste is equivalent to reducing the amount of waste, due to heat being the limiting factor in repository loading. The methods used could also be applied to minor actinides and uranium in the thorium-uranium cycle.

Table 5.1: Plutonium compositions from used fuel from different reactor designs and burn-up periods (Nuclear Decommissioning Authority, 2008)

Reactor	Mean burn-up (MW d/t)	Plutonium isotopic make-up (%)				
		Pu-238	Pu-239	Pu-240	Pu-241	Pu-242
Magnox	3000	0.1	80	16.9	2.7	0.3
	5000	N/A	68.5	25.0	5.3	1.2
CANDU	7500	N/A	66.6	26.6	5.3	1.5
AGR	18000	0.6	53.7	30.8	9.9	5.0
BWR	27500	2.6	59.8	23.7	10.6	3.3
	30400	N/A	56.8	23.8	14.3	5.1
PWR	33000	1.3	56.6	23.2	13.9	4.7
	43000	2.0	52.5	24.1	14.7	6.2
	53000	2.7	50.4	24.1	15.2	7.1

5.2 Theory

Plutonium has been produced by many different reactor designs operating under different conditions, for both civil and military purposes. This has led to stockpiles of plutonium with different isotopic compositions. Some sample plutonium compositions are given in table 5.1, along with the reactor designs and burn-up periods that produced them.

The different plutonium isotopes decay at different rates and via different processes, meaning they produce different amounts of heat as they decay. Isotopes with longer half-lives will typically not produce as much heat per second as those with shorter half-lives and similar decay processes at the moment the fuel reaches the end of its life, but the longer-lived isotopes will continue to produce heat and ionising radiation over considerable timescales, necessitating geological storage. It should be noted that plutonium isotopes all undergo multi-stage decay processes before reaching stability, meaning the properties of the daughter nuclei of the decay processes should also be considered. The half-lives, energy released per decay, and heat production per second for some plutonium isotopes are shown in table 5.2. Pu-241 in particular produces much less heat per decay than the other isotopes listed.

Table 5.2: Half-lives, energy per decay, and waste heat production of plutonium isotopes (SCALE manual, 2009)

Plutonium isotope	Half-life (years)	Energy per decay (MeV)	Heat production (W/kg)
238	$8.77\times10^{+1}$	5.591	568
239	$2.41\times10^{+4}$	5.243	1.93
240	$6.56\times10^{+3}$	5.253	7.07
241	$1.43\times10^{+1}$	0.005	3.29
242	$3.74\times10^{+5}$	4.982	0.117

This is because it decays via β-decay, unlike the others which decay by α-decay. Pu-241 produces Am-241 however, which is an α emitter, meaning the heat production resulting from it can increase, depending on the time period in question.

If plutonium is treated as fuel, rather than waste, then the heat produced by its decay is less of an issue. The fission products resulting from its use, however, also produce heat by radioactive decay. While the majority of fission products are short-lived compared to most plutonium isotopes, there are some with comparable half-lives. Further, given that the delay between use in-reactor and disposal in a geological facility is intended to be on a scale of decades, some of the shorter lived fission products will also contribute to the heat production of the waste at the time it is placed in the repository. In order to determine how the use of plutonium in reactor fuel affects the heat generated by the waste produced, the coupled depletion perturbation theory discussed in chapter 4 can be applied, using the heat production as the source vector for the DPT problem.

Once the waste heat production due to an isotope has been determined, plutonium of different compositions can be compared. In order to accurately compare the different plutonium sources, it is necessary to calculate the fuel make-up that will produce similar reactor behaviour using the method applied to the reloading problem in chapters 3 and 4. Combining the waste heat results with those for the criticality allows the heat production from fuel compositions that show similar in-reactor behaviour to be compared.

5.2.1 Plutonium re-use

A significant amount of plutonium is left in MOX fuel after it has been used in a reactor. This fuel can be reprocessed in turn and the plutonium, uranium, and other actinides can be recovered for later use, depending on the fuel cycle strategy in operation. This can be represented in the DPT model by setting the waste heat production of the recovered isotopes in the adjoint source vector to zero. If there are losses in the reprocessing method, these can be modelled by multiplying the waste heat contribution of the isotopes in question by the appropriate loss factor. The multiple re-use of plutonium is not practical in thermal systems (Baetslé and De Raedt, 1997), so this option is only considered for reactors with a fast neutron spectrum.

5.3 Method

The calculations described here were performed using the coupled depletion perturbation theory model detailed in chapter 4. The study of waste heat production, however, presents a particular challenge as the decay constants of the nuclides cover an extremely wide range of values. Allowing for a decay period after use in a reactor gives the shortest-lived isotopes time to decay away.

In order to determine the effects of the decay period on the waste heat production, the waste heat values were used as the source for an adjoint decay problem. No coupling is required in this kind of problem, as there is no flux to be affected by changes in the composition. The problem can be solved for the appropriate period, giving worths that can then be used as the source for the full adjoint transmutation problem over the burn-up period.

The minimum delay used was one hour. This reduces the range of values to be included in the burn-up problem significantly, which means the solver can produce more accurate results. The isotope helium-5 was removed manually, as its extremely high decay constant, $9.13 \times 10^{20}\mathrm{s}^{-1}$, adversely affects the solver when performing the adjoint decay problem. Decay periods of 50 and 100 years were also studied, to represent a period of interim storage before the waste is placed in the repository.

Table 5.3: Comparison of fast system waste heat worths after a 1 hour decay period from perturbed forward, uncoupled, and coupled DPT calculations

Nuclide	Worth (W/kg)		
	Perturbed forward	Uncoupled DPT	Coupled DPT
U-235	-3.05×10^{3}	$+9.32\times10^{3}$	-2.62×10^{3}
U-238	$+2.49\times10^{2}$	$+4.91\times10^{2}$	$+2.31\times10^{2}$
Pu-239	-3.61×10^{3}	$+7.23\times10^{3}$	-3.24×10^{3}
Pu-240	-5.54×10^{2}	$+1.39\times10^{3}$	-5.56×10^{2}
Pu-241	-5.55×10^{3}	$+1.02\times10^{4}$	-5.07×10^{3}
Pu-242	-3.08×10^{2}	$+1.02\times10^{3}$	-2.65×10^{2}

5.4 Results

5.4.1 Fast system heat worths

The heat production values were used as the source for the coupled DPT calculation of the fast system pin model described in chapter 4. The results were compared to those from perturbed forward calculations and are shown in table 5.3. The worths are expressed in W/kg, meaning the power produced by the waste as a result of including one kilogram of the nuclide in the initial composition. The results show a reasonable match between the values from the perturbed forward and coupled DPT calculations. The uncoupled DPT values are significantly different to those from the perturbed forward approach, showing the strong effect of the flux coupling. The differences between the perturbed forward and coupled DPT values may be a result of the approximation of the multi-group transmutation matrix.

Only U-238 has a positive worth in the perturbed forward and coupled DPT values. Increasing the amount of any of the other nuclides studied in the initial composition decreases the waste heat produced. All the uncoupled DPT values are positive, indicating this effect is manifested in the flux coupling. The decrease in waste heat is due to lower production of U-239 and Np-239. U-239 is produced by neutron capture in U-238, and then decays to Np-239. The more U-238 in the fuel, the higher the chance of this process occurring and the higher the waste heat production. Increasing the amounts of other isotopes, particularly the fissile U-235, Pu-239, and Pu-241, decreases the waste heat,

Table 5.4: Comparison of fast system waste heat worths after a 50 year decay period from perturbed forward, uncoupled, and coupled DPT calculations

Nuclide	Worth (W/kg)		
	Perturbed forward	Uncoupled DPT	Coupled DPT
U-235	5.19×10^{-1}	2.86×10^{-1}	5.05×10^{-1}
U-238	1.48×10^{-1}	1.21×10^{-2}	1.45×10^{-2}
Pu-239	2.31	2.10	2.29
Pu-240	7.77	7.75	7.78
Pu-241	9.49×10^{1}	9.46×10^{1}	9.49×10^{1}
Pu-242	2.42×10^{-1}	2.13×10^{-1}	2.35×10^{-1}

Table 5.5: Comparison of fast system waste heat worths after a 100 year decay period from perturbed forward, uncoupled, and coupled DPT calculations

Nuclide	Worth (W/kg)		
	Perturbed forward	Uncoupled DPT	Coupled DPT
U-235	4.04×10^{-1}	8.77×10^{-2}	3.91×10^{-1}
U-238	1.33×10^{-1}	9.10×10^{-3}	1.29×10^{-2}
Pu-239	2.26	1.97	2.25
Pu-240	7.73	7.70	7.74
Pu-241	9.56×10^{1}	9.52×10^{1}	9.56×10^{1}
Pu-242	2.10×10^{-1}	1.73×10^{-1}	2.04×10^{-1}

by allowing more neutrons to be captured by nuclides other than U-238.

A more realistic model would allow for the decay period after the fuel has been used in the reactor. The worths were calculated for post-use decay periods of 50 and 100 years. These values were chosen to represent a range of possible decay periods before final disposal. The values for the 50 year period are shown in table 5.4 and those for the 100 year period in table 5.5.

The values calculated with the longer decay periods show improved agreement between the perturbed forward and DPT results. All the worths become positive, as the short-term reduction due to decreased amounts of U-239 and Np-239 becomes negligible once the decay period is significantly longer than

Table 5.6: Comparison of thermal system waste heat worths after a 1 hour decay period from perturbed forward, uncoupled, and coupled DPT calculations

Nuclide	Worth (W/kg)		
	Perturbed forward	Uncoupled DPT	Coupled DPT
U-235	$+2.67\times10^{2}$	$+4.45\times10^{3}$	$+4.26\times10^{3}$
U-238	$+2.86\times10^{1}$	$+6.16\times10^{1}$	$+6.01\times10^{1}$
Pu-239	-1.20×10^{2}	$+8.66\times10^{3}$	$+8.29\times10^{3}$
Pu-240	$+4.76\times10^{2}$	$+3.49\times10^{2}$	$+3.66\times10^{2}$
Pu-241	-6.26×10^{2}	$+9.09\times10^{3}$	$+8.66\times10^{3}$
Pu-242	$+6.31\times10^{2}$	$+5.72\times10^{2}$	$+5.91\times10^{2}$

the half-lives of those isotopes. Both the uncoupled and coupled values are closer to the perturbed forward values. Some differences remain, and these are of similar size for both decay periods. From these results, it appears that increasing the length of the decay period improves the quality of the adjoint prediction. The high activities of the short-lived isotopes mean that while they are present in the waste, they dominate the heat production, and that any small change in the production of these isotopes can have a large effect on the waste heat. Many of the short-lived isotopes are fission products, whose cross sections were approximated in the multi-group transmutation matrix. Longer decay periods allow the contributions of the shorter lived isotopes to decrease, lessening their importance in determining the final value.

5.4.2 Thermal system heat worths

A similar set of calculations was performed for the waste heat produced by fuel used in the thermal system pin model described in chapter 4. The worths were found for perturbed forward, uncoupled, and coupled DPT models, with 1 hour, and 50 and 100 year decay periods. The results are shown in tables 5.6, 5.7, and 5.8 respectively.

The thermal system results show a similar pattern to that seen for the fast system, but the comparison of the perturbed forward and coupled DPT values shows larger differences. The worths of the fissile plutonium isotopes after the one hour decay period are negative, as increased amounts of these isotopes lead to lower amounts of U-239 and Np-239, as in the fast system. Additional U-235

Table 5.7: Comparison of thermal system waste heat worths after a 50 year decay period from perturbed forward, uncoupled, and coupled DPT calculations

Nuclide	Worth (W/kg)		
	Perturbed forward	Uncoupled DPT	Coupled DPT
U-235	3.09×10^{-1}	1.39×10^{-1}	1.29×10^{-1}
U-238	9.79×10^{-4}	1.50×10^{-3}	1.41×10^{-3}
Pu-239	2.04	2.19	2.17
Pu-240	8.64	9.66	9.63
Pu-241	9.46×10^{1}	9.50×10^{1}	9.50×10^{1}
Pu-242	5.13×10^{-1}	3.20×10^{-1}	3.19×10^{-1}

Table 5.8: Comparison of thermal system waste heat worths after a 100 year decay period from perturbed forward, uncoupled, and coupled DPT calculations

Nuclide	Worth (W/kg)		
	Perturbed forward	Uncoupled DPT	Coupled DPT
U-235	2.78×10^{-1}	4.20×10^{-2}	3.46×10^{-2}
U-238	9.25×10^{-4}	1.13×10^{-3}	1.07×10^{-3}
Pu-239	2.04	2.04	2.03
Pu-240	8.61	9.65	9.62
Pu-241	9.55×10^{1}	9.57×10^{1}	9.57×10^{1}
Pu-242	4.47×10^{-1}	2.45×10^{-1}	2.42×10^{-1}

also decreases the amounts of these isotopes, but the effect on the waste heat is offset by increased amounts of Kr-88 and Sr-91. Increasing the amounts of the non-fissile isotopes increases the amounts of U-239 and Np-239, in contrast to the fast system.

The longer decay periods improve the values found, although the effect is not as strong as for the fast system. The waste produced in a thermal system differs from that in a fast system, as the less energetic neutrons are more easily captured and produce more minor actinides that cannot be fissioned by thermal neutrons. The stronger effects of fission products on the thermal system also exacerbate the issues associated with the multi-group transmutation matrix

approximation. These factors may account for the differences seen between the results for the two systems.

5.4.3 Plutonium recycling

In order to use the entirety of a plutonium stockpile, the fuel is reprocessed to recover plutonium that remains at the end of the burn-up cycle. This can then be made into new fuel. This recycling is represented in the waste heat production model by setting the contributions of plutonium isotopes in the adjoint source to zero. Fission products and other actinides created from plutonium during burn-up still produce heat, but the plutonium itself is removed and re-used.

These calculations were performed for the fast system, with decay periods of 1 hour, and 50 and 100 years. The results are shown in tables 5.9, 5.10, and 5.11 respectively. The results show the same behaviour as in the fast system without recycling, the coupled DPT values improve with the length of the decay period. Comparing these results with those in section 5.4.1, a number of effects can be seen. For the worths with a 1 hour decay period, there is very little difference except for the value of Pu-242, which is decreased with plutonium recycling. This appears to be caused by the Pu-242 that remains at the end of the burn-up period being a significant contributor to the waste heat from the inclusion of Pu-242 in the initial composition. Removing Pu-242 from the fuel at the end of the cycle removes this contribution and the worth decreases accordingly.

If a 50 year decay period is allowed for, plutonium recycling has a larger effect on the worths found. Only the uncoupled DPT worth for U-235 remains constant, all other values decrease. The decrease caused by the effect of U-235 on the flux, however, is significant, which can be seen in the other two values. Recycling the plutonium has a particular effect on the worths of Pu-239 and Pu-240, which remain negative after the longer decay time. The amounts of several isotopes that contribute to the waste heat after 50 years in the EOC composition decrease as more of either of the two plutonium isotopes is added to the initial composition. In particular, the amounts of Np-239, Am-243, Cm-242, and Cm-244 are reduced. The additional Pu-239 or Pu-240 atoms appear to be absorbing neutrons that would otherwise produce minor actinides.

The waste heat resulting from Sr-90 in the EOC composition is also reduced

Table 5.9: Comparison of fast system waste heat worths with plutonium recycling after a 1 hour decay period from perturbed forward, uncoupled, and coupled DPT calculations

Nuclide	Worth (W/kg)		
	Perturbed forward	Uncoupled DPT	Coupled DPT
U-235	-3.03×10^{3}	$+9.32\times10^{3}$	-2.61×10^{3}
U-238	$+2.49\times10^{2}$	$+4.91\times10^{2}$	$+2.32\times10^{2}$
Pu-239	-3.60×10^{3}	$+7.22\times10^{3}$	-3.23×10^{3}
Pu-240	-5.58×10^{2}	$+1.39\times10^{3}$	-5.61×10^{2}
Pu-241	-5.54×10^{3}	$+1.02\times10^{4}$	-5.06×10^{3}
Pu-242	-4.80×10^{2}	$+8.43\times10^{2}$	-4.39×10^{2}

Table 5.10: Comparison of fast system waste heat worths with plutonium recycling after a 50 year decay period from perturbed forward, uncoupled, and coupled DPT calculations

Nuclide	Worth (W/kg)		
	Perturbed forward	Uncoupled DPT	Coupled DPT
U-235	$+6.05\times10^{-2}$	$+2.86\times10^{-1}$	$+6.83\times10^{-2}$
U-238	$+9.86\times10^{-4}$	$+5.21\times10^{-3}$	$+1.18\times10^{-3}$
Pu-239	-2.54×10^{-2}	$+1.71\times10^{-1}$	-2.06×10^{-2}
Pu-240	-3.16×10^{-3}	$+3.23\times10^{-2}$	-2.90×10^{-3}
Pu-241	$+3.57\times10^{-1}$	$+6.44\times10^{-1}$	$+3.66\times10^{-1}$
Pu-242	$+7.26\times10^{-2}$	$+9.64\times10^{-2}$	$+7.34\times10^{-2}$

by increased amounts of Pu-239 or Pu-240 in the BOC composition. The effects of the plutonium isotopes on the flux lower the rate of production of Sr-90, particularly from fissile isotopes such as U-235 and Pu-239.

Extending the decay period to 100 years gives similar behaviour to the 50 year decay period results. Only the uncoupled DPT worth for U-235 is unaffected. All other values are decreased compared to those found without plutonium recycling, with Pu-239 and Pu-240 still having negative worths.

Table 5.11: Comparison of fast system waste heat worths with plutonium recycling after a 100 year decay period from perturbed forward, uncoupled, and coupled DPT calculations

Nuclide	Worth (W/kg)		
	Perturbed forward	Uncoupled DPT	Coupled DPT
U-235	$+8.41\times10^{-3}$	$+8.77\times10^{-2}$	$+1.20\times10^{-2}$
U-238	$+7.04\times10^{-4}$	$+2.23\times10^{-3}$	$+7.33\times10^{-4}$
Pu-239	-1.60×10^{-2}	$+5.33\times10^{-2}$	-1.33×10^{-2}
Pu-240	-1.48×10^{-3}	$+1.11\times10^{-2}$	-1.21×10^{-3}
Pu-241	$+3.53\times10^{-1}$	$+4.53\times10^{-1}$	$+3.57\times10^{-1}$
Pu-242	$+4.77\times10^{-2}$	$+5.65\times10^{-2}$	$+4.84\times10^{-2}$

5.4.4 Uranium and plutonium recycling

To make better use of the available resources, uranium can be recycled alongside plutonium. Uranium is the main constituent of MOX fuel, and re-using it not only improves sustainability, but also significantly decreases the amount of waste produced. The values studied here are calculated per unit mass of initial composition, so the reduction of the waste mass is not seen in the worths found. Uranium re-use is included in the model in the same manner as for plutonium, setting the uranium isotope terms in the adjoint source to zero. The worths were found for a fast system with 1 hour, and 50 and 100 year decay periods, and are given in tables 5.12, 5.13, and 5.14.

Comparing the results in tables 5.9 and 5.12 shows that recycling uranium as well as plutonium increases the worths of several isotopes. The uncoupled values for the plutonium isotopes are unchanged, showing that the effect of recycling uranium on the waste heat resulting from plutonium is mediated by the flux coupling. The perturbed forward and coupled DPT values show that only U-238 has a positive waste heat worth, no matter which recycling scheme is used.

Moving to the 50 year decay period, the differences between the plutonium recycling values in table 5.10 and the uranium and plutonium recycling values in table 5.13 become very small. There are only minimal variations between the three sets of values. It appears that on a waste heat per unit initial mass

Table 5.12: Comparison of fast system waste heat worths with uranium and plutonium recycling after a 1 hour decay period from perturbed forward, uncoupled, and coupled DPT calculations

Nuclide	Worth (W/kg)		
	Perturbed forward	Uncoupled DPT	Coupled DPT
U-235	-2.41×10^{3}	$+9.31\times10^{3}$	-2.03×10^{3}
U-238	$+2.12\times10^{2}$	$+4.40\times10^{2}$	$+1.99\times10^{2}$
Pu-239	-3.07×10^{3}	$+7.22\times10^{3}$	-2.73×10^{3}
Pu-240	-4.63×10^{2}	$+1.39\times10^{3}$	-4.64×10^{2}
Pu-241	-4.78×10^{3}	$+1.02\times10^{4}$	-4.33×10^{3}
Pu-242	-4.10×10^{2}	$+8.43\times10^{2}$	-3.74×10^{2}

Table 5.13: Comparison of fast system waste heat worths with uranium and plutonium recycling after a 50 year decay period from perturbed forward, uncoupled, and coupled DPT calculations

Nuclide	Worth (W/kg)		
	Perturbed forward	Uncoupled DPT	Coupled DPT
U-235	$+6.05\times10^{-2}$	$+2.86\times10^{-1}$	$+6.83\times10^{-2}$
U-238	$+9.70\times10^{-4}$	$+5.19\times10^{-3}$	$+1.16\times10^{-3}$
Pu-239	-2.54×10^{-2}	$+1.71\times10^{-1}$	-2.05×10^{-2}
Pu-240	-3.14×10^{-3}	$+3.23\times10^{-2}$	-2.89×10^{-3}
Pu-241	$+3.58\times10^{-1}$	$+6.44\times10^{-1}$	$+3.66\times10^{-1}$
Pu-242	$+7.26\times10^{-2}$	$+9.64\times10^{-2}$	$+7.34\times10^{-2}$

basis, uranium recycling has very little effect in this scenario.

The worths for the 100 year decay period in table 5.14 also show only small changes from the values in table 5.11. The differences in the uncoupled values for the uranium isotopes mean transmutation effects have become important. This suggests that there are small contributions to the waste heat from the uranium isotopes that become more pronounced with the longer decay period.

Table 5.14: Comparison of fast system waste heat worths with uranium and plutonium recycling after a 100 year decay period from perturbed forward, uncoupled, and coupled DPT calculations

Nuclide	Worth (W/kg)		
	Perturbed forward	Uncoupled DPT	Coupled DPT
U-235	$+8.41\times10^{-3}$	$+8.76\times10^{-2}$	$+1.20\times10^{-2}$
U-238	$+6.88\times10^{-4}$	$+2.21\times10^{-3}$	$+7.16\times10^{-4}$
Pu-239	-1.60×10^{-2}	$+5.33\times10^{-2}$	-1.33×10^{-2}
Pu-240	-1.46×10^{-3}	$+1.11\times10^{-2}$	-1.20×10^{-3}
Pu-241	$+3.53\times10^{-1}$	$+4.53\times10^{-1}$	$+3.57\times10^{-1}$
Pu-242	$+4.77\times10^{-2}$	$+5.65\times10^{-2}$	$+4.84\times10^{-2}$

5.4.5 Waste heat and plutonium composition

Table 5.1 gives the compositions of plutonium produced by different reactor designs with different burn-up periods. Given these sources of plutonium, different fuel compositions that produce similar reactor behaviour can be determined using the methods developed in chapters 3 and 4. The effects of these compositions on the waste heat can be predicted, allowing the appropriate plutonium source for a given set of requirements to be selected.

The waste heat produced by the reference fast pin was calculated for the three decay periods and three recycling schemes used previously, with the values shown in table 5.15. In contrast to the previous section, the values given here are expressed in terms of the heat produced per unit mass of waste, rather than heat produced per unit mass of nuclide in the initial composition. This allows the effects of the different recycling schemes to be seen more clearly and gives a more straightforward comparison of the different plutonium source compositions.

Equivalent fuel compositions were found for all the different plutonium sources, with depleted uranium with 0.25% U-235 as the uranium feed material. The heat produced by the waste from these systems after different decay periods and under different recycling schemes was calculated. The waste masses produced by the different systems under the different recycling schemes relative to that produced with no recycling are shown in table 5.16. The

Table 5.15: Heat production (W/kg) of waste from reference fast pin for different decay periods and recycling schemes

Recycling scheme	Decay period		
	1 hour	50 years	100 years
None	8.91×10^{2}	1.75	1.57
Plutonium	9.74×10^{2}	2.25×10^{-2}	1.04×10^{-2}
Uranium and Plutonium	7.01×10^{3}	1.69×10^{-1}	7.87×10^{-2}

Table 5.16: Mass of waste produced under different recycling schemes relative to system with no recycling

Plutonium source (burn-up)	Recycling	
	Plutonium	Uranium and plutonium
Reference	0.914	0.121
Magnox (3000)	0.925	0.121
Magnox (5000)	0.923	0.121
CANDU	0.921	0.121
AGR	0.914	0.121
BWR (27500)	0.915	0.121
BWR (30400)	0.913	0.121
PWR (33000)	0.914	0.121
PWR (43000)	0.909	0.121
PWR (53000)	0.911	0.121

Table 5.17: Heat production (W/kg) of waste from a fast pin fuelled with plutonium compositions from different sources

Plutonium source	Mean burn-up (MW d/t)	Decay period		
		1 hour	50 years	100 years
Magnox	3000	8.99×10^{2}	4.41×10^{-1}	4.23×10^{-1}
	5000	8.99×10^{2}	6.55×10^{-1}	6.47×10^{-1}
CANDU	7500	8.99×10^{2}	6.67×10^{-1}	6.58×10^{-1}
AGR	18000	8.95×10^{2}	1.29	1.23
BWR	27500	8.93×10^{2}	1.86	1.60
	30400	8.83×10^{2}	1.45	1.45
PWR	33000	8.86×10^{2}	1.81	1.67
	43000	8.85×10^{2}	2.16	1.94
	53000	8.84×10^{2}	2.46	2.17

relative waste mass produced with plutonium recycling shows some variation, due to the different amounts of plutonium used to make fuel from the different sources. Once uranium is also recycled, the relative masses all show the same value, as the relative amount of waste produced from the different fuels is very similar.

The waste heat values produced by the various fuel compositions operated without recycling are shown in table 5.17. The results show that the different plutonium sources have only a small effect on the waste heat produced one hour after the end of the burn-up period. After the waste has been allowed to decay for a longer time, significant changes are seen. In general, the lower burn-plutonium sources give less waste heat, as more neutron captures are required to produce the minor actinides that make a significant contribution to the heat production. The 27500 MWd/t burn-up BWR plutonium is the only source that does not fit this pattern, which is likely to have been caused by its relatively high Pu-238 content.

If the plutonium is recycled at the end of the burn-up period, the heat produced by the waste is affected. The waste heat per unit waste mass values resulting from the use of fuel produced from the different plutonium

Table 5.18: Heat production (W/kg) of waste from a fast pin fuelled with plutonium compositions from different sources with plutonium recycling

Plutonium source	Mean burn-up (MW d/t)	Decay period		
		1 hour	50 years	100 years
Magnox	3000	9.71×10^{2}	1.84×10^{-2}	6.80×10^{-3}
	5000	9.74×10^{2}	1.94×10^{-2}	7.74×10^{-3}
CANDU	7500	9.75×10^{2}	1.95×10^{-2}	7.77×10^{-3}
AGR	18000	9.77×10^{2}	2.17×10^{-2}	9.77×10^{-3}
BWR	27500	9.71×10^{2}	2.16×10^{-2}	9.73×10^{-3}
	30400	9.67×10^{2}	2.34×10^{-2}	1.14×10^{-2}
PWR	33000	9.67×10^{2}	2.31×10^{-2}	1.12×10^{-2}
	43000	9.68×10^{2}	2.38×10^{-2}	1.17×10^{-2}
	53000	9.69×10^{2}	2.42×10^{-2}	1.21×10^{-2}

compositions are given in table 5.18. Comparing them to the values in table 5.17, it can be seen that plutonium recycling increases the heat per unit waste mass one hour after the end of the burn-up period. The heat production at this point is dominated by non-plutonium isotopes, so the main effect of the removal of the plutonium is to decrease the waste mass. Allowing for a longer decay period makes a significant difference to the results, with a reduction of at least one order of magnitude seen after 50 years and two after 100 years when compared to the values without recycling.

Including uranium and plutonium recycling in the modelling of the different plutonium compositions gives the waste heat per unit waste mass values in table 5.19. Removing the uranium from the waste makes a large difference to the mass, leading to the increased waste heat per unit mass one hour after the end of the burn-up period. A similar effect is seen after both of the longer decay periods, with the values including uranium and plutonium recycling being higher than those including only plutonium recycling, but still lower than those found with no recycling. A further point is that the values found with uranium recycling have the smallest relative range after 50 and 100 years of the three schemes. Removing the uranium and plutonium from the waste lessens the effects of using the different plutonium sources to create the fuel.

Table 5.19: Heat production (W/kg) of waste from a fast pin fuelled with plutonium compositions from different sources with uranium and plutonium recycling

Plutonium source	Mean burn-up (MW d/t)	Decay period		
		1 hour	50 years	100 years
Magnox	3000	7.09×10^{3}	1.40×10^{-1}	5.20×10^{-2}
	5000	7.09×10^{3}	1.48×10^{-1}	5.89×10^{-2}
CANDU	7500	7.09×10^{3}	1.48×10^{-1}	5.91×10^{-2}
AGR	18000	7.05×10^{3}	1.64×10^{-1}	7.37×10^{-2}
BWR	27500	7.03×10^{3}	1.64×10^{-1}	7.37×10^{-2}
	30400	6.97×10^{3}	1.76×10^{-1}	8.58×10^{-2}
PWR	33000	6.98×10^{3}	1.75×10^{-1}	8.42×10^{-2}
	43000	6.97×10^{3}	1.79×10^{-1}	8.82×10^{-2}
	53000	6.96×10^{3}	1.82×10^{-1}	9.05×10^{-2}

5.5 Conclusions

The implementation of the coupled depletion perturbation theory (CDPT) model developed in chapter 4 was applied to the problem of waste heat production. The model was used to study fast and thermal systems, with different decay periods and recycling schemes. The use of different plutonium sources and their effects on the waste heat production was also studied.

Using the CDPT model to predict the waste heat production of a fast system once again showed how the source term in the problem can affect the accuracy of the results. When compared to the perturbed forward values, the CDPT predictions became more accurate as the waste was allowed to decay for longer periods, with the effect on the source term of reducing the contributions of the short-lived nuclides. It is expected that this trend would continue for time periods longer than those studied here.

Modelling the thermal system under the same circumstances as the fast system produced similar results. The accuracy of the CDPT calculations improved with the longer decay periods, although to a lesser extent than for

the fast system. The production of minor actinides and stronger effects of fission products in the thermal system combined with the multi-group transmutation matrix approximation are believed to have caused this difference.

The effects of recycling plutonium on its own and uranium and plutonium together were studied for the three different decay periods. Plutonium recycling had only a small effect on the worths found one hour after the end of the burn-up, but once the waste was allowed to decay for longer periods, the removal of the plutonium isotopes had a significant effect, decreasing almost all the worths studied. Recycling uranium alongside plutonium changed the waste heat worths significantly for the case with a one hour decay period, but resulted in only small differences after longer periods had elapsed.

Different sources of plutonium were used to determine a set of equivalent fuel compositions for the model fast system. The effects of these different fuels on the waste heat production under different recycling schemes and with different decay periods were studied. In general, plutonium from a lower burn-up source, that contained fewer heavy plutonium isotopes, resulted in higher waste heat after a decay period of one hour and lower waste heat after 50 or 100 years. Recycling plutonium gave a significant reduction in the waste heat production, once an appropriate decay period had been included. Removing and re-using uranium as well as plutonium increased the waste heat per unit mass from the value found when recycling only plutonium, but reduced the waste mass by a large factor.

From the results obtained in this chapter, it can be concluded that although the coupled depletion perturbation theory model can be applied to the study of waste heat production, there are some associated issues. The key problem being the accuracy of the model when used with a source representing the heat produced for zero or very short decay periods. On the longer timescales the results improved, and it can be expected that this would continue if the model were used over the geological periods that are of interest for long-term waste disposal. The results of the plutonium source calculations showed that choosing the appropriate plutonium source can give a significant reduction in the heat production of the waste. It should be noted that the low burn-up plutonium that tended to give the lowest waste heat is also the material of greatest concern for proliferation issues, given its high amount of Pu-239.

There is scope for further investigation of these issues. In particular, the application of the methods developed here to more realistic full reactor models,

operated over longer time periods would be of interest. The effects of recycling higher actinides, as proposed in some fuel cycles, could also be studied. The effects of losses during reprocessing could be included in the model, by isotope or by element. Determining the optimal sequence of use of a existing plutonium stockpiles to minimise the resultant waste heat could be of significant benefit.

Chapter 6

Conclusions and Recommendations

6.1 Conclusions

The goal of the research in this thesis was the quantification of nuclide contributions to reactor properties over time, with a specific focus on criticality and the use of depleted uranium. A number of adjoint techniques have been used and developed to study these issues, although the methods used have a wide range of possible applications.

The issue of improving sustainability by making greater use of depleted uranium was used to guide the work done in this thesis. The production of power from depleted uranium necessitates the use of the uranium-plutonium cycle, and the emphasis on plutonium illustrates this connection, as well as the broader applicability of these methods.

The continuous model approximates the behaviour of a reactor over multiple burn-up cycles by describing the long-term behaviour in the form of an eigenvalue problem. The use of the adjoint problem as a method to measure the contribution of a nuclide to the reactor behaviour over time is illustrated. The reactor designs used provide examples of different possible strategies. Studying different reprocessing strategies demonstrates that recycling additional

actinides reduces the amount and radiotoxicity of the waste, although it also leads to increased amounts of higher actinide waste. The use of different feed materials shows how increased fissile feed content increases the system growth rate, and similarly increased reprocessing losses reduce the system growth rate. The low accuracy of the results obtained from the continuous model mean it is not considered suitable for detailed fuel cycle analysis.

The double adjoint method uses two different adjoint calculations, criticality and transmutation, to describe how nuclides present at the beginning of the burn-up period affect reactor behaviour at the end of the cycle. This method allows the reloading problem to be solved, making it possible to replicate reactor behaviour with fuels of different compositions. The breeding ratio definition that follows from the double adjoint method can be applied to non-equilibrium systems and allows for the effect of the feed material. The increase in breeding ratio from the use of feed materials with higher fissile content is shown, as is the increase that results from recycling additional actinides. Given the inclusion of the effects of the feed material, this definition allows a system that maintains operation using only a depleted uranium feed to be described as requiring a breeding ratio greater than or equal to one, a more accurate description than can be achieved with existing breeding ratio measures. Neglecting the coupling between the flux and transmutation effects results in less accurate values for the thermal system than the fast one. One solution to this issue is to re-define the problem to treat only actinides.

Allowing for the coupling between the composition and the flux, as in the Williams (1979) model, improves the values found for the thermal system when the entire range of nuclides is considered. The applicability of this method to different responses is shown, which also illustrates how changes in the response can affect the relative contributions of the flux and transmutation effects. The limitations of implementing the model as an addition to existing codes, instead of as an integral part, necessitates the approximation of the multi-group transmutation matrix, leaving an obvious avenue for improvement.

The importance of the source term in coupled depletion perturbation theory is also indicated by the waste heat calculations. The waste heat source contains many terms of different magnitudes, and how those terms affect the worths of other nuclides can be strongly affected by the flux. Many of the nuclides that produce significant amounts of heat are also subject to the multi-group transmutation cross section approximation. The resulting differences between

the values from the coupled DPT model and perturbed forward calculations are decreased by lessening these effects, by either allowing the short-lived nuclides to decay away or moving from a thermal to a fast system with a weaker flux coupling effect. Using the methods developed to create equivalent fuels with different plutonium compositions demonstrates that materials with similar in-reactor behaviour can lead to significantly different waste heat production. Recycling of uranium and plutonium provides significant decreases in the amounts of waste produced, although it can increase the heat produced per unit waste mass, depending on the time period considered. Analysis of the properties of the plutonium from different sources using these methods allows the optimal choice of plutonium source to be made for a given objective.

The final conclusion of this thesis must be that allowing for the different properties of nuclides at both the current moment and at later points in time produces more accurate results than considering only the present. Accurate predictions of the evolution of these properties over time can only lead to more efficient use of existing resources and better exploitation of materials that are currently under-used.

6.2 Recommendations

There are a number of possible ways to improve the methods developed in this thesis and to apply them more widely. The most obvious is the study of different responses using the coupled depletion perturbation theory model. Investigating properties such as the spontaneous neutron source would give options of working to minimise the neutron emission in order to ease reprocessing, or maximise it in order to improve proliferation resistance. Similarly, the heat produced by plutonium isotopes at the end of the burn-up period could be increased, with the goal of making the remaining material less suitable for weapons purposes. The waste heat response that was studied was determined for different times chosen to represent possible decay periods before the waste is finally placed in the repository. The time at which the waste is placed in the repository is not, however, necessarily the moment at which it produces the most heat in the repository, due to decay processes producing isotopes that have a higher heat production than their parent nuclide. Determining how the initial fuel composition affects the peak waste heat production would be of interest, although the problem would need to be carefully formulated to allow for the effect of the composition on the timing of the peak value.

The definition of breeding ratio developed in this thesis has the important advantage over many other definitions that it applies in non-equilibrium situations. It could be used to compare the capabilities of different reactor designs or different fuel cycle strategies throughout their lifetimes. The inclusion of the feed material in the definition makes comparisons of this kind possible, which is also not the case for many existing definitions. Extending the theory to use three or more points in time over the burn-up period could provide further improvement in the results, although this would require the use of additional materials beyond the two in the current model.

When discussing the use of adjoint techniques of the kind in this thesis, it is important to compare them to the perturbed forward calculation method. There is a large body of existing software that can be used for the perturbed forward approach with minimal adaptation. There are far fewer codes that can perform the adjoint calculations, particularly the adjoint eigenvalue problem with source term necessary to solve the coupled depletion perturbation theory problem. The cost of implementing these methods is a significant barrier to their use. If a commercial code were to include them, it would significantly redress the balance between the two approaches. The question of parallel computation should also be considered, as the perturbed forward method naturally lends itself to being performed in this manner. The adjoint approach, whether coupled or uncoupled, cannot be run in parallel with the same ease, particularly if performed over multiple burn-up time-steps. The ideal problem for the adjoint method is one in which the contributions of many nuclides to a single response are to be determined. Increasing the number of responses or decreasing the number of nuclides to be studied plays to the strengths of the perturbed forward approach. The linearity of the response is also an issue, with non-linear responses being poorly modelled by the adjoint approach, but also requiring more perturbed forward calculations to achieve accurate results. Expanding the adjoint method to treat higher order terms would allow better representation of these responses, with the associated increase in computational cost.

Further to the possible gains from minimising the implementation time required to use the adjoint methods, integrating them into a standardised reactor modelling code would have certain advantages. In particular, full access to the data used in the modelling code would obviate the need to approximate the multi-group transmutation matrix, improving the accuracy of the code. Other information necessary for the solution of the coupled problem could

also be passed directly to the appropriate code, as opposed to being read from output files as in the current implementation. The transmutation problem is currently solved twice, in different forms, by the codes used. A more integrated approach could remove this redundancy and improve the consistency of the code. The need to redo the transmutation calculation stems from the difference between the coupled model, which used the flux shape and amplitude from the beginning of the time-step to perform the burn-up, and the reactor modelling code that employs a predictor-corrector approach, using an approximation of the flux at the middle of the time-step for the burn-up calculation. If the model could be adapted to use the predictor-correct approach, that would also resolve this issue.

Although the work in this thesis has focussed on modelling the in-reactor behaviour of different nuclides, external processes play an important part in the nuclear fuel cycle, particularly in scenarios involving the repeated use and reprocessing of e.g. plutonium. The modelling of reprocessing here has been performed on only a basic level. An improved model would lead to a better representation of reality in the results. Of particular interest would be any shifts in the isotopic composition due to chemical processes, the time taken for the various stages of reprocessing and how decay changes the composition, losses of different nuclides during reprocessing, and the uncertainty in the final composition.

Bibliography

C. R. Adkins. The breeding ratio with correlation to doubling time and fuel cycle reactivity variation. *Nuclear Technology*, **13**, 114, 1972.

L. H. Baetslé and C. De Raedt. Limitations of actinide recycle and fuel cycle consequences. A global analysis part 2: Recycle of actinides in thermal reactors: impact of high burn up LWR-UO_2 fuel irradiation and multiple recycle of LWR-MOX fuel on radiotoxic inventory. *Nuclear Engineering and Design*, **168**, 203, 1997.

A. R. Baker and R. W. Ross. Comparison of the value of plutonium and uranium isotopes in fast reactors. Technical report, Argonne National Laboratory, 1963. ANL-6792.

S. Behnel et al. Cython: The best of both worlds. *Computing in Science & Engineering*, **13**, 31, 2011.

J. Bernstein. *Plutonium: A history of the world's most dangerous element.* Joseph Henry Press, 2007.

D. Boccaletti and G. Pucacco. *Theory of Orbits Volume 2: Perturbative and Geometrical Methods.* Springer, 1998.

R. C. Borg. *Impact of delays in plutonium use on the stationary doubling time for fast breeder reactors.* Ph.D. thesis, Purdue University, 1976.

P. N. Brown, G. D. Byrne and A. C. Hindmarsh. VODE, A Variable-Coefficient ODE Solver. *SIAM Journal on Scientific and Statistical Computing*, **10**, 1038, 1989.

N. Chapman and A. Hooper. The disposal of radioactive wastes underground. *Proceedings of the Geologists' Association*, **123**, 46, 2012.

R. G. Cochran and N. Tsoulfanidis. *The Nuclear Fuel Cycle: Analysis and Management*. American Nuclear Society, second edition, 1999.

T. Downar. Depletion perturbation theory for burnup dependent microscopic cross sections. *Annals of Nuclear Energy*, **19**, 27, 1992.

J. J. Duderstadt and L. J. Hamilton. *Nuclear Reactor Analysis*. John Wiley & Sons, 1976.

ERDO. Shared solutions for spent fuel and radioactive wastes. Technical report, European Repository Development Organisation (ERDO) Working Group, 2011.

P. V. Evans (ed.). *Proceedings of the London Conference on Fast Breeder Reactors*, 1967. Appendix: Definitions of Fast Reactor Breeding and Inventory. Fast Breeder Reactors.

F. M. Fernández. *Introduction to Perturbation Theory in Quantum Mechanics*. CRC Press, 2001.

G. Girardin et al. Development and characterization of the control assembly system for the large 2400 MWth generation IV gas-cooled fast reactor. *Annals of Nuclear Energy*, **35**, 2206, 2008.

N. A. Hanan, R. C. Borg and K. O. Ott. Interpretation of the isotopic breeding worth. *Transactions of the American Nuclear Society*, **28**, 386, 1978.

H. Hökmark et al. Strategy for thermal dimensioning of the final repository for spent nuclear fuel. Technical Report R-09-04, Swedish Nuclear Fuel and Waste Management Company, 2009.

J. D. Hunter. Matplotlib: A 2D graphics environment. *Computing in Science & Engineering*, **9**, 90, 2007.

IAEA. Fast reactor database 2006 update. Technical Report IAEA-TECDOC-1531, International Atomic Energy Agency, 2006.

ICRP. Dose coefficients for intakes of radionuclides by workers. *Annals of the ICRP*, **24**, 1994. International Commission on Radiological Protection (ICRP) Publication 68.

M. A. Jessee, M. L. Williams and M. D. Dehart. Development of generalized perturbation theory capability within the scale code package. In *Proceedings of International Conference on Mathematics, Computational Methods, and Reactor Physics (M & C 2009)*. Saratoga Springs, New York, 2009.

E. Jones et al. SciPy: Open source scientific tools for Python. `http://www.scipy.org/`, 2001–.

P. J. Maudlin, K. O. Ott and R. C. Borg. Instantaneous fuel growth rates for breeder reactors. *Nuclear Science and Engineering*, **72**, 140, 1979.

Nuclear Decommissioning Authority. NDA plutonium options. `http://www.nda.gov.uk/documents/upload/Plutonium-Options-for-Comment-August-2008.pdf`, 2008.

OECD NEA/IAEA. Uranium 2009. Technical Report NEA No. 6891, Organisation for Economic Co-operation and Developement (OECD) Nuclear Energy Agency (NEA) and International Atomic Energy Agency (IAEA), 2010.

T. E. Oliphant. *Guide to NumPy*, 2006.

K. O. Ott. An improved definition of the breeding ratio for fast reactors. *Transactions of the American Nuclear Society*, **12**, 719, 1969.

K. O. Ott and R. C. Borg. Derivation of consistent measures for the doubling of fast breeder reactor fuel. *Nuclear Science and Engineering*, **62**, 243, 1977.

K. O. Ott and R. C. Borg. Fast reactor burnup and breeding calculation methodology. *Progress in Nuclear Energy*, **5**, 201, 1980.

K. O. Ott and R. J. Neuhold. *Introductory Nuclear Reactor Dynamics*. American Nuclear Society, 1985.

K. O. Ott et al. Description of reactor fuel breeding with three integral concepts. *Nuclear Science and Engineering*, **72**, 152, 1979.

K. O. Ott et al. Integrated fuel-cycle models for fast breeder reactors. *Annals of Nuclear Energy*, **8**, 371, 1981.

S. Pillon et al. Aspects of fabrication of curium-based fuels and targets. *Journal of Nuclear Materials*, **320**, 36, 2003. Proceedings of the 2nd Seminar on European Research on Material for Transmutation.

G. C. Pomraning. Variational principle for eigenvalue equations. *Journal of Mathematical Physics*, **8**, 149, 1967.

R. Rhodes. *The Making of the Atomic Bomb*. Simon & Schuster Paperbacks, 1986.

W. Romberg. Vereinfachte numerische integration. *Det Kongelige Norske Videnskabers Selskab Forhandlinger*, **28**, 30, 1955.

M. Salvatores. Fast reactor calculations. In Y. Ronen (ed.), *Handbook of Nuclear Reactor Calculations*, volume III, 263–363. CRC Press, 1986.

SCALE manual. *SCALE: A Modular Code System for Performing Standardized Computer Analyses for Licensing Evaluation*. Oak Ridge National Laboratory, 2009. ORNL/TM-2005/39 Version 6 Vols. I-III. Available from Radiation Safety Information Computational Center at Oak Ridge National Laboratory as CCC-750.

L. B. Silverio and W. de Queiroz Lamas. An analysis of development and research on spent nuclear fuel reprocessing. *Energy Policy*, **39**, 281, 2011.

W. M. Stacey. *Variational Methods in Nuclear Reactor Physics*. Academic Press, 1974.

H. F. Stripling, M. Anitescu and M. L. Adams. A generalized adjoint framework for sensitivity and global error estimation in time-dependent nuclear reactor simulations. *Annals of Nuclear Energy*, **52**, 47, 2013.

U.K. Nirex Ltd. Heat capacity in deep geological disposal concepts. Technical report, United Kingdom Nirex Ltd., 2004.

W. F. G. Van Rooijen. *Improving Fuel Cycle Design and Safety Characteristics of a Gas Cooled Fast Reactor*. Ph.D. thesis, Delft University of Technology, 2006.

A. E. Waltar, D. R. Todd and P. V. Tsvetkov (eds.). *Fast Spectrum Reactors*. Springer, 2012.

J. R. White. The development, implementation, and verification of multicycle depletion perturbation theory for reactor burnup analysis. Technical Report ORNL/TM-7305, Oak Ridge National Laboratory, 1980.

M. L. Williams. Development of depletion perturbation theory for coupled neutron/nuclide fields. *Nuclear Science and Engineering*, **70**, 20, 1979.

M. L. Williams. Perturbation theory for nuclear reactor analysis. In Y. Ronen (ed.), *Handbook of Nuclear Reactor Calculations*, volume III, 63–188. CRC Press, 1986.

World Nuclear Association. Nuclear fuel cycle overview. `http://www.world-nuclear.org/info/inf03.html`, 2011.

Summary

This thesis describes the application of adjoint techniques to fuel cycle analysis, in order to provide a more accurate description of the effects of nuclides on reactor behaviour. Transmutation and decay processes change the composition of the fuel. Allowing for these changes makes it possible to create different fuel compositions that yield similar reactor behaviour. This approach can then be used to improve the sustainability of nuclear energy, for example by reducing the heat produced by radioactive waste.

Chapter 2 reviews and extends the continuous fuel cycle model described in Ott and Borg (1980). This approach approximates the long-term behaviour of the reactor using an eigenvalue problem, removing the complexity associated with the discrete operating cycles. The model provides reasonable predictions of the behaviour of a sodium cooled fast reactor model, although extending it to include additional nuclides decreases the quality of the results significantly. The use of a constant power constraint in place of the reactivity constraint makes little difference to the results. Applying the model to a negative growth system gives worse results than those found for the breeder system, with the growth rate prediction being particularly poor. The effects of fuel cycle strategies such as different feed materials and recycling schemes on the negative growth system are also studied. Recycling additional actinides decreases the waste radiotoxicity, while including more light uranium isotopes in the feed material increases the amount of Pu-239 and decreases the amount of other plutonium isotopes in the fuel.

The double adjoint method is developed in chapter 3. This approach relies on using the nuclide worths found from an adjoint reactivity calculation as the source values for a time adjoint problem. This allows the contributions of nuclides present at the start of the burn-up period to the reactivity at the end of it to be determined. Combining this measure with reactivity worths found at the beginning of the burn-up period yields a method that can be used to produce a new fuel composition that gives very similar reactor behaviour to that seen with the original composition. This leads to a breeding gain definition that includes the effects of the feed material and that can be applied to non-equilibrium situations. The importance of including the effects of the compound material in the calculation is demonstrated. Results are found for both fast and thermal systems, with the indirect effects causing inaccuracies

in the worths of up to 50% in the worst cases.

The coupled perturbation theory proposed by Williams (1979) is used in chapter 4 to allow for the indirect effects that are neglected in chapter 3. Including the coupling to the flux allows for accurate results to be found for both the fast and thermal systems. The effects of studying a different response are also investigated, with the flux coupling having a larger effect on results for the Pu-239 response than for the reactivity response. The scale of the coupling effect is illustrated by comparison between the values found using the coupled and uncoupled approaches. The use of longer burn-up periods increases the importance of the flux coupling. This implementation of the coupled model relies on an approximation to produce some of the multi-group cross sections, and it is expected that the use of more accurate data would improve the results.

Chapter 5 describes the application of the coupled model to waste heat production. The model is used with fast and thermal systems, and the effects of different post burn-up decay periods are considered. The waste heat worths for different isotopes are found with no recycling, with plutonium recycling, and with uranium and plutonium recycling. Equivalent fuel compositions using plutonium from different sources are determined and the resulting waste heat is calculated, with the results showing that plutonium from lower burn-up sources tends to produce less waste heat, by up to a factor of 5 in the extreme cases. The effects of different recycling schemes on the waste produced by these fuels are determined, and both the waste heat per unit mass and the total waste mass are examined.

The methods developed in this thesis demonstrate some of the potential uses of adjoint techniques in fuel cycle analysis. Quantifying how nuclides present at the beginning of the burn-up period affect the reactor behaviour at the end of the period allows a better comparison of fuels of different compositions. One possible application of such comparisons is demonstrated in the study of the waste heat produced by different fuels. There is a wide range of other possibilities, some of which are described in the recommendations given in the final chapter.

Samenvatting

Dit proefschrift beschrijft het toepassen van geadjugeerde technieken op de analyse van de splijtstofcyclus, om een nauwkeurigere beschrijving van de effecten van nucliden op reactorgedrag te verkrijgen. Transmutatie en vervalprocessen beïnvloeden de samenstelling van het brandstofmengsel gedurende opbrand. Het correct verdisconteren van deze veranderingen maakt het mogelijk om verschillende brandstofmengsels te creëren die leiden tot vergelijkbaar gedrag van de reactor. Deze benadering kan dan toegepast worden om de duurzaamheid van nucleaire energie te verbeteren, bijvoorbeeld door de warmte die door radioactief afval geproduceerd wordt, te verminderen.

In hoofdstuk 2 wordt het continue splijtstof cyclus model, beschreven in Ott en Borg (1980), besproken en uitgebreid. Deze aanpak benadert het lange termijn gedrag van de reactor met behulp van een eigenwaarde probleem, zodat de complexiteit die gepaard gaat met discrete herladingscyclus verdwijnt. Het model geeft redelijke voorspellingen van het gedrag van een natriumgekoelde-snelle reactor, hoewel de kwaliteit van de resultaten significant afneemt, als extra nucliden in het model worden opgenomen. Het gebruik van een constant vermogenvoorwaarde, in plaats van de reactiviteitsvoorwaarde, maakt weinig verschil voor de resultaten. Door het model toe te passen op een negatief groeisysteem worden slechtere resultaten verkregen dan die gevonden worden voor het kweeksysteem, waarbij vooral de voorspelling van de groeisnelheid tegenvalt. De effecten van splijtstof-cyclus-strategieën, zoals gebruik van verschillende grondstoffen en recyclingschema's, op het negatieve groeisysteem worden ook bestudeerd. Het hergebruiken van extra actiniden verlaagt de radiotoxiciteit van het afval, terwijl het opnemen van meer lichte uraniumisotopen in de grondstoffen de hoeveelheid Pu-239 verhoogt en de hoeveelheid van andere plutoniumisotopen verlaagt in de brandstof.

De dubbel-geadjugeerde methode wordt ontwikkeld in hoofdstuk 3. Deze benadering is gebaseerd op het gebruik van de nuclide-waardes die middels een geadjugeerde reactiviteitsberekening gevonden worden als de bronwaardes van een tijds-geadjugeerd probleem. Op deze manier kunnen de bijdragen van de nucliden die aanwezig zijn aan het begin van de opbrandperiode tot en met de reactiviteit aan het einde daarvan, bepaald worden. Het combineren van deze maat met reactiviteitswaardes die bepaald worden aan het begin van de opbrandperiode, geeft een methode om een nieuwe splijtstofsamenstelling te

genereren die resulteert in reactorgedrag dat sterk lijkt op het gedrag met de originele samenstelling. Dit leidt tot een definitie van kweekfactor waarbij de effecten van de grondstoffen zijn inbegrepen en die toegepast kan worden op niet-evenwicht situaties. Het belang van het verdisconteren van de effecten van samengestelde materialen in de berekening wordt gedemonstreerd. Resultaten zijn gevonden voor zowel snelle als ook voor thermische systemen, waarbij de indirecte effecten onnauwkeurigheden veroorzaken in de waardes van tot wel 50% in de slechtste gevallen.

De gekoppelde verstoringstheorie, voorgesteld door Williams (1979), wordt gebruikt in hoofdstuk 4 om indirecte effecten die verwaarloosd werden in hoofdstuk 3, toe te staan. Door de koppeling met betrekking tot de flux op te nemen, kunnen accurate resultaten gevonden worden voor zowel de snelle als ook de thermische systemen. De effecten (van het bestuderen) van verschillende responsies worden ook bestudeerd, waarbij de fluxkoppeling een groter effect heeft op de resultaten van de Pu-239 responsie dan voor de reactiviteitsresponsie. De schaal van het koppelingseffect wordt geïllustreerd aan de hand van een vergelijking tussen de waarden die gevonden worden met en zonder de koppelingsmethode. Het gebruik van langere opbrandperiodes maakt de fluxkoppeling nog belangrijker. Deze implementatie van het gekoppelde model hangt af van een benadering om enkele van de multi-groep doorsneden te produceren en het licht in de lijn der verwachting dat het gebruik van nauwkeuriger data de resultaten verder zal verbeteren.

Hoofdstuk 5 beschrijft de toepassing van het gekoppelde model op afvalwarmte-productie. Het model wordt gebruikt voor zowel snelle als ook thermische systemen en de effecten van verschillende vervalperiodes na de opbrandperiode worden behandeld. De afvalwarmte-waarden worden gevonden voor verschillende isotopen zonder hergebruik, bij hergebruik van het plutonium en bij hergebruik van zowel uranium als ook plutonium. Equivalente splijtstofcomposities met plutonium van verschillende bronnen worden bepaald en de resulterende afvalwarmte wordt berekend, waarbij de resultaten laten zien dat plutonium afkomstig van lagere opbrandperiodes in de regel minder afvalwarmte produceert tot wel een factor 5 in de meest extreme gevallen. De effecten van verschillende hergebruikschema's op het geproduceerde afval met deze splijtstoffen worden bepaald en zowel de afvalwarmte per eenheid massa en de totale afvalmassa worden bestudeerd.

De methoden die ontwikkeld zijn in dit proefschrift demonstreren enkele van

de mogelijke toepassingen van geadjugeerde technieken op de analyse van de splijtstofcyclus. Door te kwantificeren hoe nucliden die aan het begin van de opbrandperiode aanwezig zijn, het gedrag van een reactor aan het einde van deze periode beïnvloeden, zorgt voor een betere vergelijking tussen splijtstoffen met verschillende composities. Een mogelijke toepassing van dergelijke vergelijkingen is gedemonstreerd aan de hand van het onderzoek naar afvalwarmte, dat geproduceerd wordt door verschillende splijtstoffen. Er bestaan diverse andere mogelijkheden; deze worden beschreven in de aanbevelingen in het laatste hoofdstuk.

Dutch translation provided by Jurriaan Peeters.

Acknowledgements

First, I must thank Tim van der Hagen and Jan Leen Kloosterman for giving me the opportunity to do my PhD in PNR/NERA. Their input has shaped my research into the thesis that you have in your hands. The supervision provided by Danny Lathouwers was invaluable, particularly his ability to discuss problems in such a way as to make the solution pop into my head.

I would like to thank the rest of the group, past and present, for all the talks and fun we had over the years. Thank you to the staff, Martin, Dick, Peter, August, Hugo and Eduard. Special thanks go to Ine, for keeping things going and always being willing to help. There have been quite a few postdocs over the years, all of whom have taken an interest and offered help and advice, even on problems well outside their fields. So thank you to Denis, Norbert, József, Dimitrios, Christophe, and Ming. My fellow PhDs, Gert Jan, Jurriaan, Wim, Valentina, Frank, Bart, Károly, Amer, Stavros, Brian, Johan, and Jitka, thank you for sharing this experience with me. I enjoyed working with you, even when we didn't want to be, and socialising with you even when we shouldn't have been. I must give special thanks to Luca, a wonderful office mate, and to Zoltán, who not only coped with my supervision, but was also organised enough to have the software I needed for many of my calculations. I would also like to thank Bauke, the other survivor of my supervisory efforts, for all his hard work.

Regular visits to the bar are a vital part of the life of any Englishman, and I would like to thank all those who made 't Koepeltje so much fun every week. In particular, thank you to Léon and Stefan, who always took arguments seriously on Friday evenings, but never let them carry over to Monday mornings.

The support from my family has been vital throughout the whole PhD process and before. Without their love and encouragement, I would never have made it this far.

Finally, of course, I have to thank Edith. She has been there for me through the ups, downs, and round-and-rounds. She has been happy and sad, angry and elated for me. I hope, therefore, that she will understand exactly what I mean when I say, from the bottom of my heart and with all my love, thank you.

List of publications

S.A. Christie, D. Lathouwers, J.L. Kloosterman, Double adjoint method for determining the contribution of composition to reactivity at different times, *Annals of Nuclear Energy*, Volume 51, January 2013, pages 50-59

J.A.B. van Rhijn, S.A. Christie, D. Lathouwers, J.L. Kloosterman, Modelling fuel behaviour in a reactor park using fuel cycle kinetics, *Annals of Nuclear Energy*, Volume 51, January 2013, pages 27-37

S.A. Christie, D. Lathouwers, J.L. Kloosterman, T.H.J.J. van der Hagen, Extending the Continuous Fuel Cycle Model with Additional Nuclides and Constraints, *Proceedings of GLOBAL 2011*, Japan

S.A. Christie, D. Lathouwers, J.L. Kloosterman, T.H.J.J. van der Hagen, The Continuous Fuel Cycle Model and the Gas Cooled Fast Reactor, *Proceedings of GLOBAL 2011*, Japan

Z. Perkó, S. Fehér, J.L Kloosterman, S.A. Christie, Recycling of VVER minor actinides in a gas-cooled fast reactor, *Proceedings of PHYSOR 2010*, USA

Curriculum Vitae

Stuart Alexander Christie was born in Northampton in the United Kingdom on April 23rd 1982. He grew up in Milton Keynes and attended Bedford Modern School. He studied a combined Master's undergraduate degree in physics at Imperial College London.

After his first degree, Stuart moved to Chiba City, Japan, and spent three years teaching English to elementary and junior high school students. He then returned to the United Kingdom to study for a Master of Science degree in the physics and technology of nuclear reactors at the University of Birmingham.

Stuart moved to Delft to perform his PhD research in the then Physics of Nuclear Reactors (now Nuclear Energy and Radiation Applications) group, the results of which are presented in this thesis.

TU Delft
Delft
University of
Technology